Universitetet
i Stavanger

FACULTY OF SCIENCE AND TECHNOLOGY

MASTER'S THESIS

Study program/specialization: Petroleum engineering / Natural gas engineering	Spring / Autumn semester, 2020 Open / Confidential
Author: Zongqiang Luo	………………………… (Signature of author)
Program coordinator: N/A Supervisor(s): Pål Ø. Andersen, Carita Augustsson	
Title of master's thesis: A LSSVR-PSO machine learning model for the estimation of reservoir porosity from petrophysical well logs	
Credits: 30	
Keywords: Porosity prediction; Well logging; Support Vector Machine; Particle Swarm Optimization; Machine learning;	Number of pages: 78 +supplemental material: 29 Stavanger, Jun.10th / 2020

Abstract

Reservoir porosity is a key parameter in the reservoir evaluation and geomechanics. To obtain accurate measurement of porosity can be time-consuming and expensive by core sampling or applying various well logging tools. Core sampling can also be limited to a small number of wells or partially sections of a wellbore. In this thesis, a more effective and economical method is introduced to provide porosity estimation. A least square support vector regression (LSSVR) model is developed to predict the reservoir porosity based on 1260 well logging data and porosity from routine core analysis from four wells in the Varg field, North Sea. Regularization and kernel parameters are the two primary components in the LSSVR algorithm, and they are optimized by employing particle swarm optimization (PSO) algorithm. A combined LSSVR-PSO model is developed to predict porosity by using petrophysical logs from Varg Field. As comparison, two unoptimized machine learning approaches k-nearest neighbors (KNN), support vector regression (SVR) and a hybrid porosity estimation method of density log, neutron log and sonic log are utilized. Feature selection is conducted and sonic log, gamma-ray log, deep resistivity log, density log and compensated neutron log are selected as input features while caliper log is discarded as insufficient correlation relationship with porosity. The predicted porosity result from LSSVR-PSO model for well 15/12-20S, showing higher accuracy with R^2 =0.945, Root mean square error (RMSE) = 0.01341 comparing with KNN, SVR and the hybrid porosity estimation method. The proposed LSSVR-PSO model for porosity prediction is reliable in the datasets range and it can be a more general porosity estimation model by varying the scale of the data samples and the number of wells.

Keywords: Porosity prediction; Well logging; Support Vector Machine; Particle Swarm Optimization; Machine learning;

Acknowledgements

I would like to express my appreciation for the useful help from my supervisor Pål Ø. Andersen and Carita Augustsson at University of Stavanger, Norway.

I feel grateful to complete my master program and write my master thesis at University of Stavanger in Norway.

Table of Contents

List of Tables

List of Figures

Nomenclature

Symbol	Description	Unit
t, s	Arbitrary vector	-
ω_a	Arbitrary positive weight function	-
I	Current	A
C	Conductivity	$S \cdot m^{-1}$
P_{curr}	Current position	-
Γ	Complete gamma function	-
d	Calculated distance	-
cc_1	Cognitive weight	-
c_d	Distance correlation constant	-
D_{corr}	Distance correlation co-efficient	-
ϕ_{den}	Density estimated porosity	$\mu s \cdot f^{-1}$
E	Electrical potential	V
c	Electrical conductance	S
Z	Estimated porosity by logs	-
r	Electrical resistance	Ω
x	Feature value	-
ρ_{fluid}	Fluid density	$gm \cdot cc^{-1}$
Q_1	First quartile	-
ω	Feature co-efficient vector	-
$Gbest$	Group best individual position	-
A	Horizontal area	m^2
ω_{in}	Inertia weight	-
Δt_{log}	Interval transit time of formation	$\mu s \cdot f^{-1}$
Δt_{matrix}	Interval transit time of matrix	$\mu s \cdot f^{-1}$

Δt_{fluid}	Interval transit time of pore fluid	$\mu s \cdot f^{-1}$
ϕ	Joint characteristic equation of vectors	-
K	Kernel function	-
σ	Kernel parameter	-
$\tau i, \tau i*, \alpha, \alpha i, \alpha i*$	Lagrangian multiplier	-
R_{Lower}	Lower range	-
L_f	Lagrangian function	-
ρ_{matrix}	Matrix density	$gm \cdot cc^{-1}$
ρ_{bulk}	Measured formation bulk density	$gm \cdot cc^{-1}$
N_{SVM}	Number of supporting vectors	-
y	Observation value	-
$Pbest$	Previous best individual position	-
P	Pearson correlation co-efficient	-
P_{old}	Previous position	-
R	Resistivity	$\Omega \cdot$ m
L	Regularization norm	-
C_p	Regularization penalty parameter	-
ϕ_{sonic}	Sonic estimated porosity	%
$\varepsilon, \mu_i, \mu^*$	Slack variable	-
cc_2	Social weight	-
Q_3	Third quartile	-
R_{Upper}	Upper range	-
u	Velocity	-
T	Weight co-efficient	-

1 Introduction

Porosity is defined as a key petrophysical factor to determine the fluid storage capacity of aquifer, gas and oil fields, the space connection relationship between formation pore spaces with different mineral components. Porosity is also utilized for the indication of petrophysical metrics and lithofacies database in hydrocarbon reservoir evaluation and geoscience model establishment (Wendt et al., 1985). A detailed description of porosity can be used for reservoir engineers and production engineers to determine the reservoir exploration plan and production schedule.

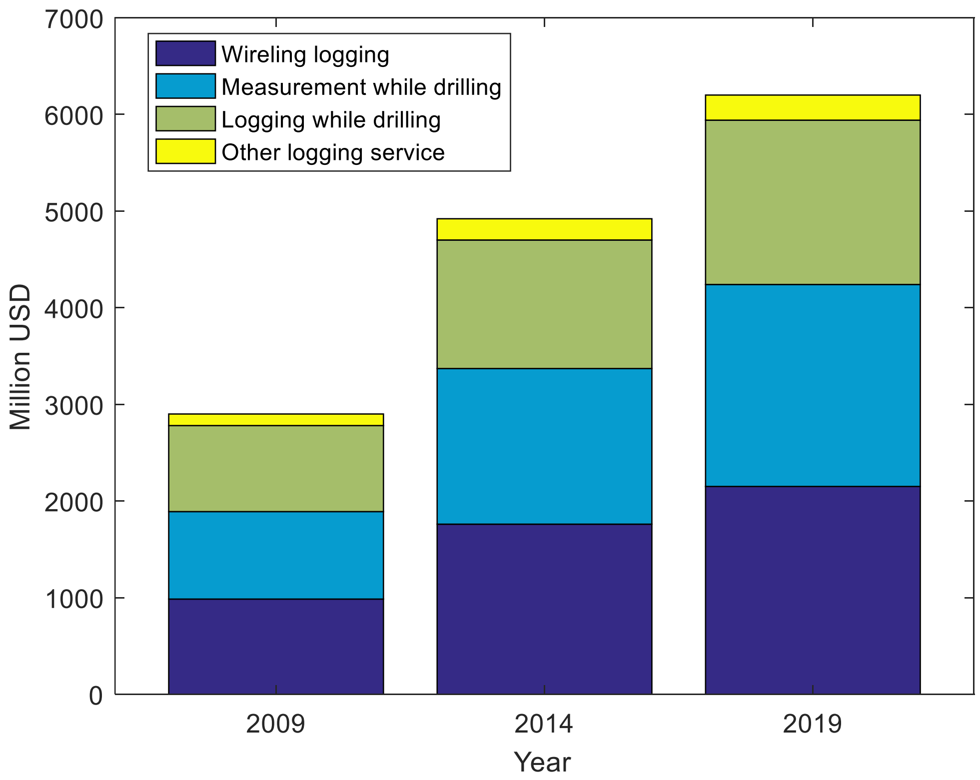

Figure 1 Logging & Measuring Service Cost (Freedonia Group, 2015)

Remarkable expense and time are spent on well-logging operation and core analysis laboratories about specific sections of the wellbores to acquire a comprehensive database of the rock properties within a targeted hydrocarbon reservoir section (Zhang, et al.,2018). Freedonia Group (2015) indicated that the total cost of the logging and measurement service cost in 2019 would be approximately 6.2 billion US dollars as Figure 1 shows. Additionally, to obtain accurate quantitative values of porosity is complicated and uneasy due to the uncertainties in well logging operation procedure and unclear interaction between formations and reservoir fluids (Ghiasi-Freez, et al., 2014). Though the accuracy of porosity can be increased by calibrating with more core samples, the number of core sampling operation is also limited by time and cost. Various empirical equations have been proposed to provide the calculation base for porosity estimation with well logs (Wyllie, et al., 1958; Raymer et al., 1980; Krief et al., 1990; Pu et al., 2006; Li et al., 2009), but it is still a challenge to apply for these estimated formulas as most empirical equations are developed on specific reservoir conditions like unconsolidated carbonate, sandstone or inhomogeneous porous reservoir. Therefore, it is essential to improve the exploration efficiency of the conventional petroleum reservoir to maintain the economical competence of fossil fuels. Acquiring more accurate measurement of rock properties like porosity can contribute to the exploration optimization and production arrangement to enhance recovery with less investment.

The aim of this master's thesis is to develop a machine learning model that the porosity prediction of a single well can be accomplished by only inputting a series of petrophysical well logging data of the single well. This model is trained by the well logging data and the true porosity from routine core analysis laboratory from other wells in the same field.

In this thesis, some methods for the estimation of porosity in the Varg oil field, North Sea, was done by applying a hybrid conventional porosity estimation model with petrophysical logs, and a developed machine learning model of applying LSSVR and PSO algorithms. The Varg field is chosen because petrophysical logs and comparative data from different logs are available for this field. The hybrid conventional porosity estimation method is established on density logs, sonic logs, and neutron logs. The LSSVR model is developed and optimized by a PSO algorithm based on several common well logs like a sonic log, resistivity log, caliper log, etc. Additionally, two SVR and KNN machine learning models are also constructed for comparison purpose.

For this master's thesis work, the thesis content is organized as follows:

Chapter 2 represents the theoretical basics required to understand porosity concept, the measurement of porosity and introduction of several commonly used petrophysical logs in petroleum well logging operation.

Chapter 3 illustrates the basics of machine learning theory and algorithms applied in this thesis and introduces studies for porosity measurement in well logging, examples application of machine learning in the petroleum industry and various optimization methods for support vector machine algorithm.

Chapter4 describes the detailed methodologies of the LSSVR-PSO model, how to apply the LSSVR-PSO model to the well log dataset, and introduction for data preparation and parameter setting of the LSSVR-PSO model. This chapter also gives the overview of Varg field and some statistical evaluation metrics used in this thesis.

Chapter 5 lists the feature selection of LSSVR-PSO model and the model comparison results between LSSVR-PSO, KNN, SVR and the hybrid porosity estimation method are described. A sensitivity analysis is conducted for investigating the relationship between input features and predicted porosity.

Chapter 6 gives illustration of the LSSVR-PSO model results, advantages and limitation of LSSVR-PSO model are discussed.

Chapter 7 concludes the LSSVR-PSO model performance and thesis findings.

Bibliography summarizes the references cited in this thesis.

2 Basic Well Logs and Porosity Measurement

Porosity is a parameter that is defined as the empty volume fraction over the total volume. The space between porous rock is an ideal location for the storage of hydrocarbon. Thus, a high percentage of porosity would suggest that more hydrocarbon could be stored in the pore space than a low percentage of porosity. Due to the pressure difference between formations, the reservoir hydrocarbon can flow in the pore spaces. The higher the porosity of the rock is, the easier fluids like hydrocarbon could flow in a more porous condition as Figure 2 shows.

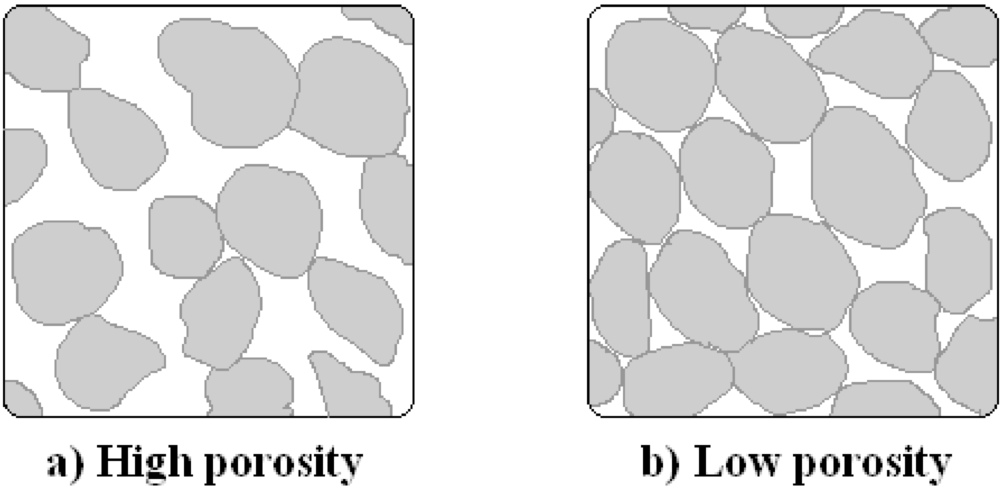

Figure 2 Simplified examples of materials with high and low porosity (Höök et al.2010)

Well logging is a widely used operation to measure geological properties in the wellbore by physical recording or the response received from the well logging tools during the exploration, drilling, completion and production period of a petroleum reservoir development. In this thesis, frequently used well logs including the gamma ray log, the caliper log, the deep resistivity log, the density log and the compensated neutron log are detailed described here as these six logs are available in the Varg field.

Gamma ray log

The gamma-ray logging tool is defined as a widely applied tool in petrophysical parameter measurement by measuring the natural radioactivity for fluid, mud, or formation sections in the reservoir. Gamma-ray log data represents the concentration of radioactive components for measured target by evaluating the energy loss when gamma radiation emanates in the formation. Normally, the gamma radioactivity from the formation is usually evaluated in API units and a higher gamma-ray reading can be obtained in shale than in clean sandstone and carbonates as shale contains more radioactive material. It is worthy to mention that the existence of potassium feldspar and mica, including glauconite can cause a high gamma-ray reading figure even in clean sandstone (Asquith et al., 2004).

Table 1 provides a summary of the gamma radiation reference value for some common minerals and lithologies. When the gamma-ray reading value is higher than 80 in API units, it probably suggests that the logged interval is primarily composed of shale rocks with low porosity. However, porosity estimation can be hard when the gamma-ray reading value is between 10 and 30, which requires other well logging tools to determine the lithologies. The measurement accuracy or reliability of the gamma-ray log is constrained by the initial intensity of gamma-ray emission and the amount of Compton scattering that gamma rays meet (Glover, 2000). Therefore, the gamma-ray logging tool is always equipped with a radioactive source like thorium, potassium, and uranium (Asquith et al., 2004).

The gamma-ray logging tool is useful in the lithological classification and geological assessment or shale volume calculation, it can be a single well logging tool and it can also be combined with other well logs like neutron log, density log, resistivity log, and caliper log. Additionally, the gamma-ray logs can also be utilized in-depth matching, cased hole correlation, recognition of radioactive mineral deposits, and facies depositional environment analysis (Glover, 2000).

Table 1 Gamma radiation reference value for some common minerals and lithologies (Pirson,1963)

Mineral or Lithology	Composition	Gamma Radiation (API Units)
Pure Mineral		
Calcite	$CaCO_3$	0
Dolomite	$CaMg(CO_3)_2$	0

Halite	$NaCl$	0
Anhydrite	$CaSO_4$	0
Gypsum	$CaSO_4(H2O)_2$	0
Sulphur	S	0
Mica	-	200-350
Quartz	SiO_2	0
Lithology		
Limestone	-	5-10
Dolomite	-	10-20
Sandstone	-	10-30
Shale	-	80-140
Others		
Lignite	$CH_{0.849}\ N_{0.015}\ O_{0.221}$	0
Anthracite	$CH_{0.358}\ N_{0.009}\ O_{0.022}$	0

Caliper log

The caliper logging tool is designed with several flexible arms in the tool and the basic objective of this tool is to provide a measurement of wellbore diameter and wellbore shape by detecting the electrical signal changes when the arms are released or withdrawn from the tool.

The diameter and shape of the wellbore can always be changed when drilling through different lithologies, or other causes like the occurrence of mud cake. A combination of caliper log and gamma-ray log can be helpful in the lithological assessment, the bit size is regarded as an optimal measurement reference to monitor the diameter and shape along the wellbore.

Generally, there are three kinds of measuring scenarios for caliper log operation:

(1) Wellbore diameter equals to bit size:

This measurement may suggest that the tool is running through a pretty consolidated formation with relatively low permeability and possible lithologies can be massive sandstone or calcareous shale.

(2) Wellbore diameter is larger than bit size:

This measurement may suggest that the tool is running through a relatively soft formation and possible caving-in occurs. The possible lithologies can be unconsolidated sandstone or gravel.

(3) Wellbore diameter is smaller than bit size:

This measurement may indicate that part of the formation had already fell back into the wellbore and the existence of mudcake. The possible guessing for lithologies can be porous sandstone or carbonate.

The Caliper log has become a useful indicator in computing mudcake thickness, wellbore volume and required cement volume. The quality of wellbore determines the correctness of most well logging tools as the logging quality can be affected by the poor hole size setting. Thus, the caliper log also is often used as a reference wellbore correction for other well logging tools that are run under poor wellbore conditions. Furthermore, possible lithology information from the caliper log can offer additional help in wireline pressure tests and recovery of fluid samples (Glover, 2000).

Resistivity log

Resistivity logging tool is a widely favorable tool in the determination of the existing zones of hydrocarbon by measuring the electrical resistivity of rocks and depositional sediments. The application of resistivity logging tool can be categories into three primary parts:

(1) Clarification of hydrocarbon layers and water-bearing layers;

(2) indicate permeable zones;

(3) Calculation of resistivity porosity (Asquith et al., 2004).

Here some basic concepts and Ohm's law about resistivity are restated and a remarkable contribution of Georg Ohm is the study that clearly illustrates the relationship between current, voltage and resistance (Georg Ohm, 1827). With a given conductor I, there is a proportional relationship existing between the current flowing from two points and the changes of electrical potential ΔE. The constant of proportionality can be defined as the electrical conductance c and the electrical resistance r is characterized as the inverse of the conductance.

Here, the conductor I between two points X and Y can be defined as:

$$I = c\,\Delta E \tag{1}$$

$$r = \frac{1}{c} \tag{2}$$

Then, substitute Eq.(2) into Eq.(1):

$$I = \frac{\Delta E}{r} \tag{3}$$

Suppose that there are two different faces X and Y in a cube rock with horizontal area A and length of the cube L. The current I can be estimated by measuring the electrical potential changes ΔE and then the resistivity R of the rock in the horizontal direction can be computed with Eq.(4):

$$R = \frac{\Delta E}{I}\frac{A}{L} \tag{4}$$

Hence, the conductivity C can be rewritten as Eq.(5):

$$C = \frac{1}{R} = \frac{I}{\Delta E}\frac{L}{A} \tag{5}$$

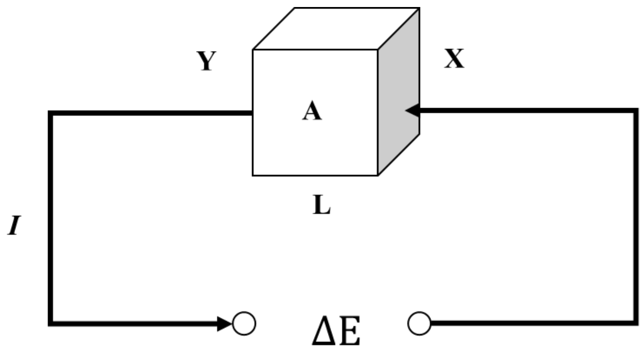

Figure 3 Electrical potential change in rock

The two primary types of resistivity logs that are applied in petrophysical parameter measurement are induction log and electrode log. Normally, the measuring result either is a direct measurement of resistivity or a direct measurement of conductivity, thus both measurement results can be used to get the measured resistivity results. In terms of sediments, formation water and water-based mud are detected low resistivity readings in resistivity log. On the contrary, hydrocarbon components like oil and gas always have higher resistivity than water or water-based mud. Thus, the resistivity log can be useful in identifying the hydrocarbon zones and non-hydrocarbon zones when combined with other petrophysical logs.

Sonic log

The sonic logging tool is basically equipped with one sound transmitter and two or more sonic receivers and the formation response reflects the transmitting capacity of the formation by recording the interval transit time (Δt). Lithology and porosity are characterized as key factors for the interval transit time (Δt) thus once the seismic velocity of the rock matrix u_{matrix} and pore fluid u_{fluid} are known or assumed, the porosity values can be estimated with Eq.(6) (Wyllie et al., 1958). Typical velocity and interval transit time reference values are given in the Table 2. It shall be mentioned that Eq.(6) is applicable on the condition that the rock material is perfectly homogenous (Wyllie et al., 1958).

$$\phi_{sonic} = \frac{\Delta t_{log} - \Delta t_{matrix}}{\Delta t_{fluid} - \Delta t_{matrix}} \tag{6}$$

Table 2 Sonic velocities and Interval Transit Times for different lithologies (Schlumberger, 1974)

Item	u_{matrix} (f/s)	Δt_{matrix} $(\mu s/f)$	Δt_{matrix} $(\mu s/f)$ Commonly used
Sandstone	18 to 19.5	55.5 to 51	55.5 to 51
Limestone	21 to 23	47.6 to 43.5	47.6
Dolomite	23 to 26	43.5 to 38.5	43.5
Anhydrite	20	50	50
Salt (Halite)	15	66.7	67
Casing (Iron)	17.5	57	57

Density log

The density logging tool is defined as an equipment to provide the bulk density curves of the measured formation within a well log interval by recording the returned gammy ray count after the impaction of Compton scattering and photoelectric absorption (Tittaman and Wahl, 1965). The density log is comprised with a gammy ray source that transmits gamma ray into the formation during the well logging operation and normally Cobalt-60 or Cesium-137 would be selected as the gamma ray source.

Density porosity can be computed with the condition that the density of matrix and fluid are known. Combined with the measured bulk density record, the density porosity is estimated by Eq.(7) and typical values of matrix density for different lithologies in the Table 3. Some commonly used value for fluid density are 1.1 gm/cc for salt mud, 1.0 gm/cc for fresh water and 0.7 gm/cc for gas (Glover, 2001).

$$\phi_{den} = \frac{\rho_{matrix} - \rho_{bulk}}{\rho_{matrix} - \rho_{fluid}} \tag{7}$$

Table 3 Matrix densities of different lithologies (Schlumberger, 1974)

Item	ρ_{matrix} (gm/cc)
Sandstone	2.65
Limestone	2.71
Dolomite	2.88
Anhydrite	2.98
Salt (Halite)	2.03

Neutron log

The neutron logging tool is designed with a chemical source within the equipment to measure the hydrogen ion concentration of the formation. The neutrons are emitted from the source into the logging formation and due to the collision process between neutrons and other formation material, the energy loss of the neutrons is related with the formation porosity, where the maximum amount of energy loss is a function of hydrogen concertation in the formation. Therefore, the responses from neutron log can be collected to measure the formation porosity. Neutron log responses can be affected lithology type, detector position placement and spacing between source and detectors, which can bring uncertainties for the estimated porosity.

In terms of the real rock formation, the hydrogen components exist both in the rock matrix and the fluids occupying the rock pore space, which can greatly influence the measurement of porosity in neutron log. This issue is handled by introducing limestone calibration for the neutron log tool as few other elements except hydrogen can contribute to measured response in pure limestone where the limestone can be assumed to be saturated with water (Glover, 2001). As Figure 4 shows, the apparent limestone neutron porosity reading matches the true porosity in limestone layers. If the logged interval lithologies are not limestone, then the apparent limestone neutron porosity needs to be calibrated to get the true porosity readings. It is noted that the calibrated charts can vary by different compensated neutron logging tool

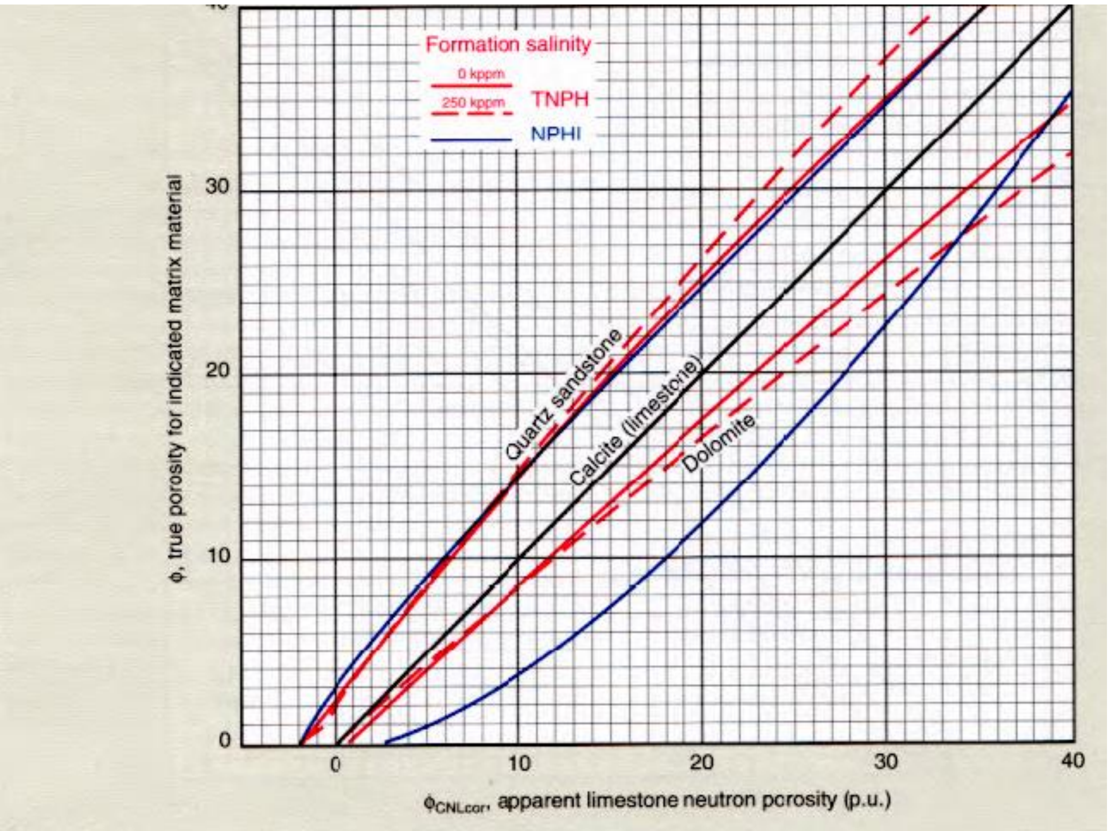

Figure 4 CNL neutron chart for lithology and scale conversions (Crain et al. 2006)

The core analysis laboratory is an ideal and expensive approach to measure a great majority of petrophysical rock properties. However, clear limitation from economical perspective and specific sections of interests can been seen, but it is still recommended as an effective method to get the most accurate measurement of the formation like porosity in petroleum industry. In this section, a summary towards Routine Core Analysis Laboratory (RCAL) and Special Core Analysis Laboratory (SCAL) will be briefly introduced to show what the petrophysical properties are measured in these two techniques.

Routine core analysis laboratory

Routine core analysis laboratory (RCAL) is widely used to acquire petrophysical properties from reservoir formation or other intervals of interests. The standard RCAL report contains horizontal and vertical permeability, porosity, pore saturation, grain density as Figure 5 shows. This petrophysical information can be collected by core plugs from the formation. Once the process of core sampling is completed and core samples are retrieved to the surface, consolidated methods are needed for core samples to avoid drying of interface sensitive clays or permeability reduction on the way to be delivered to laboratory (Glover, 2001). In terms of the porosity measurement methods in laboratory, the most used two methods are imbibition and mercury injection. By immersing the core sampling rock within a fluid with known density, the weight difference of the core sample before and after immersion can be obtained. Then the pore volume of core sample can be computed, which is referred as connected porosity. As for mercury injection, the core sampling rock is immersed within mercury and gradual pressure change would lead to the displacement changes of mercury within the core sampling rock. The weight difference of mercury lost can be measured to compute the pore volume and porosity.

COMPANY : STATOIL
WELL : 15/12-5
FIELD : 15/12
STATE : NORWAY

FINAL REPORT

CORE NO.: 2

PAGE: 1

DATE: JUNE 1986

GECO
Petroleum laboratory

Plug No.	Depth (meter)	Permeability (mD), horizontal		vertical		Porosity (%)		Pore saturation		Grain dens.	Formation Description
		k_a	k_{el}	k_a	k_{el}	He	Sum.	S_o	S_w	g/cc	
	2910.50										
29	2911.00	0.79	0.61	0.042	0.031	10.5	12.7	0	87.5	2.67	SstGryVF-gr,SbangVW-cmtw-srtCl-lam
30	2911.25	0.078	0.058	0.048	0.035	9.1				2.67	A.A. w/Mic.
31	2911.50	0.11	0.080	<0.04	<0.02	10.2				2.66	A.A.
32	2911.75	0.34	0.26	<0.04	<0.02	8.5				2.68	A.A.
33	2912.00	0.099	0.073	<0.04	<0.02	9.2	12.9	0	88.4	2.66	A.A.
34	2912.25	0.046	0.034	<0.04	<0.02	9.2				2.65	A.A.
35	2912.50	0.058	0.043	<0.04	<0.02	9.3				2.66	A.A.
36	2912.75	1.5	1.2	<0.04	<0.02	8.5				2.66	A.A.
37	2913.00	0.094	0.070	<0.04	<0.02	9.5	12.0	0	84.7	2.67	A.A.

Figure 5 RCAL report for Well 15/12-5, Varg Field (Statoil,1986)

Special core analysis laboratory

Compared with RCAL, Special core analysis laboratory (SCAL) can provide a wide range of petrophysical parameters by conducting fluid laboratory towards the core sampling from the geological formation. More analysis work is involved in SCAL to offer approaches to capillary pressure, relative permeability, wettability etc. With more detailed information from SCAL, it can help optimize the procedure of Enhanced Oil Recovery plan with a better geological and petrophysical understanding of the reservoir formation in petroleum industry compared to RCAL. Meanwhile, necessary plug preservation methods like wax coating are suggested during the pore sampling and delivery process (Glover, 2001).

3 Machine Learning and Optimization Techniques

3.1 Machine Learning basics

Machine learning can be defined as a training process of finding models that are derived from data and there are various definitions of machine learning from different perspectives. Samuel (1959) described machine learning as a procedure that programming computers can learn from experience and eliminate the requirement of detailed programming effort. In Mitchell's (1997) work, machine learning is defined that a computer program is said to learn from experience E with respect to some class of tasks T and performance measure P, if its performance at tasks in T, as measured by P, improves with experience E. (Mitchell, 1997). Due to the rapid development of computation ability and information technology industrialization, a large amount of data is created. Machine learning is a power tool that are widely used in statistics, artificial intelligence and predictive analysis. Despite the commercial application like house price prediction and spam email classification, machine learning has a great impact on data-oriented researches in numerous industries.

Hastie et al. (2009) suggested that learning from data in the perspective of statistics can be illustrated as a procedure to extract important patterns and trends, and understand "what the data says". A more recent definition of machine learning is expressed as a combination of hacking skills, mathematics and statistics knowledge and substantive expertise (Conway & White, 2012).

The aim of conducting machine learning is to learn an approximately behavioral function g(x) to describe a certain pattern of a dataset where an unknown pattern function f(x) may exist. By introducing a cost function or fitness function in machine learning and minimizing the error value or fitness value, a series of hyper-parameter can be discovered to make the machine learning model to have the best approximate pattern estimation of the dataset. A hyper-parameter is defined as a model parameter that needs to be set manually rather than learning from the data such as the number of neighbors in KNN algorithm and regularization parameter in SVM algorithm.

Basically, there are three major categories of machine learning: supervised learning, unsupervised learning and reinforcement learning. These three learning types are classified by whether the output data of learning result is desired or not. For instance, the identification of a spam email belongs to a supervised learning problem as the fact that an email is known to be classified into spam or not spam. A customer segmentation shall be dimed as unsupervised learning problem as the features and outcome of segmentation is unknown before applying machine learning. Furthermore, the machine learning applied in this thesis is supervised machine learning model as the model is provided with labeled input datapoints and desired outputs.

The standard approach of supervised machine learning is to obtain the desired output by feeding the algorithm with a vast number of labeled inputs to train the model. In the example of rock porosity prediction based on petrophysical logs, the objective of the supervised machine learning model is to predict the rock porosity values with known petrophysical log samples. The fitness function in the prediction of rock porosity is the spread values between predicted rock porosity and measured porosity from RCAL.

A more detailed definition of the supervised machine learning model in this thesis can be suggested as follows: The task T is making a prediction of the rock porosity, the experience E can be expressed by the labeled input data of petrophysical logs, the performance measure P can be described by the spread value of fitness function and improved by feeding more samples of the input data from petrophysical logging records. Model fitting performance can be evaluated by introducing a fitness function, which is widely used to describe the model performance in pattern extraction and recognition. Overfitting and underfitting are two major issues that may occur when it comes to supervised machine learning (Müller, 2016).

Overfitting is described as the supervised model is particularly fitting to a set of data rather than capturing the pattern of the remaining training set and unable to be used for new data. On the contrary, underfitting is when a supervised model basically ends up failing to capture the patterns of most data within the training set. The graphic figure for illustrating overfitting and underfitting is showed in Figure 6.

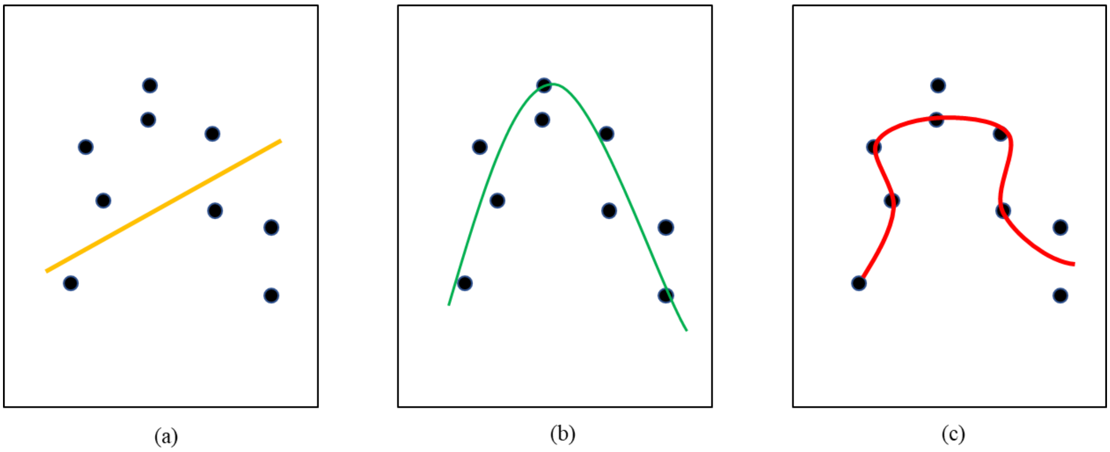

Figure 6 Graphic illustration of (a) underfitting , (b) good fitting, (c) overfitting.

In the supervised machine learning model, the plan is to establish a trained model to make a relatively accurate estimation on unknown data with the same label as the training dataset. If the estimation turns out to be accurate, then it is concluded that this model can generalize from the training dataset to test dataset and generation is used to describe the robustness of the supervised model.

Additionally, a sweet pot is represented as the best generalization performance. The relationship of overfitting and underfitting is further described in Figure 7. Generally, a model with less complexity is estimated to achieve low accuracy for the training dataset than a model with higher complexity, so this model is underfitted for the training dataset. With more features to be added or optimization of hyper-parameter, the accuracy and generalization of the model for the training dataset can be increased till the sweet spot is reached. Once the model complexity overpassed the sweet spot, the model generalization tends to decline despite that the model accuracy for the training dataset is still rising, where this model is overfitted for the training dataset and may not be generalized enough for other datasets.

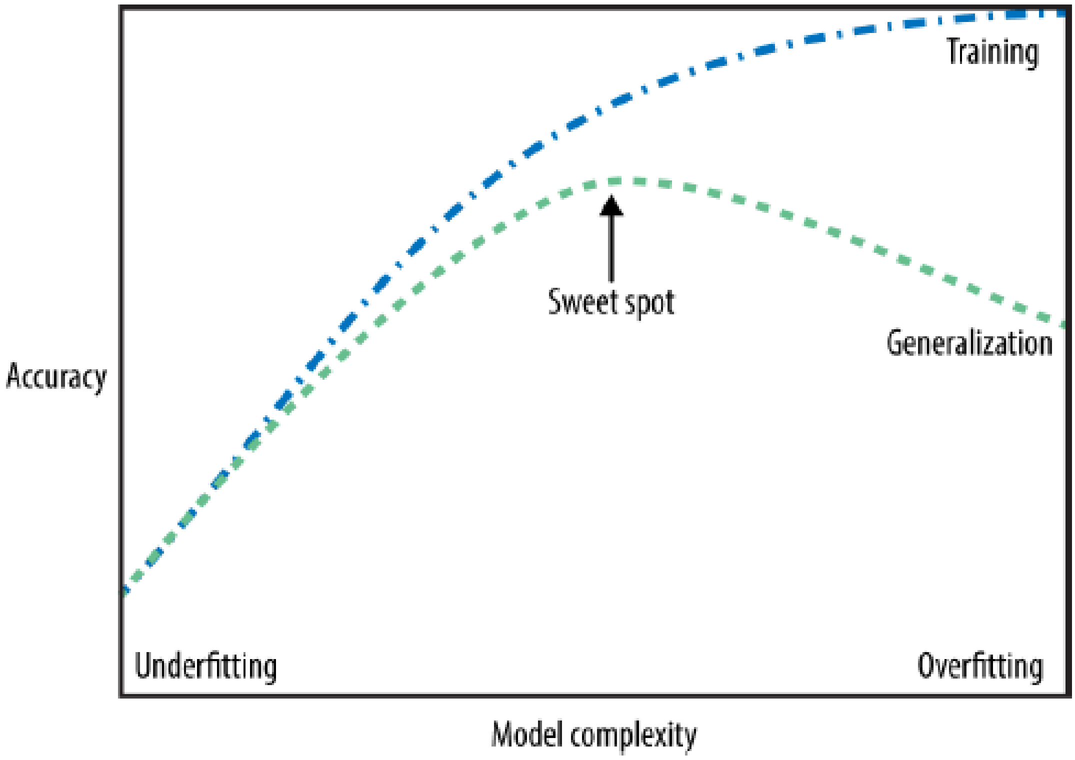

Figure 7 Trade-off of model complexity against training and test accuracy (Müller, 2016)

In order to avoid overfitted or underfitted model, data augmentation and hyper-parameter adjustment are the two frequently used ways in supervised machine learning. The purpose of data augmentation is to increase the dataset size and diversity for both training set and test set by collecting more data or revising the existing data as new samples. Data augmentation is deemed as a standard regularization method and label preserving transformation can be utilized to manually increase samples in the dataset (Yaeger et al., 1996).

In terms of hyper-parameter adjustment, hyper-parameters are referred to as model parameters in machine learning like input weighting, bias etc., and the machine learning performance is highly influenced by the hyper-parameter settings before training the model on the training set. It is essential to choose a proper number of hyper-parameters in machine learning because a small number of hyper-parameter may lead to the overfitted model whereas too many hyper-parameter can also cause the model training inefficient or time-consuming in actual practice.

Regularization is an effective method to prevent the machine learning model from overfitting as regularization penalties are always introduced to minimize the error by adding extra information. There are two major ways to add the regularization penalties into the machine learning model: L1 norm and L2 norm in Eq.(11)-(12):

$$L_1 = C_p \sum_{i=1}^{n} |y_i - f(x_i)| \tag{8}$$

$$L_2 = C_p \sum_{i=1}^{n} \big(y_i - f(x_i)\big)^2 \tag{9}$$

Support Vector Machines

Vapnik (1995) firstly proposed Support vector machines (SVMs) as one effective algorithm for model pattern recognition (Vapnik et al., 1995) and it is a fundamental method that the SVMs can solve nonlinear functions by leveling the data into a higher dimensional space and introducing an optimal hyperspace in the space through kernel functions. SVMs can be further divided into two categories: Support vector classification (SVC) and Support vector regression (SVR). SVR is developed on the basics of SVC with the same methodology. Therefore, some definition and properties of SVC are restated as follows:

State that we have a series of data samples (x_i,y_i), i=1,…,n where $x_i \in R^n$ and $y_i \in [-1,1]$ in a linear SVC problem. By solving the Quadratic Programming (QP) equation, an ideal hyperplane of classification can be found with the condition of given constraint function. The object function is written as a maximizing problem in Eq.(10):

$$\max \frac{1}{\|\omega\|} + C_p \sum_{i=1}^{L} \varepsilon_i \,, i = 1, \dots \ , L \tag{10}$$

Obviously, the maximizing problem can be transformed into the corresponding minimizing problem as follows:

$$\min \frac{1}{2} \|\omega\|^2 + C_p \sum_{i=1}^{L} \varepsilon_i \,, i = 1, \dots \ , L \tag{11}$$

Subject to:

$$y_i(\omega^T x_i + b) \geq 1 - \varepsilon_i, \varepsilon_i \geq 0, i = 1, \dots, L \tag{12}$$

Penalty parameter C_p and slack parameter ε are introduced to avoid outliers and misclassification of the dataset. Date points from the original dataset that are significantly different from other observations, which can be called as outliers. Outliers can have great impact on the application of SVC when limited data points in the dataset can be fed as training set. As Figure 8 shows, the existence of an outliner leads to a different hyperplane A that is far away from other observation with a smaller margin. However, if the outlier can be identified or eliminated, Hyperplane B can be represented to have a better classification performance.

Then an ideal hyperplane can be illustrated with known values of ω and b as it can be defined as Eq.(13).

$$\omega^T x + b = 0 \tag{13}$$

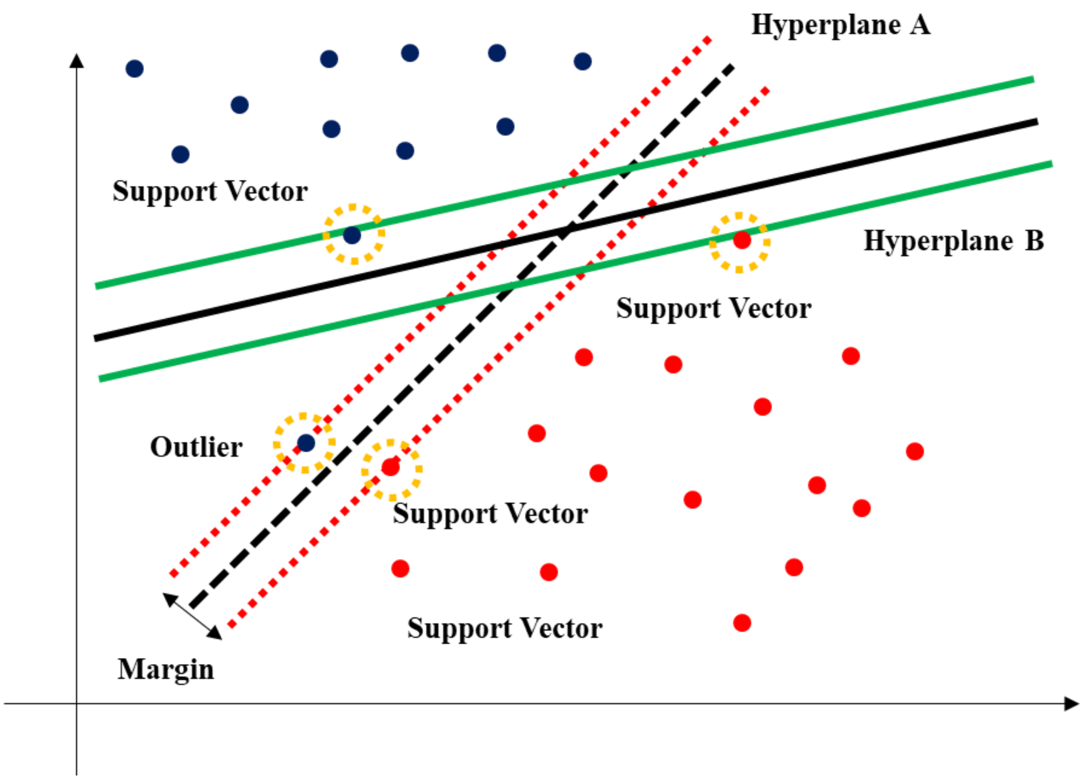

Figure 8 Graphic illustration of SVM hyperplane separation with outlier

As this problem is a typical minimization dual problem with specific constraints, then the Wolfe dual problem equation can be introduced to write the objective function as:

$$\min_{\alpha} \frac{1}{2} \sum_{i=1}^{L} \sum_{i=1}^{L} y_i y_j (x_i, x_j) \alpha_i \alpha_j - \sum_{j=1}^{L} \alpha_j \tag{14}$$

Here, α_j is the Lagrangian multipliers and this equation is subjected to:

$$\sum_{i=1}^{L} \alpha_i y_i = 0\,,0 \leq \alpha_i \leq C, i = 1, \dots, L \tag{15}$$

Then, the ideal separating hyperplane can be illustrated by computed ω and b with Eqs. (14) – (15) and a clear hyperplane drawing can be used to separate the dataset points into two categories with a given maximum margin as Figure 15 illustrates.

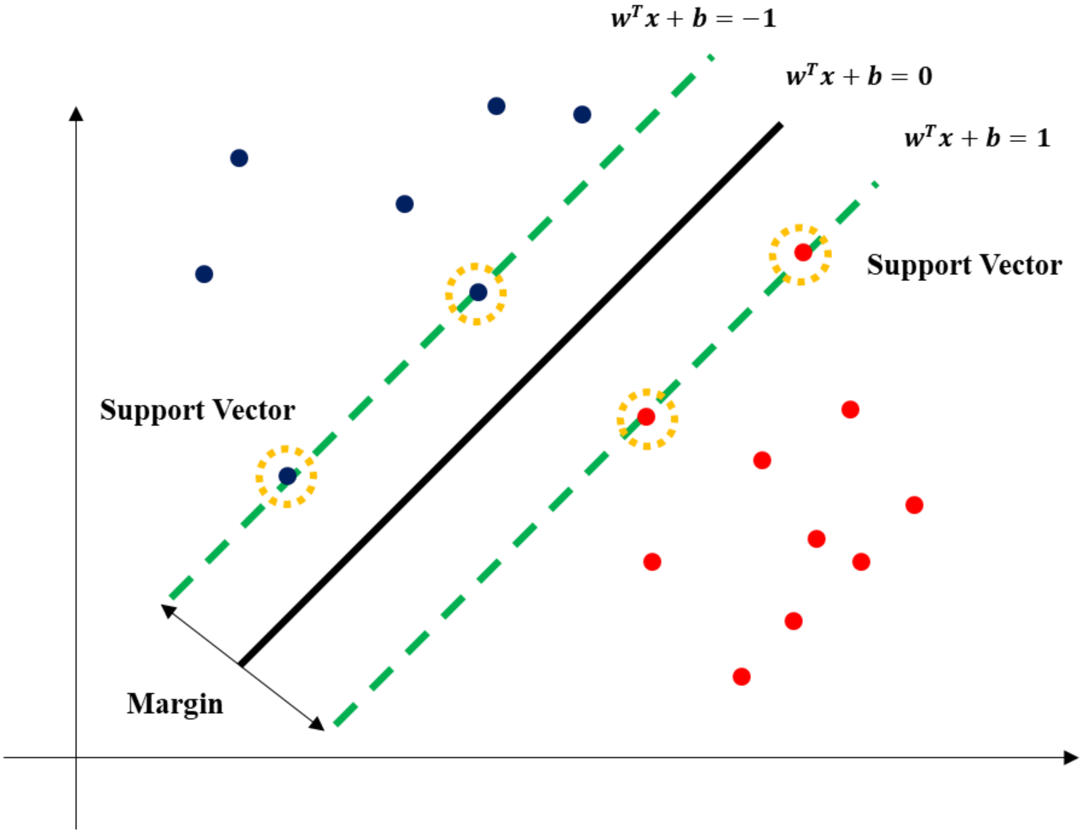

Figure 9 Graphic illustration of SVM with hyperplane separation

$$\omega = \sum_{i=1}^{L} \alpha' x_i y_i \tag{16}$$

$$b = \frac{1}{N_{SVM}} \left(y_j - \sum_{i=1}^{N_{SVM}} \alpha' K(x_i, y_i) \right) \tag{17}$$

The SVR algorithm was further developed in application of conducting regression analysis and solving time series prediction problems (Müller et al. 1997). The detailed theory basics and concepts are reviewed as follows:

Compared with the parameters and principle of SVC, SVR is aimed at solving the convex optimization problem under constraints, another loss function and two different slack variables μ_i, μ^* are introduced to balance the infeasible constraints in the optimization problem (Bennett and Mangasarian, 1992). Thus, the objective function of the optimization problem can be expressed by Eq.(18) and $\langle ., . \rangle$ represents the dot product.

$$\min \frac{1}{2}\|\omega\|^2 + C_p \sum_{i=1}^{L}(\mu_i + \mu_i^*) \tag{18}$$

Subject to:

$$y_i - \langle \omega, x_i \rangle - b \leq \varepsilon + \mu_i \ (i = 1,2, \ldots, L) \tag{19}$$

$$\langle \omega, x_i \rangle + b - y_i \leq \varepsilon + \mu_i^* \ (i = 1,2, \ldots, L) \tag{20}$$

$$\mu_i \geq 0 \tag{21}$$

$$\mu_i^* \geq 0 \tag{22}$$

Then, the loss function can be rewritten as equation as below and a graphic illustration is described as Figure 10 shows.

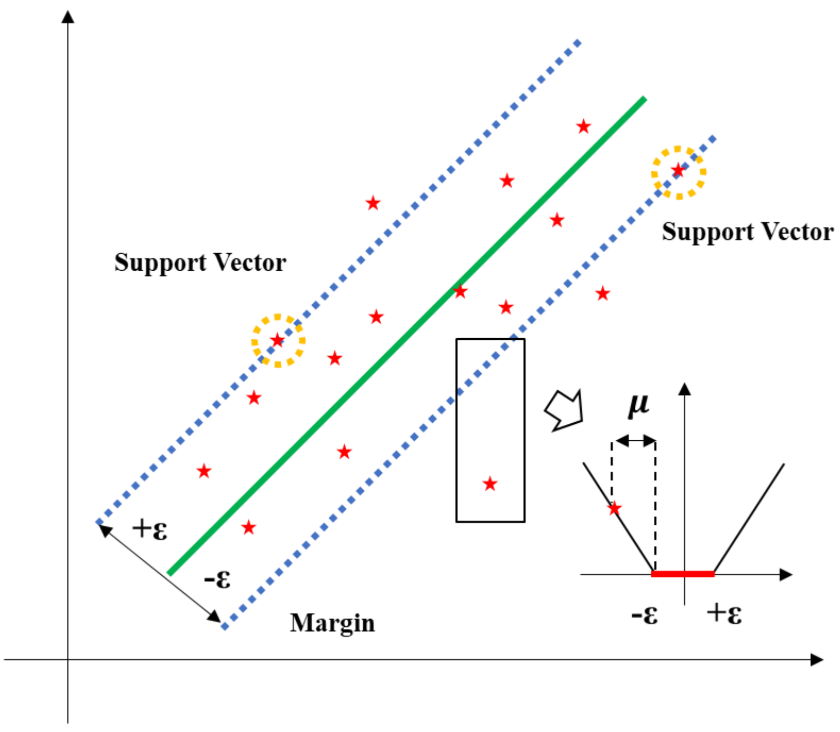

Figure 10 Graphic illustration of SVR algorithm

$$|\mu|_{\varepsilon} = \begin{cases} 0 & if\ |\mu| \leq \varepsilon \\ |\mu| - \varepsilon & others \end{cases} \tag{23}$$

Furthermore, Lagrange multiplier is used in the objective function and then it proceeds as below:

$$L' = \frac{1}{2}\|\omega\|^2 + C\sum_{i=1}^{L}(\mu_i + \mu_i^*) + \sum_{i=1}^{L}(\tau_i\,\mu_i + \tau_i^*\mu_i^*)$$

$$-\sum_{i=1}^{L}\alpha_i(\varepsilon + \mu_i - y_i + \langle\omega, x_i\rangle + b)$$

$$-\sum_{i=1}^{L}\alpha_i^*(\varepsilon + \mu_i^* + y_i - \langle\omega, x_i\rangle - b) \tag{24}$$

Here, then take the partial derivatives of Eq.(24):

$$\frac{\partial L}{\partial b} = \sum_{i=1}^{L}(\alpha_i + \alpha_i^*) \tag{25}$$

$$\frac{\partial L}{\partial \omega} = \omega - \sum_{i=1}^{L}(\alpha_i + \alpha_i^*)x_i \tag{26}$$

$$\frac{\partial L}{\partial \mu_i^*} = C - \alpha_i^* - \tau_i^*(i = 1,2 \dots L) \tag{27}$$

Then, substitute Eqs.(25)-(27) into the objective function and constraints and eliminate the dual variables τ_i, τ_i^*:

$$\max\left(-\frac{1}{2}\sum_{i,j=1}^{L}(\alpha_i + \alpha_i^*)(\alpha_j + \alpha_j^*)\langle x_i, x_j\rangle\right) \tag{28}$$

$$\max\left(-\varepsilon\sum_{i=1}^{L}(\alpha_i + \alpha_i^*) + \sum_{i=1}^{L}y_i(\alpha_i + \alpha_i^*)\right) \tag{29}$$

Subject to:

$$\sum_{i=1}^{L}(\alpha_i + \alpha_i^*) = 0 \tag{30}$$

$$0 \leq \alpha_i \leq C_p \tag{31}$$

$$0 \leq \alpha_i^* \leq C_p \tag{32}$$

Eventually, the objective function can be expressed as Eq.(34):

$$\omega = \sum_{i=1}^{L} (\alpha_i - \alpha_i^*)\, x_i \tag{33}$$

$$f(x) = \sum_{i=1}^{L} (\alpha_i - \alpha_i^*)\, \langle x_i, x_j \rangle + b \tag{34}$$

To conclude, SVM is a useful tool to solve linear and non-linear classification or regression problems as nonlinearity in the dataset can be solved by introducing kernel methods to be further linearly in a higher dimensional space, which provides the mathematic theory basics and parameters for LSSVR.

K-Nearest Neighbors

K-Nearest Neighbors (KNN) algorithm is a widely applied algorithm for solving regression and classification problems in data mining and machine learning. KNN algorithm normally means that the pattern of each sample in the dataset can be illustrated or represented by the data values of k nearest neighbors.

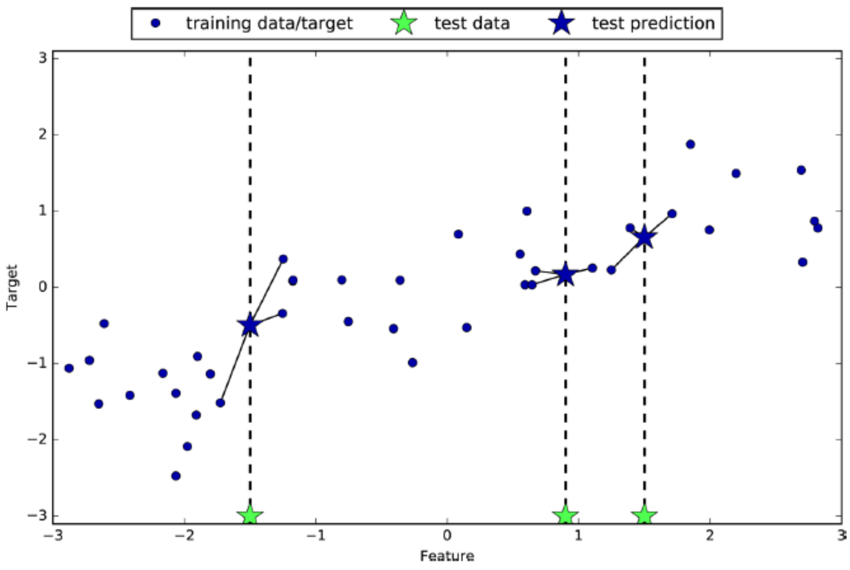

Figure 11 Predictions made by three-nearest-neighbors regression on the wave dataset (Müller, 2016)

The primary concept of the KNN algorithm is that a certain sample is assumed in the feature space having the same pattern or characteristics as the k nearest neighbor samples. If the k nearest neighbors also share the same patter or characteristics, then it can be concluded that this sample belongs to the category as what k nearest neighbor samples belong to as Figure 11 shows. Distance calculation and number of neighbors are the two primary factors in applying KNN algorithm, the advantages of using KNN algorithm can be seen in two ways:

(1) The KNN algorithm itself is intelligible and easy to apply in practice;
(2) No specific parameter adjustment is required other than choosing numbers of neighbors (normally the selection of a number is between 6 and 10) and distance between data points (Müller, 2016).

The KNN algorithm may be optimal to be used in the dataset with many features as the speed of calculation can be slow as a result of heavy computing load.

Particle Swarm Optimization

The PSO algorithm is described on a number of individual particles with an original population size of 20-50. Each particle is defined by three major parameters: the current position P_{curr_i}, the velocity u_i and the previous best individual position $Pbest_i$. The term swarm describes all the searching particles. The objective of PSO algorithm is to optimize the model parameters and increase model performance. A fitness function is evaluated and computed for individual particle with their current location.

By comparing its previous location P_{old_i}, the present location and best location within the particles group, each particle can determine its action with iteration algorithm. Ultimately, a best fitness function would be found on the conditions that an acceptable good fitness result is obtained or a maximum iteration number is met. The whole process to find the optimal objective function is like the foraging behavior of birds.

In this method, coordinates are used to describe the current position P_{curr_i} of the particle as a point in the space. The present particle position is treated as a problem solution during the iteration process. If the position is better than any that had been discovered so far, it would be assigned to a new vector p_i and the best function result will be stored in a variable that is called P_{best_i} among all the iterations. By continuous updating the values of better position p_i and best position P_{best_i}, the new position value will be updated by adding the velocity u_i to x_i by Eqs.(35)-(36) (Poli et al., 2007).

$$u_{i_{new}} = \omega_{in} u_{i_{old}} + cc_1 \times rand(\quad) \times (P_{best_i} - x_i) + cc_2 \times rand(\quad) \times (G_{best_i} - x_i) \quad (35)$$

$$P_{i_{new}} = P_{i_{old}} + u_{i_{new}} \quad (36)$$

By introducing ω_{in} as inertia weight, the scope of researching ability of particles can be managed to obtain the balance of global searching and individual optimization with smaller steps and larger steps respectively. With a relatively large value of ω, the particles may be intended to focus more on global searching rather than individual optimization and the particles can be stuck into local optimum with a relatively small value of ω. In terms of dealing with particles that are falling out of the search scope, another study had proved that those particles can be handled by giving a new random location within the designed search scope (Bemani et al., 2020) and they can be computed with the Eq.(37):

$$P_{ji_{new}} = (P_{j,max} - P_{j,min}) \times rand(\quad) + P_{j,min} \quad (37)$$

Here, P_{max}, P_{min} are referred to the vectors with maximum and minimum values among the whole particles within the given searching area. A more detailed flow chart for a general PSO algorithm is showed in Figure 12.

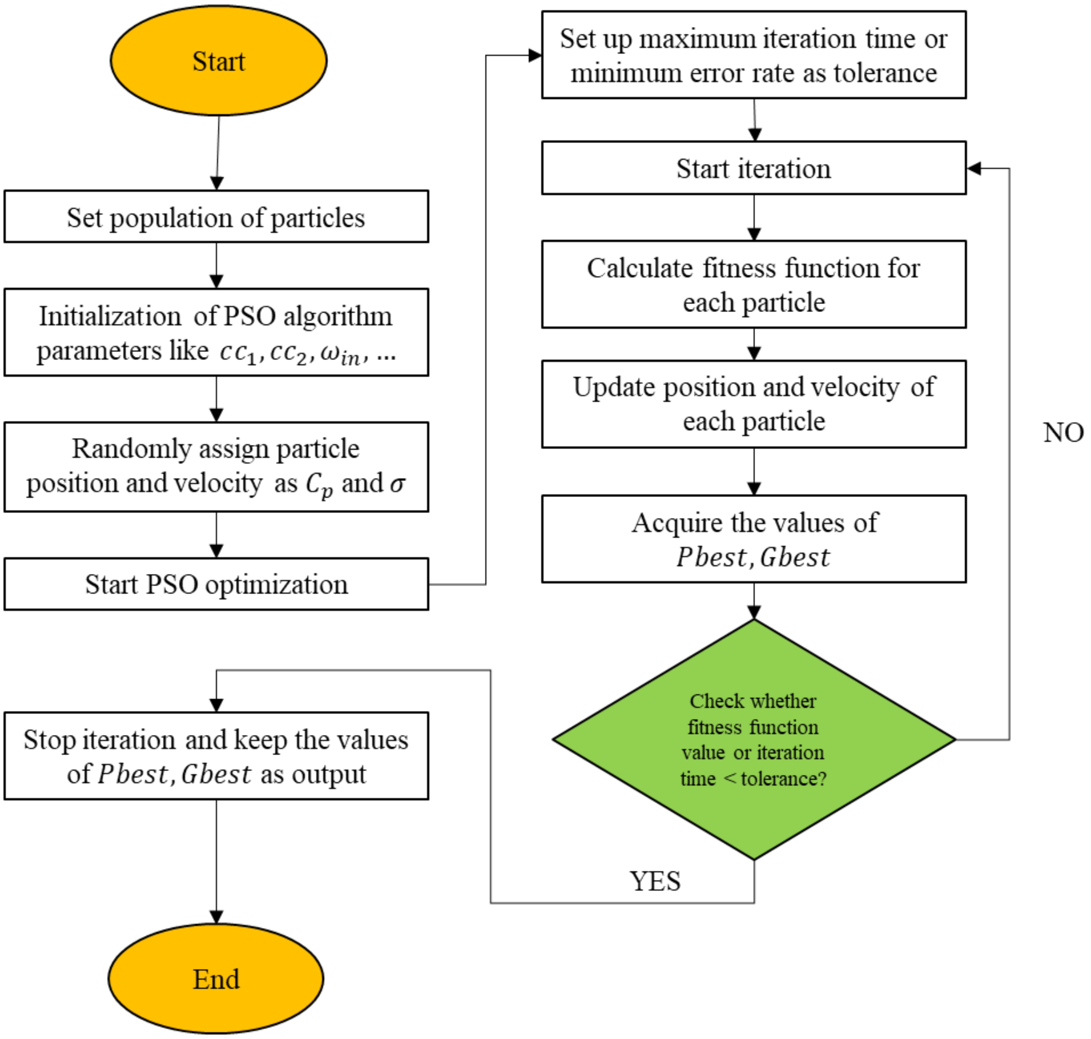

Figure 12 Graphic illustration of PSO algorithm

3.2 Description of Optimization techniques for SVMs

Regularization parameter and penalty parameter are introduced in the SVM that are required to be optimized due to the variance of input database. The performance of SVMs can be decided by data size, model running time, accuracy of setting parameters and memory ability of constraints (Shawe et al., 2011). Therefore, a proper selection of optimization methods can be utilized to improve the SVMs performance in classification and regression problems.

Over the past decades, there are some literatures for optimization methods in SVMs such as Interior Point Algorithm, Chunking and Sequential minimal optimization

(SMO), Coordinate descent etc. (Shawe et al., 2011). Some basics and concepts about these optimization methods are reviewed and summarized as follows:

Interior point algorithm

Interior point algorithm is designed to solve linear and non-linear convex optimization problems and it was firstly proposed in the 1950s and widely studied and discussed during 1960s (Fiacco & McCormick, 1990). Once a method for solving linear programming based on a new polynomial-time algorithm was proposed (Karmarkar, 1984), the usages of interior point algorithm became a great option for investigating convex optimization and programming problems. Another advantage of interior point algorithm is that it shows high reliability and competence when dealing with small or moderate datasets containing less 5000 examples, so interior point algorithm may not be an ideal option for large dataset due to the notably expensive cost for computing large scale data (Shawe et al., 2011). A possible solution for applying interior point algorithm in large scale dataset was suggested (Schölkopf & Smola, 2002) and their study indicates that a satisfying reverse matrix can be computed by applying a hybrid methodology of interior point algorithm and sparse greedy matrix estimation.

Chunking and Sequential Minimal Optimization

Chunking algorithm is described as a method that a sequence is divided into several blocks to maintain the information. In order to guarantee a certain time complexity, normally an array of n elements is divided into $\sqrt{n}$ subsets, and each subset also has $\sqrt{n}$ elements. Therefore, the complexity of the general subset algorithm is combined with a root sign and each subset is set by the solutions from the previous subset. An improved decomposition algorithm to solve quadratic programming(QP) problem by dividing the large quadratic programming problems into subproblems was presented (Osuna et al., 1997), the contribution of Osuna's work shows that quadratic programming problems can be subdivided into subsets to gain a better convergence result without making assumption of the support vector numbers. As for Sequential minimal optimization (SMO), it was firstly described by Platt (Platt, 1998) and it is a well-developed algorithm solving QP issues by computing two examples with analytical solutions, which is significantly more efficient than solving QP problem with numerical solutions.

(Vapnik, 1982). Nevertheless, the process of running SMO for convergence with high accurate solution requirement can be slow (Platt, 1998).

Coordinate descent

Coordinate descent is described as a simple and efficient non-gradient optimization algorithm in solving optimization problems. Compared with the gradient optimization algorithm that searches the minimum value of the function along the direction of the steepest gradient descent, the coordinate descent algorithm sequentially minimizes the objective function value along the coordinate axis. a dual coordinate descent method for large scale linear SVM was conducted (Hsieh et al., 2008) and the primary methodology of coordinate descent is to solve a series of simple optimization problems rather than computing a complex optimization problem.

3.3 Application of Machine Learning in Petroleum Industry

Recently, the evolution and application of artificial intelligence (AI) has enabled an optional way to obtain accurate prediction result by utilizing different machine learning methods. Four primary Machine learning methods are now being widely used in petroleum industry: Evolutionary Algorithms (EA), Swarm Intelligence (SI), Fuzzy Logic (FL) and Artificial Neural Networks (ANN) (Donaselaar et al.,2005; Kadkhodaie et al., 2017; Onalo et al., 2018).

For lithofacies classification, Dell'Aversana (2019) compared six different machine learning methods and Random Forest and Adaptive Boosting were regarded slightly more reliable than Naïve Bayes, Decision Tree and CN2 Rule Induction in lithofacies classification problems, SVM has a good classification performance. Another study further investigated the application of SVM in lithology classification and it is noted that SVM performs poor classification result in crystalline rocks when the training samples are imbalanced (Deng et al., 2017). Another case study for the Appalachian basin in the USA indicated that accurate prediction of facies and fractures in sedimentary rocks can be performed by using Bayesian Network and Random Forest methods based on petrophysical logs (Bhattacharya & Mishra, 2018).

Some researchers have successfully initialized the application of artificial intelligence for petrophysical analysis, petroleum exploration and field production. An automatic identification approach by using support vector machine for depositional microfacies based on well logs is possible (Dahai et al, 2019) and it can be limited by applying it to tight sandstone gas reservoirs. The ANN method is applied to predict compressional wave transit time and shear wave transit time with real gamma ray and formation density log (Dang et al., 2017) and it is also applicable to the correction and supplementing of well log curves (Salmachi et al., 2013). Also, some studies are more focused on the estimation of rock properties by machine learning approaches. A combination method, ADA-SVR, is proposed to predict rock porosity with good robustness performance (Li, et al., 2019). A case study in the South Pars gas field utilizes a hybrid algorithm of ANN and imperialist competitive algorithm has successfully made an estimation of porosity and permeability (Jamshidian et al., 2015).

In other areas of petroleum industry, proficient prediction of water versus gas ratio, cycle time and injection rates can be obtained by evolutionary algorithm in Chen et al. (2010). In the work of Salmachi et al. (2013), a reservoir simulator with optimization method and economic objective function is developed to find the optimal locations of infill wells for coal bed methane reservoirs. In the Norne field in the Norwegian Sea, hydrocarbon WAG performance evaluation can be performed by using hybrid GA-PSO machine learning methods to enhance oil recovery (Mohagheghian 2016). Fuzzy logic is an intelligent tool in evaluating the uncertainties by implementing fuzzy variables. Zhou (2016) proposed an estimated model for corrosion failure likelihood of oil and gas pipeline based on the fuzzy local approach. Shahabi (2016) established the selection of water reservoirs in Malyasia by fuzzy logic methods.

4 Methodology

4.1 LSSVR-PSO Algorithm

LSSVR is an advanced regression analysis technique, which is improved based on SVMs (Suykens,1999). Comparing with the SVMs technique, LSSVR approaches a new optimization problem by reforming the inequality constrains in SVM into equality constraints and introducing Lagrangian multipliers and RBF kernel functions.

Here, the difference between LSSVR algorithm and SVR algorithm is that LSSVR algorithm is established to gain a satisfying regression model by only solving equations under linear constraints rather than solving quadratic programing equations under non-linear constraints in SVR.

$$\min J(\omega, \varepsilon) = \frac{1}{2}|\omega|^2 + \frac{1}{2}C_p \sum_{i=1}^{n} \varepsilon^2 \tag{38}$$

Subject to:

$$y_i[\omega' \phi(x_i) + b] = 1 - \varepsilon_i, i = 1,2, \ldots, n \tag{39}$$

Where, C_p is introduced as penalty parameter to balance the trade-off between the flatness of the function and the amount up to which deviations larger than ε are tolerated. Then, introducing the Lagrangian multipliers:

$$L = J - \sum_{i=1}^{n} \alpha_i [y_i(\omega^T g(x_i) + b) + \varepsilon_i - 1], i = 1,2, \ldots, n \tag{40}$$

The partial derivatives of Eq.(40):

$$\frac{\partial L}{\partial \omega} = 0 \ \rightarrow \omega = \sum_{i=1}^{n} \alpha_i y_i \phi(x_i) \tag{41}$$

$$\frac{\partial L}{\partial \varepsilon_i} = 0 \ \rightarrow \ \varepsilon_i = \frac{\alpha_i}{C_p} \tag{42}$$

$$\frac{\partial L}{\partial b} = 0 \rightarrow \sum_{i=1}^{n} \alpha_i y_i = 0 \tag{43}$$

$$\frac{\partial L}{\partial \alpha_i} = 0 \rightarrow \sum_{i=1}^{n} y_i[\omega' \phi(x_i) + b] + \varepsilon_i - 1 = 0 \tag{44}$$

By substituting ω and ε_i, Eq.(40) could be simplified as follow:

$$\begin{bmatrix} 0 & {I_\alpha}^T \\ I_\alpha & \tau + C_p^{-1} I \end{bmatrix} \begin{bmatrix} b \\ \alpha \end{bmatrix} = \begin{bmatrix} 0 \\ Y \end{bmatrix} \tag{45}$$

Where:

$$Y = [y_1 \phi(x_1), y_2 \phi(x_2), \dots, y_n \phi(x_n)] \tag{46}$$

$$I_\alpha = [1,1, \dots, 1]^T \tag{47}$$

$$\alpha = [\alpha_1, \alpha_2, \dots, \alpha_n]^T \tag{48}$$

$$\tau = \left[y_i y_i \phi(x_i)' \phi(x_j)\right]_{n \times n} \tag{49}$$

Therefore, the objective function is written as:

$$y(x) = \sum_{i=1}^{n} a_j y_j K(x, x_i) + b \tag{50}$$

For nonlinear dataset, normally it could be tough to directly find the appropriate mapping for computation. Thus, the introduction of a kernel function in LSSVR is to map the input dataset into a higher dimensional space where the computed results are displayed. Depending on the dataset, there are several types of kernel functions to be applied like linear, polynomial and radial basis function (RBF) as Table 4 shows.

Table 4 Kernel function Categories

Kernel Type	**Kernel Expression**
Linear	$K(x, x_i) = x \cdot x_i$
Polynomial	$K(x, x_i) = (x \cdot x_i + 1)^m$
Gaussian RBF	$K(x, x_i) = \exp\left(-\frac{\|x - x_i\|^2}{2\sigma^2}\right)$

Among all the kernel functions, RBF is proved to have excellent generalization performance and low computational cost in nonlinear regression problem (Suykens et al., 1999). In this case, RBF kernel function is applied due to the complicated and nonlinear dataset obtained by well logging. Once the vector values of α and b are solved, the estimate result $y(x)$ could be expressed with new dataset with known α and b by using Eq.(51):

$$y(x) = \sum_{i=1}^{n} \alpha_i K(x, x_i) + b \tag{51}$$

Here, x_{new} and x_i are vectors of size m (m is the number of parameters)

$$x_{new} = \begin{bmatrix} x_1 \\ \vdots \\ x_m \end{bmatrix}, x_i = \begin{bmatrix} x_{1,i} \\ \vdots \\ x_{m,i} \end{bmatrix}, \|x - x_i\|^2 = \sum_{q=1}^{m} \left(x_q - x_{q,m}\right)^2 \tag{52}$$

$$y(x) = \sum_{i=1}^{n} \alpha_i \exp\left(\frac{\sum_{q=1}^{m}\left(x_q - x_{q,m}\right)^2}{2\sigma^2}\right) + b \tag{53}$$

Furthermore, an appropriate setting of kernel parameter σ and regularization parameter C_p would lead to a better outcome of generalization performance. With the purpose of a better prediction outcome, optimization techniques are chosen to optimize these parameters.

4.2 LSSVR-PSO Model Design

The LSSVR-PSO model is established by utilizing Python and this model is programmed and trained to search for the prediction value of porosity with well logging dataset from the Varg field. Therefore, Figure 13 illustrates the flow chart of applying the LSSVR-PSO model and the specific procedure of model implement using LSSVR and PSO algorithm are as follows:

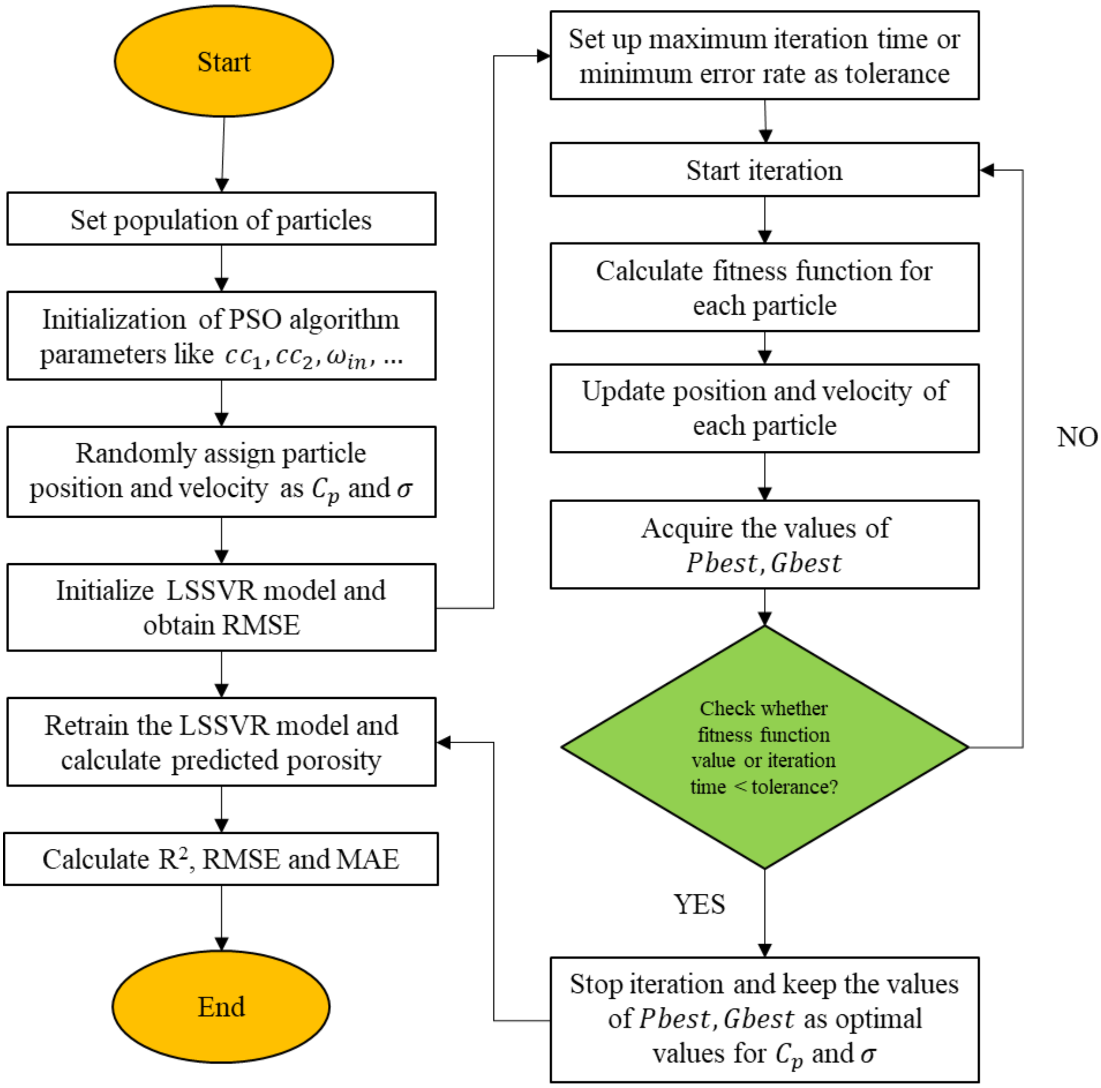

Figure 13 Flow chart of LSSVR-PSO model

(1) Load pre-proceed well logging dataset.

(2) Initialize PSO and create random kernel parameter σ and regularization parameter C_p.

(3) With the initial values of σ and C_p, proceed the LSSVR model and calculate the RMSE for the training data and make RMSE as validate error.

(4) The validate error is set as fitness value. P_{best} and G_{best} in PSO will be update based on the fitness value, then use equation in PSO to update particle position and velocity to get the new values of σ and C_p of LSSVR.

(5) Once the maximum iteration number is satisfied, the optimal values of σ and C_p are obtained.

(6) Retrain the LSSVR with the optimal σ and C_p, then establish LSSVR-PSO model.

(7) With the established LSSVR-PSO model, run the test dataset and evaluate the model performance.

4.3 Data Preparation

The accuracy, performance and quality of any suggested model can be highly affected by the consistency of the original dataset and appropriate model parameter settings. Thus, data pre-processing and outlier handling can be necessary and essential to make the dataset become representative. a total of series of 1260 data samples from four wells in Varg Field (well 15/12-5, well 15/12-6S, well 15/12-9S, well 15/12-20S) have been collected to form the comprehensive database.

All the data points employed in this thesis contain actual well logging recordings or RCAL data for Sonic Transit Time (DT), Caliper (CA), Gamma Ray (GR), Deep Resistivity (DR), Bulk Density (RHOB), Compensated Neutron Log (CNC), and Total Porosity (POR).

It is necessary to outline the statistical index of all the data points fed to the LSSVR-PSO model. In order to fit and tune the parameters in machine learning model, the database can be randomly divided into training dataset and validation dataset with given percentage. All the datapoints from well 15/12-5, well 15/12-6S, well 15/12-9S are divided randomly into two groups respectively as training dataset and validation dataset by a total series of 1100 data points with the percentage of 80% and 20% respectively. It is worthy to set another 160 sets of data samples from well 15/12-20S were chosen as blind well for pure prediction.

In the practice of data pre-processing, the prediction accuracy can be enhanced by scaling the novel data with mathematic approaches, which would eliminate the unbalance between great numerical ranges and smaller numerical ranges or other implicit numerical issues (Liu et al., 2018). Some studies suggest that it is applicable for SVMs to normalize the dataset into the different range [0.1,0.9] or [0.15, 0.85] (Kalanaki et al., 2013; Liu et al., 2018) to have a better performance.

Therefore, each of the dataset is scaled and two scaling methods are employed in this thesis. The first way is to scale the datapoint into the range of [-1,1] with the following steps: Calculate the maximum value (MaxVal) and minimum value (MinVal) of the parameters on the complete training dataset and compute the middle point value (MidVal) and scale with equations. Then, calculate the scaled value (ScalVal) and this method scales all the parameters into [-1,1] with Eqs.(54)-(56):

$$MidVal = \frac{MaxVal + MinVal}{2} \tag{54}$$

$$Scale = \frac{MaxVal - MinVal}{2} \tag{55}$$

$$ScalVal = \frac{y_i - MidVal}{Scale} \tag{56}$$

The other way of scaling method is to apply logarithmic transformation on data points related with resistivity logs, which includes significant difference in magnitudes. Logarithmic transformation is utilized in basic research studies to enable the normal distribution of the data points and eliminate or reduce the skewness.

Outlier handling normally contains outlier identification and outlier modification to maintain the data features especially when it comes to the small-scale database. In terms of outlier identification, Tukey's test is introduced where the outlier identification is explained (Tukey, 1949) and the main idea of Tukey's test is to identify a specific range where the upper and lower bounds are defined in Eq.(57)-(58):

$$R_{Lower} = Q_1 - 1.5(Q_3 - Q_1) \tag{57}$$

$$R_{Upper} = Q_3 + 1.5(Q_3 - Q_1) \tag{58}$$

A data sample that is out of the range of $[R_{Lower}, R_{Upper}]$ can be dimed as an outlier. When the outliers in data sets are clarified and the number of outliers is notable compared with the scale of the datasets, three common ways of outlier modification are:

(1) Delete the outlier data samples;

(2) Replace the outlier data samples with average value;

(3) Substitute the outlier data samples with the average value of the data points before and after the outliers.

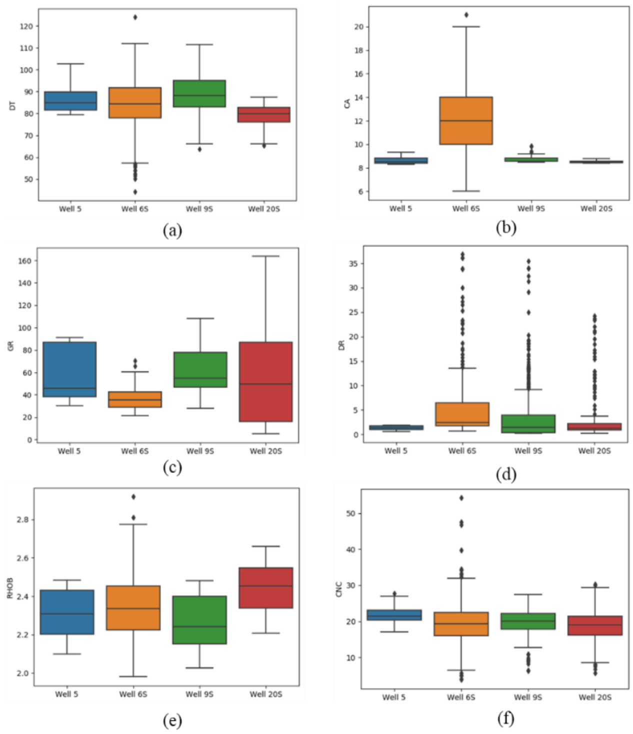

Figure 14 Data statistical analysis: (a) DT (b) CA (c) GR (d) DR (e) RHOB (f) CNC logs

The statistical distribution analysis for each log is conducted as Figure 14 shows, outliers in each log are marked as black and few outliers appear in DT, CA, GR, RHOB logs and these data points may not have a significant influence on the model performance, thus all the data samples in those four logs are included. A larger number of outliers is filtered out in DR and CNC logs, but outliers in DR and CNC logs are caused by the detection of hydrocarbon components during the well logging, therefore the outliers in DR and CNC shall be kept and no modification is needed.

Additionally, it is beneficial to have a glimpse of the data distribution of all the related datasets, Table 5-7 display the statistical indexes of the database used in this thesis and machine learning models.

Table 5 Statistical index of all petrophysical logging data in this thesis

Parameter	Min	Max	Average	P10	P90
DT ($\mu s/f$)	44.08	124.06	83.75	70.09	98.36
CA (inch)	6.00	21.00	12.20	9.00	15.50
GR (API)	21.45	70.27	37.38	25.89	51.37
DR (OHMM)	0.69	36.82	4.465	0.96	10.53
RHOB (gm/cc)	1.98	2.92	2.36	2.14	2.55
CNC (%)	3.81	54.27	20.12	15.89	24.78
POR	0.02	0.38	0.17	0.08	0.29

Table 6 Statistical index of petrophysical logging data used for training and validation

Parameter	Min	Max	Average	P10	P90
DT ($\mu s/f$)	44.08	124.06	87.15	77.97	98.80
CA (inch)	6.00	21.00	9.75	8.46	13.00
GR (API)	21.45	108.29	53.23	30.19	86.17
DR (OHMM)	0.19	36.82	3.74	0.31	9.88
RHOB (gm/cc)	1.98	2.92	2.29	2.13	2.46
CNC (%)	3.81	54.27	20.12	15.90	24.78
POR	0.02	0.38	0.20	0.10	0.31

Table 7 Statistical index of all petrophysical logging data used for blind well prediction

Parameter	Min	Max	Average	P10	P90
DT ($\mu s/f$)	65.46	87.42	78.94	70.22	85.34
CA (inch)	8.40	8.80	8.51	8.42	8.64
GR (API)	5.15	163.59	53.54	9.85	97.37
DR (OHMM)	0.26	24.21	3.60	0.54	12.15
RHOB (gm/cc)	2.21	2.66	2.44	2.28	2.59
CNC (%)	5.73	30.34	18.92	13.38	25.53
POR	0.03	0.24	0.14	0.07	0.21

4.4 Feature Selection

Feature selection is described as a primary process in machine learning and its primary purpose is to select input features for the machine learning model based on the relevance between features and model output. A good feature selection can increase the model performance with lower error rate, and it can also enhance the model generalization and avoid overfitting problem at the same time. Pearson correlation and distance correlation are two frequently used methods in feature selection, so some concepts of those two methods are illustrated in the following content.

4.4.1 Pearson Correlation

In terms of Pearson correlation, p_j represents a value in the range of +1 and -1 considering with the given dataset $\{(x_1, y_1), \ldots, (x_n, y_n))\}$ by using Eq. (59) and it can reveal the correlations between x and y, where +1 refers to total positive correlation and -1 refers to total negative correlation. Therefore, the absolute value of correlation coefficient is closer to 1, it indicates higher correlation relationship between variables. For Pearson Correlation, the correlation relationship is measured by the absolute values of p_j , which means a higher absolute value suggests higher correlation between the dependent variable y and x. The different sign of p_j shows that whether the dependent variable y would follow the changes of the increase or decrease of x. Table 8 lists out the interpretation of Pearson correlation coefficient value.

$$p_j = \frac{\sum_{i=1}^{n}(x_{j,i} - \bar{x}_j)(y_i - \bar{y})}{\sqrt{\sum_{i=1}^{n}(x_{j,i} - \bar{x}_j)^2 \sum_{i=1}^{n}(y_i - \bar{y})^2}} \,, j = 1, \ldots n \tag{59}$$

Table 8 Interpretation of Correlation coefficient values

Correlation coefficient value	Interpretation
±1	Perfect positive/negative relationship
±0.8	Fairly strong positive/negative relationship
±0.6	Moderate strong positive/negative relationship
0	No relationship

4.4.2 Distance Correlation

Székely et al., (2007) proposed Distance Correlation as a new approach to evaluate the all categories of dependence between random vectors. The definition and properties of Distance Correlation are reviewed as follows:

Distance Correlation (Dcorr) is defined to evaluate the correlation between two random vectors P and Q:

(1) Dcorr (P, Q) is characterized for P and Q with arbitrary dimensions, P and Q are not compulsorily required to be in the same dimensions.
(2) P and Q are identified as independent only when Dcorr (P, Q) = 0.
(3) Dcorr (P, Q) ∈ [0,1].

Meanwhile, Distance covariance (Dcov) is defined as a calculation distance between the joint characteristic equation $\phi_{P,Q}$ of P and Q. the marginal characteristic equations of P and Q are introduced as the product metrics $\phi_P \phi_Q$ (Székely et al., 2007)

$$Dcov^2(P,Q) = \left\| \phi_{P,Q}(t,s) - \phi_P(t)\phi_Q(s) \right\|_{\omega}^2$$

$$= \int_{R^{X+Y}} \left|\phi_{P,Q}(t,s) - \phi_P(t)\phi_Q(s)\right|^2 \omega(t,s)dtds \tag{60}$$

A detailed study provides the detailed proof steps of Lemma 1 (Székely & Rizzo, 2005) and the simplified form of Lemma 1 is described as follows:

$$\omega(t,s) = (c_X c_Y |t|_X^{1+X} |s|_Y^{1+Y})^{-1} \tag{61}$$

$$c_d = \frac{\pi^{\frac{1+d}{2}}}{\Gamma\left(\frac{1+d}{2}\right)} \tag{62}$$

Combine Eqs.(61)-(62), then the standardized form of Distance correlation is expressed as Eq.(63):

$$Dcorr(P,Q) = \frac{Dcov^2(P,Q)}{\sqrt{Dcov^2(P,Q)}} \tag{63}$$

For Distance Correlation, the distance correlation is evaluated by the absolute values of D_{corr} , which indicates that a higher absolute value means higher correlation relationship between the dependent variable P and Q.

4.5 Porosity Estimation by well logs

In this thesis, the neutron log, the sonic log and the density log are the three main logs employed to make a prediction of porosity based on the calibrated model with true porosity. Therefore, some prerequisites and assumptions are made in the employment of conventional approaches as follows:

(1) Matrix density and fluid density in the logged interval for density logging are assumed to be constant (Glover, 2002).

(2) Matrix transit time and fluid transit time in the logged interval for sonic logging are assumed to be constant (Glover, 2002).

(3) The same linear calibration is applied for neutron log, density log and sonic log and calibrated with true porosity from RCAL for the dataset of well 15/12-5,

well 15/12-6S and well 15/12-9S to make a porosity prediction on well 15/12-20S.

As for sonic log and density log, once the related variables are dimed as constant in Eqs.(6)-(7) and the matrix density, fluid density in density log and matrix transit time, fluid transit time can be recomputed by calibrating with the true porosity from RCAL. Due to difference in dataset quality in the practical well logging operations, the actual measurements from these three logs may not be equally evaluated and utilized for porosity estimation. Thus, specific weights are assigned to each log porosity estimation to balance the quality of data samples and prediction accuracy as Eq.(64) shows. The exacta values for weights can be aligned with regression r square results in each log and the weights shall be added to one.

$$Z(POR_{DT}, POR_{RHOB}, POR_{CNC}) = T_1 \times POR_{DT} + T_2 \times POR_{RHOB} + T_3 \times POR_{CNC} \quad (64)$$

4.6 Statistical Evaluation

Several statistical evaluation methods are listed to assess the derivation between the observation data and predicted data and performance of the model:

(1) Root Mean square error (RMSE):

$$RMSE = \sqrt{\frac{\sum(x_0 - x)^2}{n}} \quad (65)$$

(2) Average absolute error (MAE):

$$MAE = \frac{\sum|x_0 - x|}{n} \quad (66)$$

(3) Pearson Coefficient of determination (R^2):

$$R^2 = 1 - \frac{\sum\left(y_i - y_i^{pred}\right)^2}{\sum(y_i - \bar{y})^2} \quad (67)$$

(4) Distance Correlation:

$$Dcorr(P,Q) = \frac{Dcov^2(P,Q)}{\sqrt{Dcov^2(P,Q)}} \tag{68}$$

4.7 Varg Field Overview

The Varg field is in the central area of the North Sea, situated about 230km southwest of Stavanger. The discovery and filed production started in 1984 and 1998 respectively, the well 15/12-5 and the well 15/12-6S were drilled as two appraisal wells to confirm the discovery of the Varg field. The production of the Varg field had already been stopped and new decommissioning operation was approved in 2015 and the decommissioning operation shall be completed by the end of 2021 per schedule.

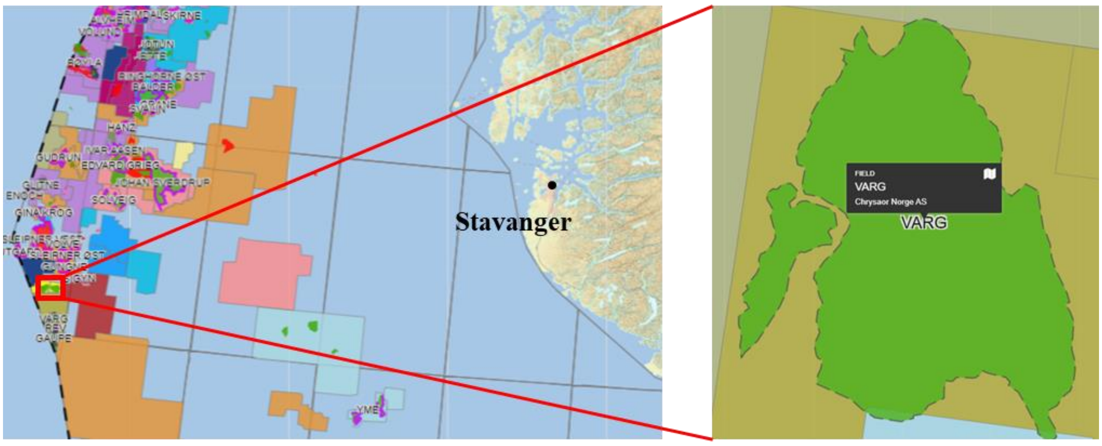

Figure 15 Location of Varg Field (Norwegian Petroleum Directorate,2020)

Table 9 Summary of Varg field wells

	15/12-5	15/12-6S	15/12-9S	15/12-20S
Well type	Appraisal	Wildcat	Appraisal	Wildcat
Water depth (m)	84	84	84	84
Total depth(MD) [m RKB]	3150	3050	3848	4192
Final vertical depth(TVD) [m RKB]	3149	3034	3213	3141.5
1st level with HC,age	Late Jurassic	Late Jurassic	Late Jurassic	Late Jurassic
1st level with HC,formaiton	Ula FM	Intra Heather FM SS	Intra Heather FM SS	Sleipner FM
Oldest penetrated age	Late Triassic	Triassic	Triassic	Late Triassic
Oldest penetrated formation	Skagerrak FM	Skagerrak FM	Skagerrak FM	Skagerrak FM
Target upper depth (m)	2895.75	2855.75	3389	3815
Target lower depth (m)	2942	2964	3554.75	3897.5

With the available and comparable well logging data samples in well 15/12-5, well 15/12-6S, well 15/12-9S and well 15/12-20S, Table 4 presents a summary of basic well information for these four wells used in the thesis. The target upper depth and target lower depth define the target zone where core samples are taken during RCAL. Therefore, more focus will be on the sections within the target zone for lithological description for well 15/12-5, well 15/12-6S, well 15/12-9S whereas no completion well report for 15/12-20S is provided, so 15/12-20S lithology description is not included here.

For well 15/12-5, the target zone is located between 2895.75m and 2942m depth, which can be divided into two sections. The first section from 2895.75m – 2918m depth belongs to the Heather Formation of the Viking Group. Siltstone, claystone and shale are the primary lithologies in the Heather Formation and its age is middle Oxfordian to early Kimmeridgian(Upper Jurassic).

Table 10 Well 15/12-5 Lithology Summary

Lithology	Color	Hardness	Description
Siltstone	Dark grey	Firm – Hard	Locally weakly laminated siltstone with very find sand
Claystone	Medium grey	Hard	Massive silty in parts and non-calcareous
Shale	Dark grey	Hard - Brittle	Fissile, slightly carbonaceous and non-calcareous

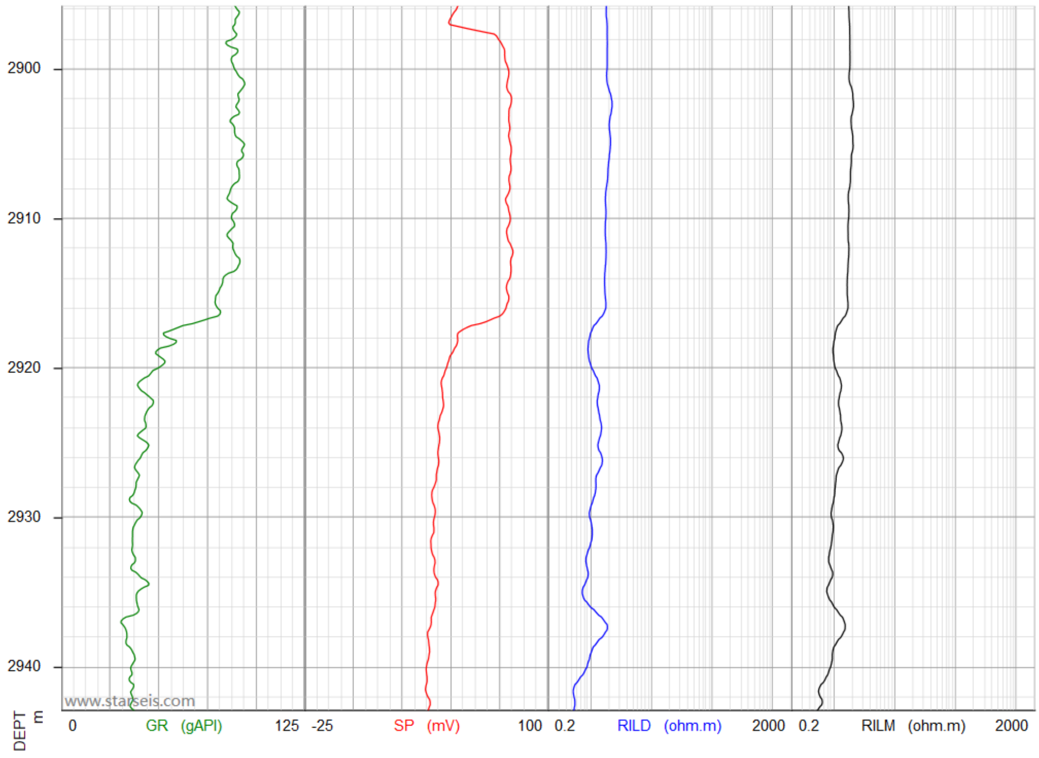

Figure 16 Gamma Ray log, SP log, Deep resistivity log and medium resistivity log for well 15/12-5

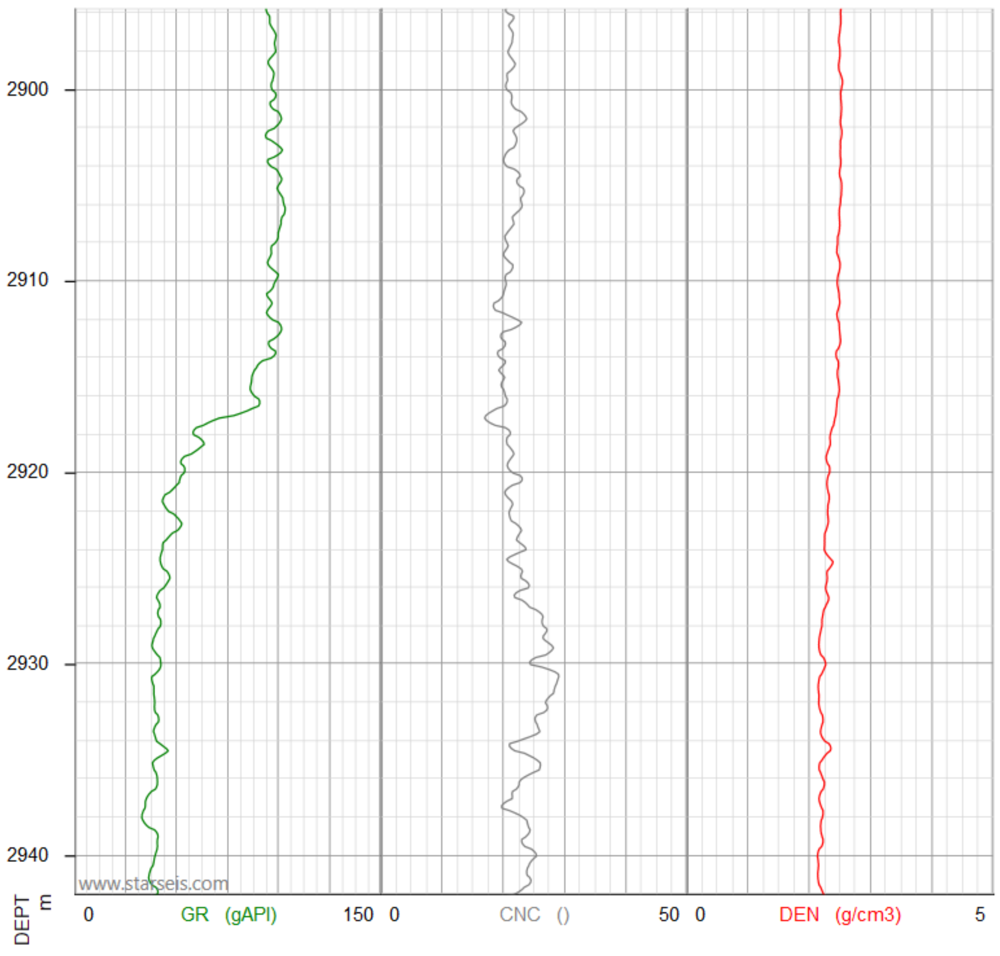

Figure 17 Gamma ray log, neutron log, density log for well 15/12-5

A series of high gamma ray readings shall be noted between 2895m and 2915m from the Figure 16 and 17 and some key lithological information can be gained from Statoil (1986) and described in Table 10. The other section from 2918m – 2942m depth belongs to the Vestland Group with Oxfordian Sandstone Unit.

For well 15/12-6S, the target zone is located between 2855.75m and 2964m depth, which can be divided into two sections. The first section from 2855.75m – 2933m depth belongs to the Oxfordian Sandstone of the Vestland Group. Sandstone is the primary lithology in the Oxfordian Sandstone and its age is early to late Oxfordian (Late Jurassic). Pale to dark yellow brown oil stained sandstone, coal fragments and mica are common in the formation. The grains in the sandstone vary from very fine to very coarse sand.

The other section from 2933m – 2964m depth belongs to the Sleipner Formation, where the age is Middle Jurassic with terrestrial / deltaic depositional environment from Statoil (1990). This section is mainly composed of layers of sandstone, claystone and coal. Additionally, some key lithological information can be obtained from Statoil (1990) as showed in Table 11.

Table 11 Well 15/12-6S Lithology Summary

Lithology	Color	Hardness	Description
Sandstone	Light grey	Very hard	Cemented with silica and no visible porosity
Claystone	Moderate brown to greyish red	Soft - Firm	Very silty and sandy in some parts
Coal	Black to brownish black	Hard	Slightly micaceous and no visible porosity

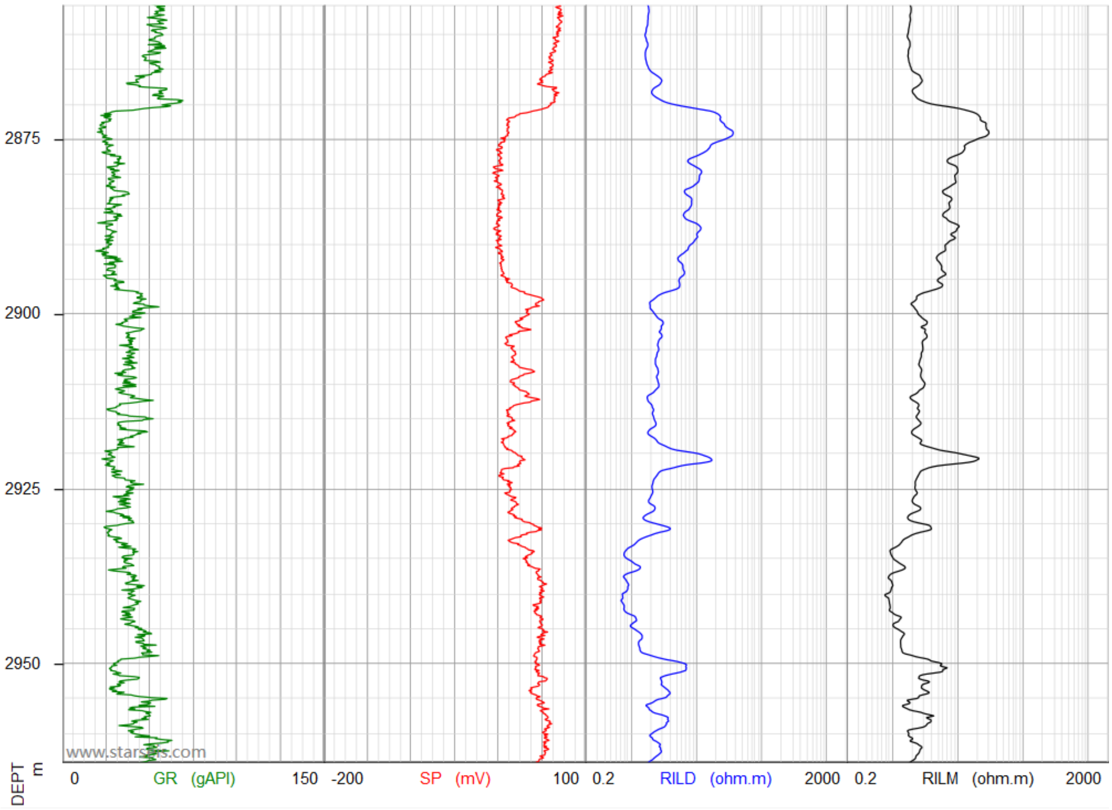

Figure 18 Gamma Ray log, SP log, Deep resistivity log and medium resistivity log for well 15/12-6S

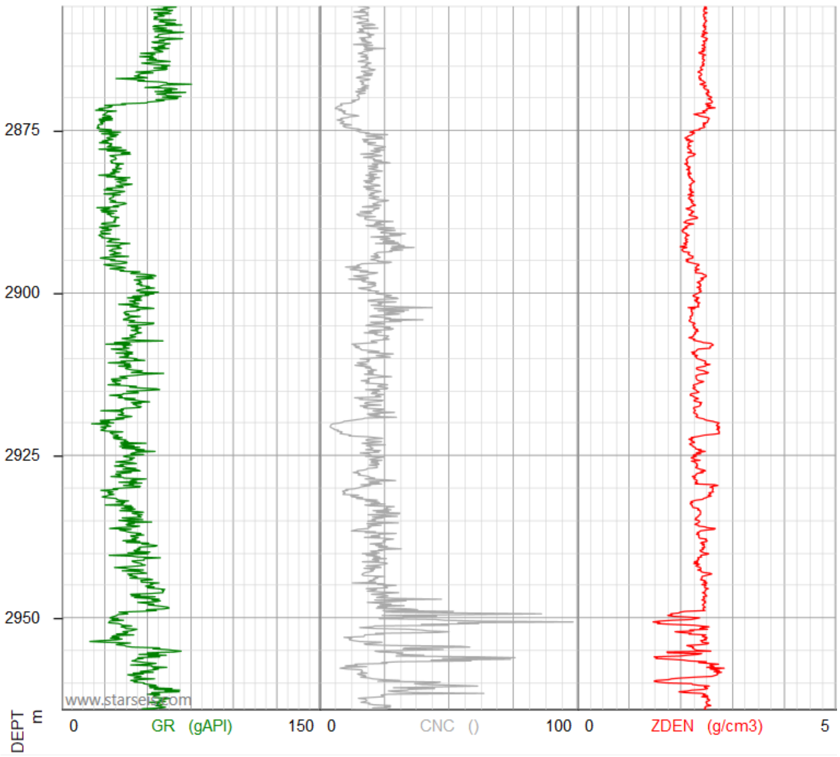

Figure 19 Gamma ray log, neutron log, density log for well 15/12-6S

For well 15/12-9S, the target zone is located between 3389m and 3554.75m depth, which belongs to the Oxfordian Sandstone of the Vestland Group. Sandstone is the primary lithology in the Oxfordian Sandstone with a narrow layer of dolomite between 3440m and 3444m. The formation age is Lower Oxfordian to Lower Kimmeridgian with Marine shelf depositional environment.

The sandstone in the Oxfordian Sandstone formation varies by depth, relatively pure and clean sandstone exist in the upper layer of the formation, which can be seen from Fig.(8)-(9) and the well completion report (Statoil, 1993). The sandstone in the lower layers is composed of clean sandstone with stingers of limestone. Additionally, some key lithological information can be obtained from the well completion report (Statoil, 1990), Figure (20)-(21) and showed in Table 12.

Table 12 Well 15/12-9S Lithology Summary

Lithology	Color	Hardness	Description
Sandstone	Grey	Hard - Very hard	Silty, argillaceous and cemented with silica
Sand	Light brown, brownish grey	Soft	Slightly bioturbated with poor visible porosity
Dolomite	Yellow grey to brownish grey	Hard	Sandy and calcareous in some parts

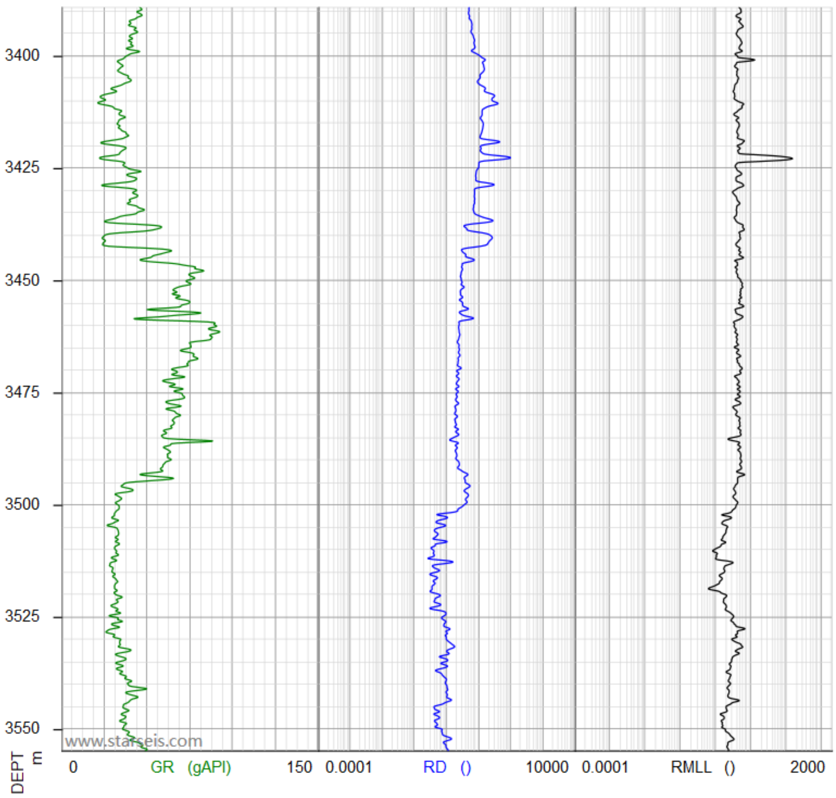

Figure 20 Gamma Ray log, Deep resistivity log and medium resistivity log for well 15/12-9S

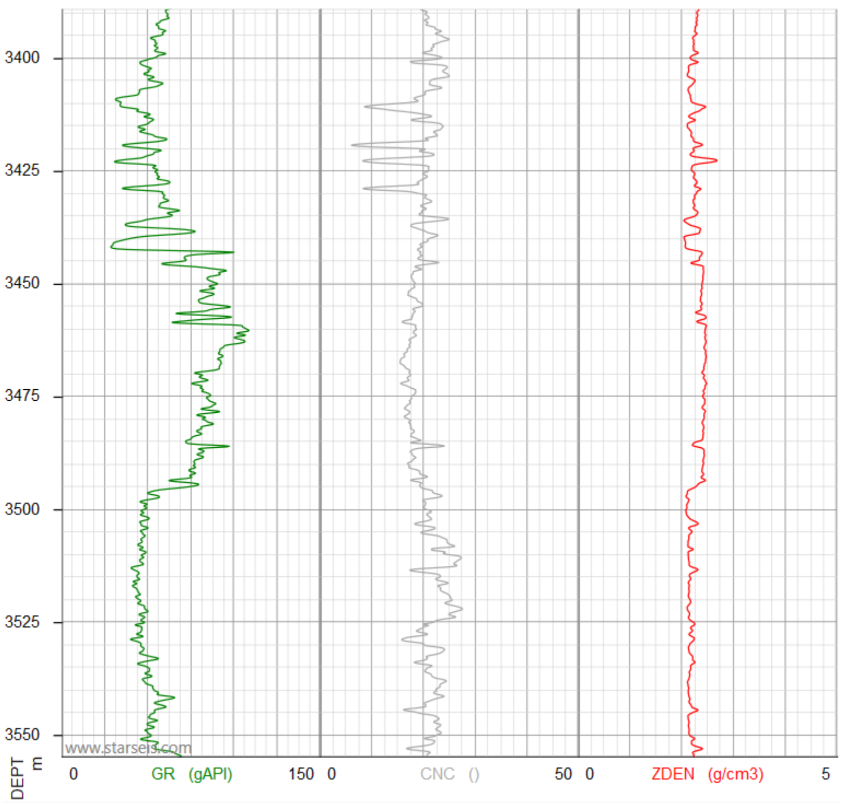

Figure 21 Gamma ray log, neutron log and density log for well 15/12-9S

4.8 Model Parameter Setting

After the optimization of applying PSO for initial LSSVR, the model parameters employed in LSSVR (regularization parameter C_p and kernel parameter σ) are optimized before feeding the training and validation datasets again to have an ideal LSSVR-PSO model as Table 13 shows. Here, the range of some parameters are defined as: $C_p \in [2, 2^{10}]$, $\sigma \in [2^{-6}, 2]$. The optimization parameter setting for PSO (population of particles, maximum iteration time, cognitive weight cc_1, social weight cc_2 and inertia weight ω) are listed in Table 14. Additionally, the parameter setting of another two machine learning models SVR and KNN for comparison are listed in Table 15.

Table 13 Parameter setting for LSSVR algorithm

Model	Item	Value / Type
LSSVR-PSO	Number of input features	6
	Kernel function	RBF
	Kernel parameter (σ)	0.571
	Regularization parameter (C_p)	13.105
	Number of training data samples	880
	Number of validation data samples	220
	Total data samples	1100

Table 14 Parameters employed in PSO algorithm

Model	Item	Value
PSO	Population of particles	50
	Maximum iteration time	100
	Cognitive weight cc_1,	2.05
	Social weight cc_2	2.05
	Inertia weight ω_{in}	0.9

Table 15 Model parameter settings for SVR and KNN algorithms

Model	Item	Value
SVR	Regularization parameter (C_p)	10
	Kernel parameter (σ)	0.5
KNN	Number of Neighbor	5

5 Model Results and Sensitivity analysis

5.1 Model Feature Selection

Normally, the model performance is highly affected by the input features for training and validation, because excessive input features will lead to information redundancy and reduced interpretability of the model, so it is necessary to screen the input features. In this thesis, the correlation relationship between well logs and porosity needs to be measured by correlation co-efficient and higher correlation co-efficient values of the well log would be relevant to porosity. Therefore, the well logs with high correlation co-efficient values are selected and fed as input features for the prediction LSSVR-PSO model.

Unlike other known correlation approaches, as for the Distance Correlation approach, the correlation between random vectors would be classified as independent only when the distance correlation value equals to zero. Furthermore, the equal dimensions or linearity are not required, and no specific constraints or assumption are needed for the compared vectors in Distance Correlation approach, which enables more generalization than classical Pearson Correlation where normal distribution assumption needs to be made. Hence, Pearson Correlation and Distance Correlation methods are utilized for the training and validation datasets to figure out the relationship between petrophysical logging data and porosity and determine what will be fed to the LSSVR-PSO model.

All the five conventional parameters have different correlation with porosity as Figure 22 shows. CA and DR are less significant compared with others with p ~-0.21 and p ~ 0.04 respectively. RHOB dependence shows the most notable correlation p ~ -0.73 and the correlation values for DT, GR and CNC are p ~ 0.53, p ~ -0.44, p ~ 0.35. It is noted that GR is in negative correlation with porosity as high GR values always indicate less porous rock space for shale where the rock porosity is remarkably low.

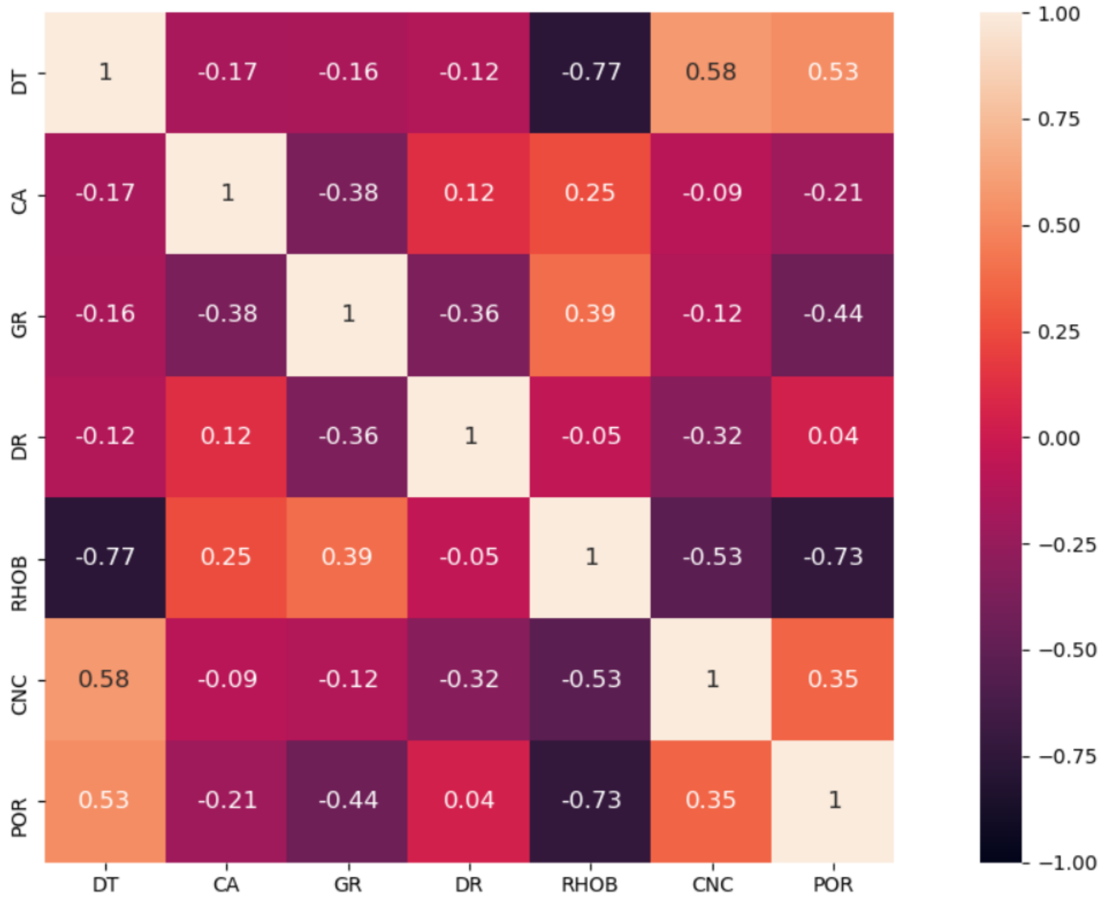

Figure 22 Pearson correlation result for training and validation datasets

The correlation summary for all five logs is represented in Figure 23 and it can be seen that CA is the parameter with lowest correlation values with D_{corr} ~ 0.26 in the correlation with porosity. The highest correlation value is obtained in RHOB with D_{corr} ~ 0.75 and the correlation values for DT, DR, GR, CNC are D_{corr} ~ 0.61 , D_{corr} ~ 0.27 , D_{corr} ~ 0.51 and D_{corr} ~ 0.45 respectively.

Considering the two correlation analysis results from Pearson Correlation and Distance Correlation, DT, DR, GR, RHOB, CNC are selected as input features of LSSVR-PSO model in the thesis because it is most likely that a relationship among DT, DR, GR, RHOB, CNC and porosity exists.

Figure 23 Distance correlation result for training and validation datasets

5.2 LSSVR-PSO Model Validation and Calibration

Once the LSSVR model is initialized with training dataset and run the LSSVR model for validation dataset to acquire the predicted porosity. The LSSVR-PSO predicted porosity can be compared with true porosity from core analysis and demonstrated in the Figure 24. The data in validation dataset are marked with red triangle and the blue line is described as the fitting line that indicates the accuracy of predicted porosity versus true porosity with R^2 =0.769.

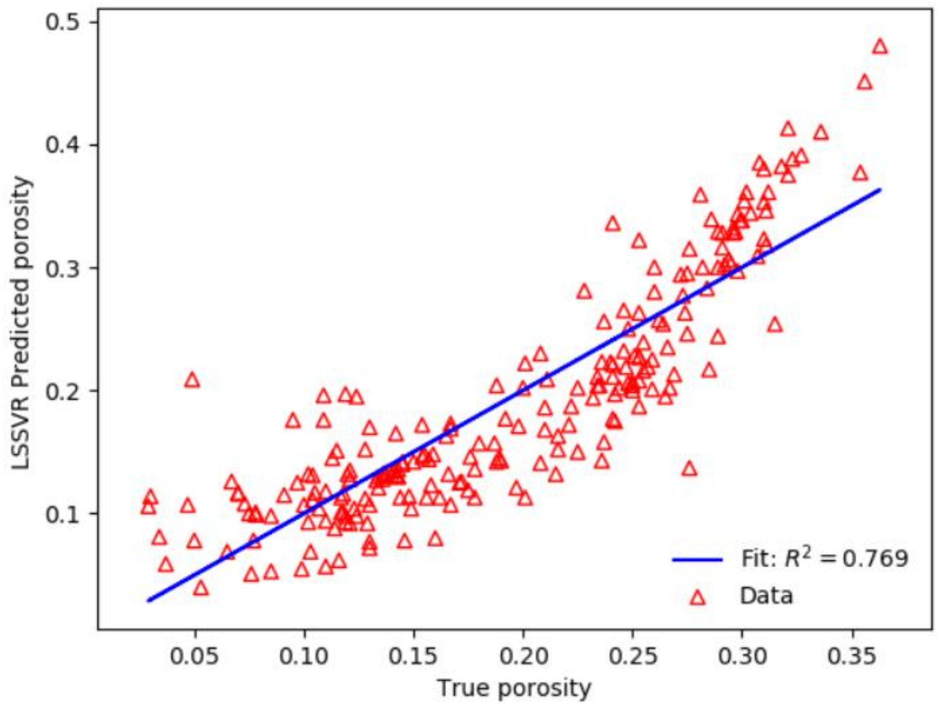

Figure 24 Scatter plot of LSSVR predicted porosity versus true porosity for validation dataset

For the next step, the hyper-parameter in the LSSVR model is optimized by employing PSO algorithm for the training dataset, the optimized parameters in the optimal LSSVR-PSO model were found: C_p = 13.105 and σ = 0.557. As the Figure 25 represents, a comprehensive graphic comparison is conducted between LSSVR-PSO predicted porosity and true porosity with high accuracy performance where R^2 = 0.979 after applying PSO algorithm for the validation dataset.

Since the calibrated LSSVR-PSO model has addressed high accuracy porosity prediction in validation dataset, then this calibrated model can be further utilized in the prediction of a blind well to verify the generalization and robustness of the model. As Figure 26 depicts, a graphic comparison is represented between the LSSVR-PSO predicted porosity and the true porosity with a great fitness with R2 =0.945 for the blind well dataset.

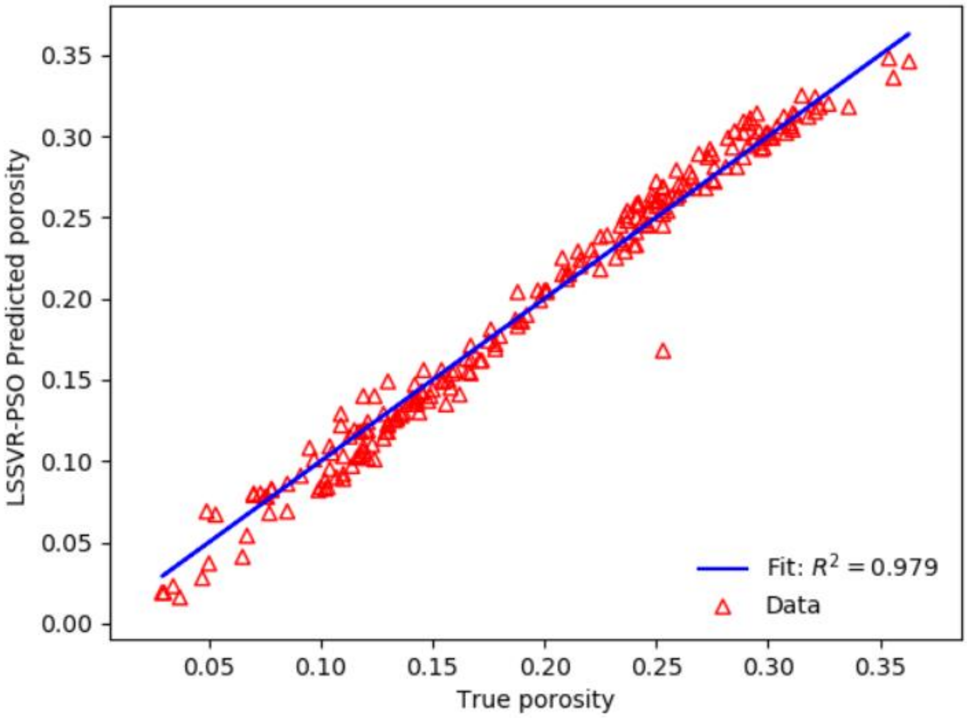

Figure 25 Regression plot of LSSVR-PSO predicted porosity versus true porosity for validation dataset

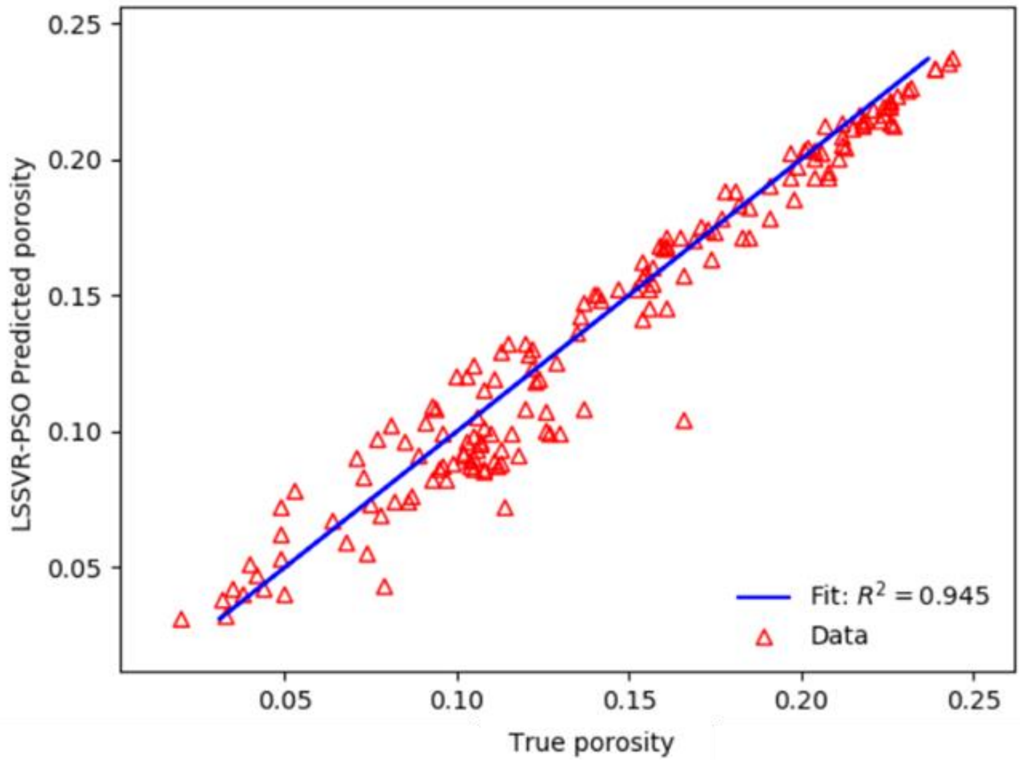

Figure 26 Regression plot of LSSVR-PSO predicted porosity versus true porosity for blind well dataset

Furthermore, a data distribution plot has been drawn for showing the porosity deviation percentage between the predicted porosity and true porosity. As showed in Figure 26, the prediction deviation is relatively within about 10%-20% when the true porosity is larger than 0.15. However, when it comes to tight rock where porosity is lower than 0.15, the predicted porosity result from LSSVR-PSO model becomes unreliable with significantly large error.

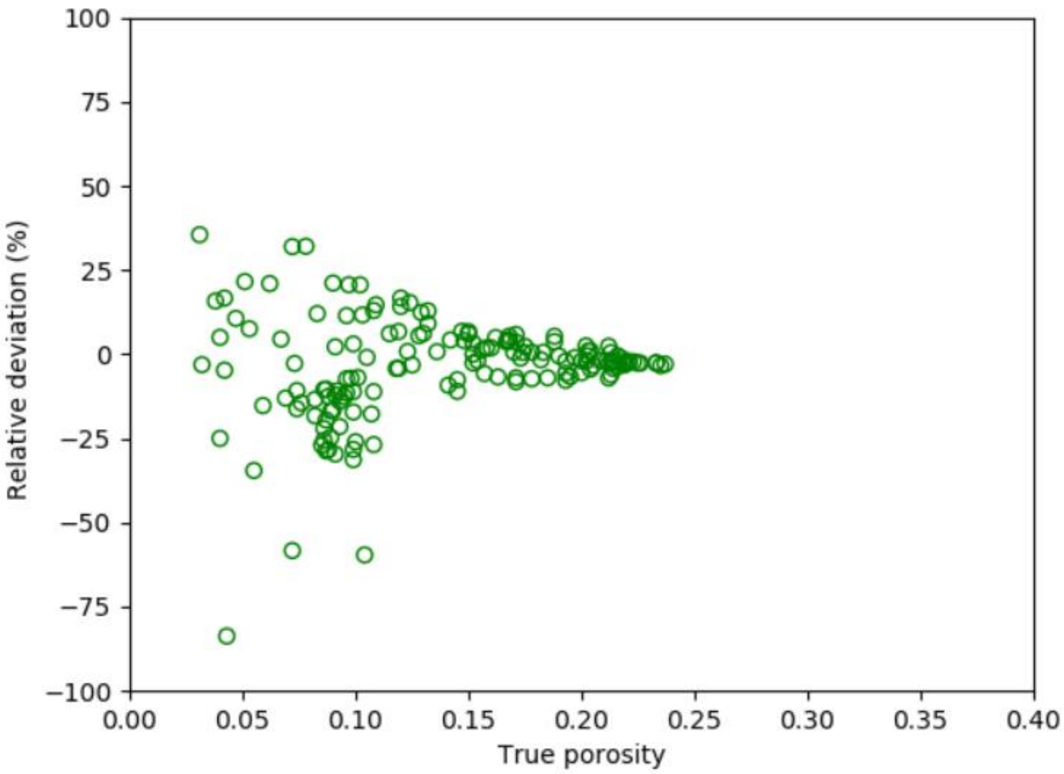

Figure 27 Relative deviation of LSSVR-PSO predicted porosity versus true porosity for blind well dataset

In order to understand the deviation distribution among all input features in LSSVR-PSO model, Fig. 27-31 are constructed by performing the LSSVR-PSO model versus DT, GR, DR, RHOB and CNC. Most of the recorded data samples from DT, RHOB and CNC logs are in good coordination level with the deviation between true porosity and predicted LSSVR-PSO porosity. It is worthy to demonstrate that the significant deviations occur when the recorded GR is larger than 100 API as Figure 28 shows.

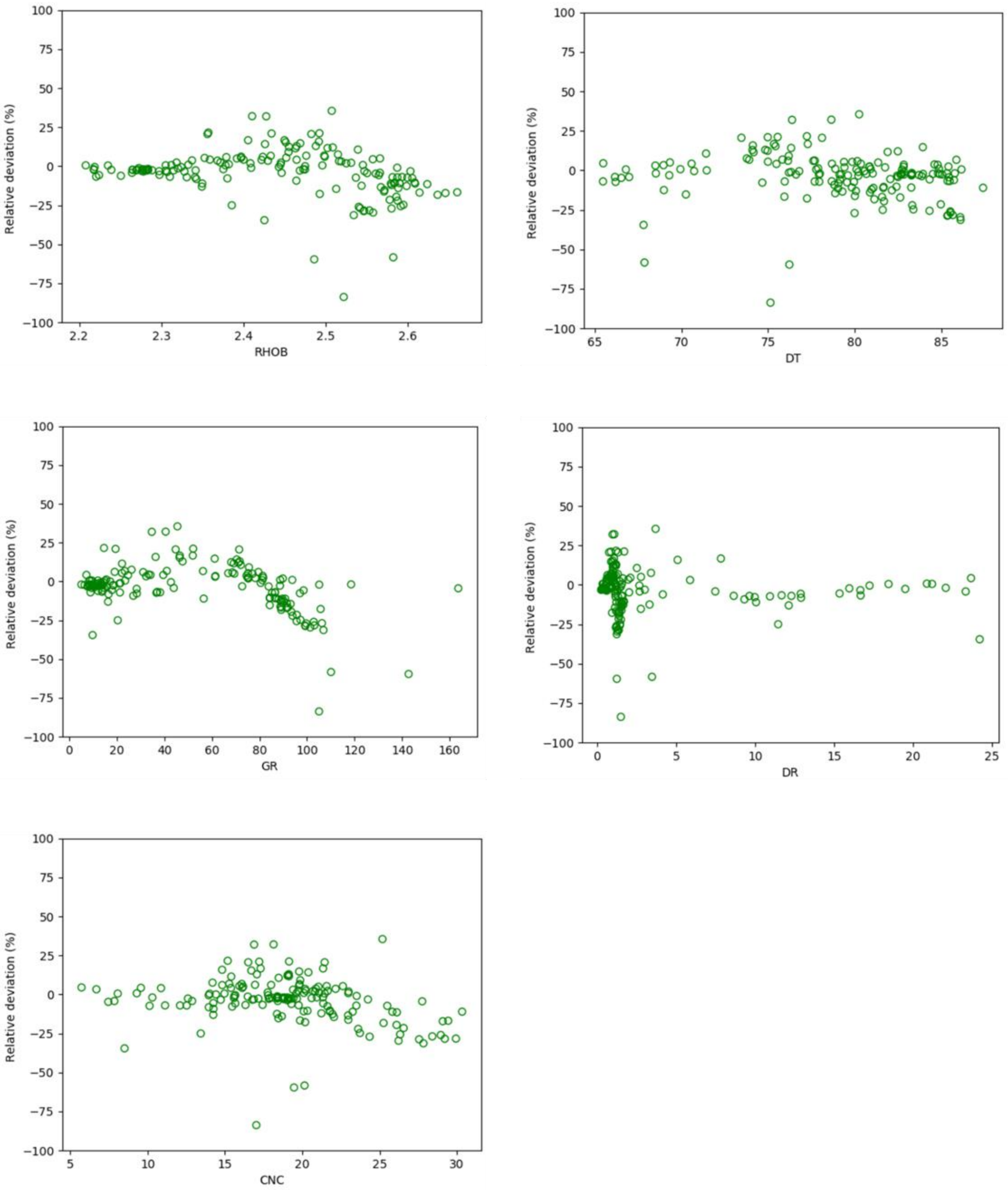

Figure 28 LSSVR-PSO Predicted porosity deviation versus petrophysical logs

5.3 Model Performance Comparison

To compare and evaluate the prediction performance of the LSSVR-PSO model, the two machine learning methods KNN and SVR are introduced and employed with the same datasets and input features. As Figure 29-30 show, the scatter plots illustrate the prediction accuracy of porosity in KNN method with five neighbors and estimation deviation between KNN predicted porosity and true porosity from RCAL. The correlation co-efficient between true porosity and predicted porosity for the blind well R^2 =0.839.

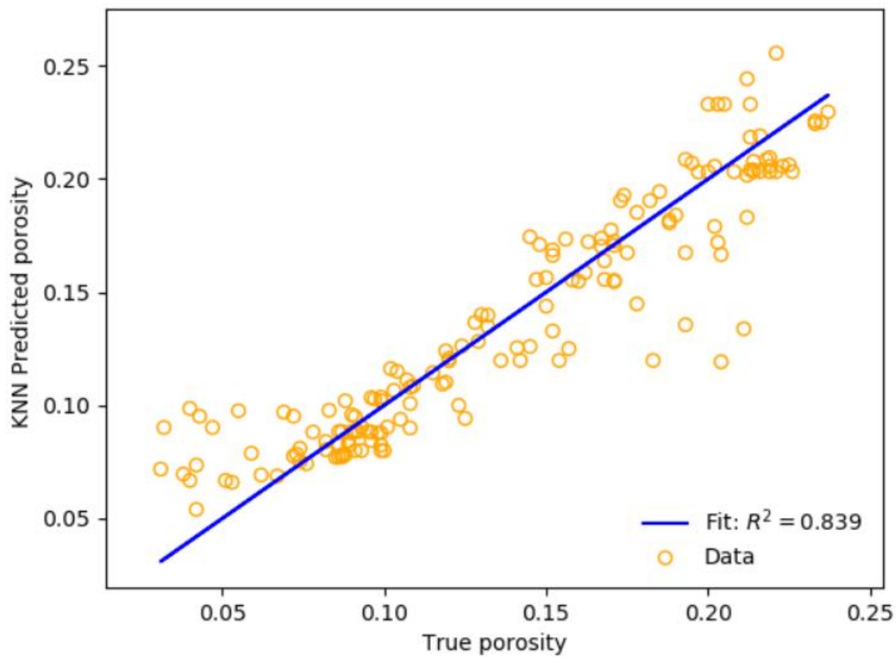

Figure 29 Regression plot of KNN predicted porosity versus true porosity for blind well dataset

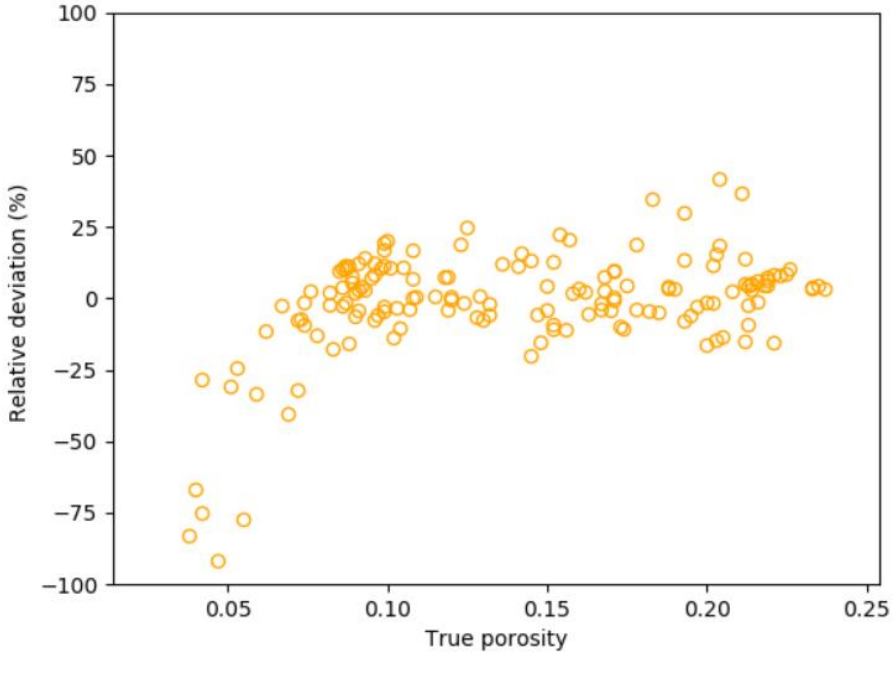

Figure 30 Relative deviation of KNN predicted porosity versus true porosity for blind well dataset

Similarly, the porosity estimation and prediction deviation distribution can be illustrated from Fig. 31-32 for the SVR machine learning method, the accuracy of this approach is higher than for the KNN method with the correlation co-efficient value R^2 =0.898.

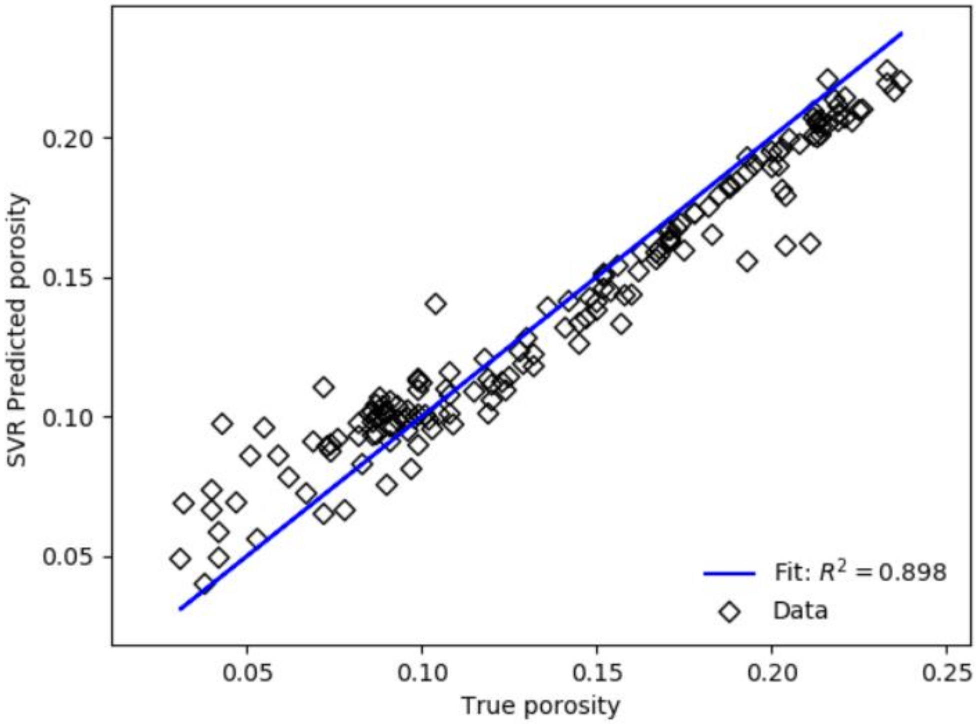

Figure 31 Regression plot of SVR predicted porosity versus true porosity for blind well dataset

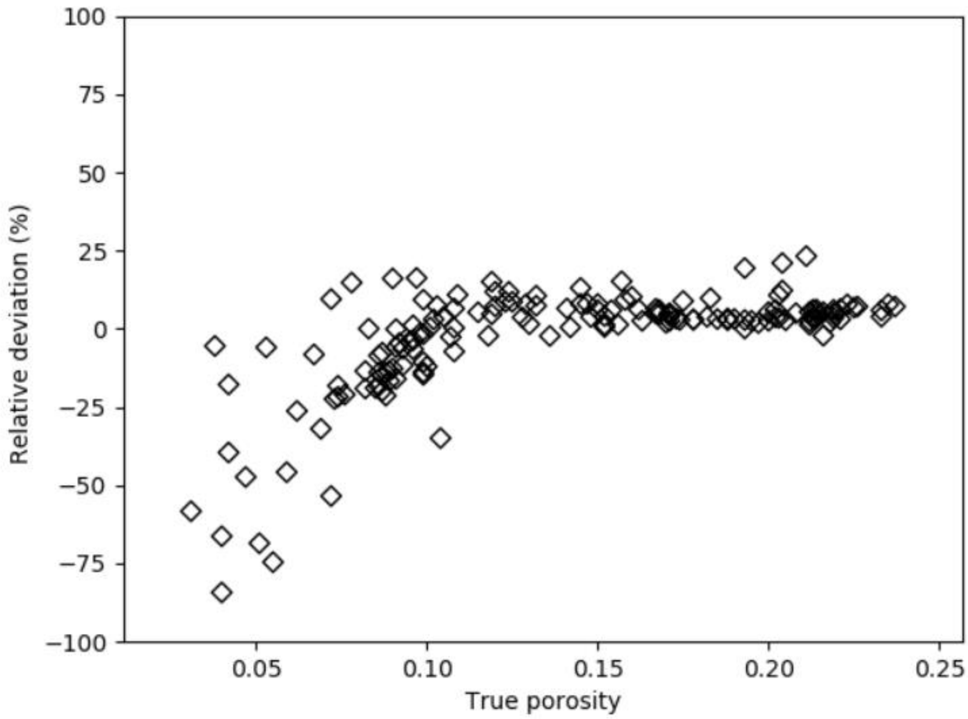

Figure 32 Relative deviation of SVR predicted porosity versus true porosity for blind well dataset

As it is mentioned in section 4.5, a suggested hybrid porosity estimation based on well logs is introduced for comparison, thus four constant variables for density log and sonic log can be calculated by plotting the scatter plots of data samples of three logs with true porosity from the training database composed of well 15/12-5, well 15/12-6S and well 15/12-9S. As Figure 36-38 show, the correlation co-efficient R^2 are 0.2813, 0.5294 and 0.1217 for sonic log, density log and neutron log respectively. The recalculated values of matrix density, fluid density, interval transit time of matrix and interval transit time of fluid are 2.79 gm/cc, 0.36 gm/cc, 41.956 $\mu s/f$, and 1.3 $\mu s/f$ respectively.

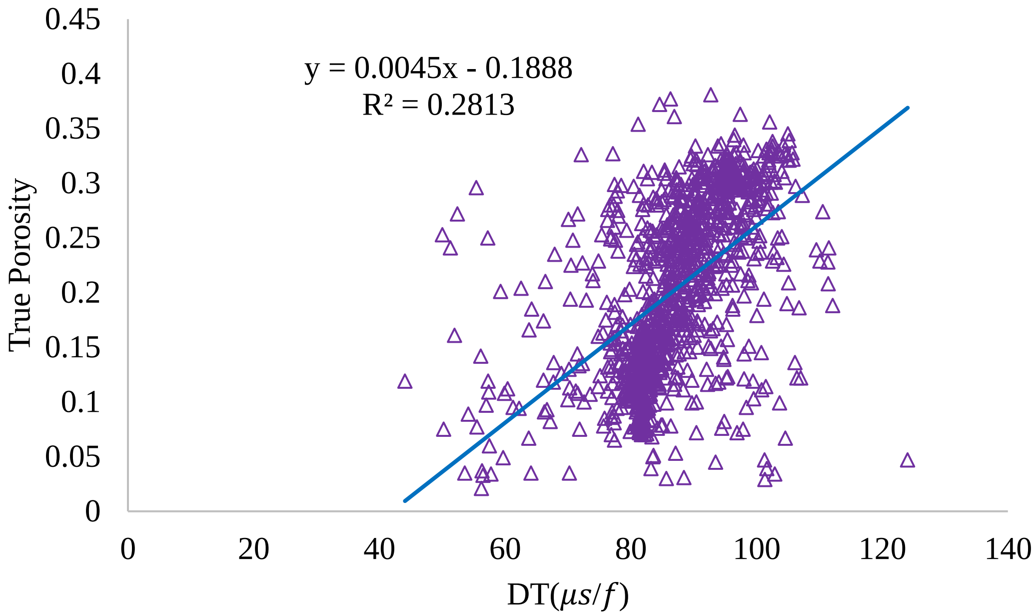

Figure 33 Linear regression plot of DT versus true porosity in training dataset

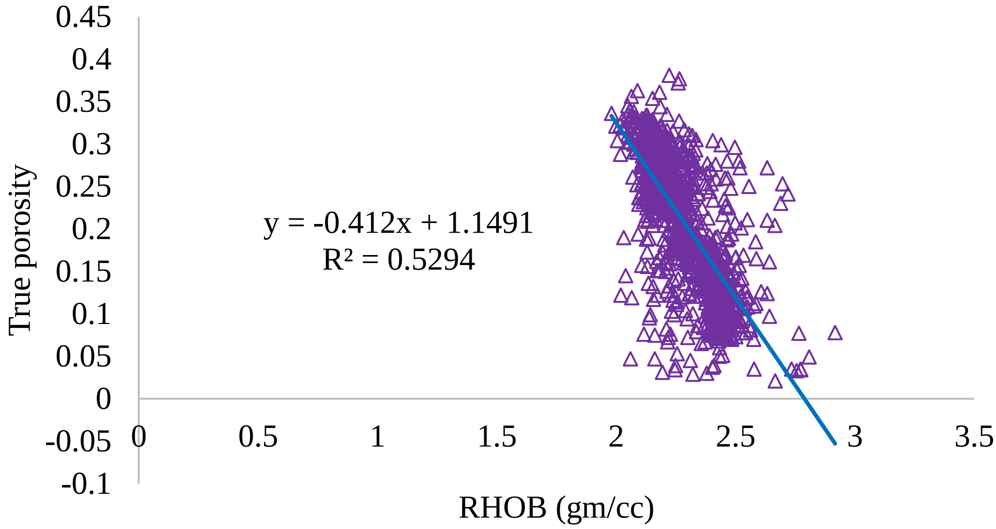

Figure 34 Linear regression plot of RHOB versus true porosity in training dataset

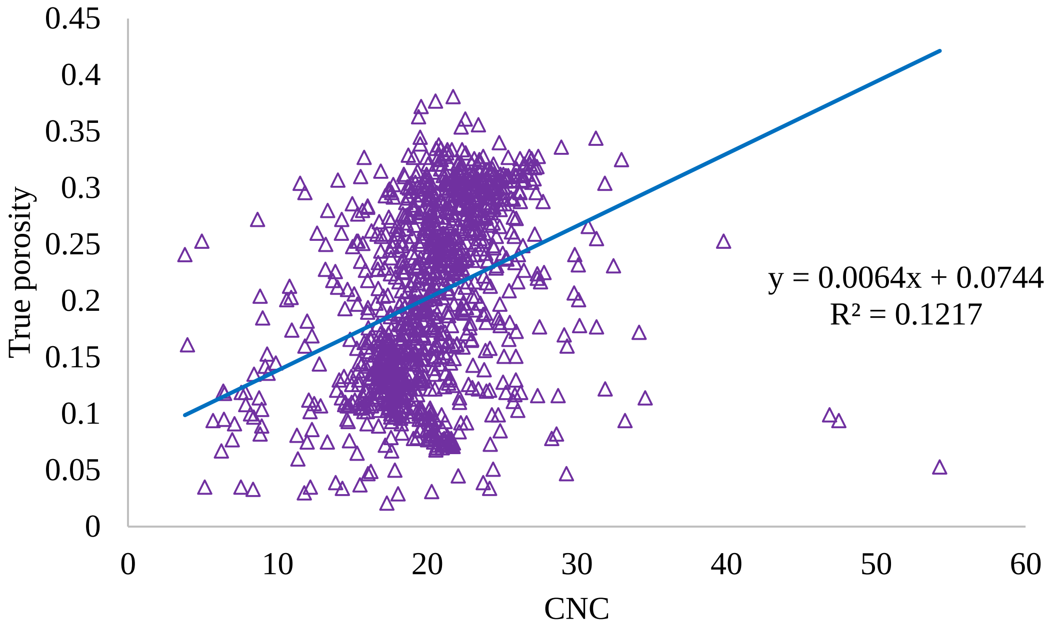

Figure 35 Linear regression plot of CNC versus true porosity in training dataset

Table 16 Constant variables in DT log and Density log obtained by calibrated linear regression by true porosity

Constant variable	Value
ρ_{matrix}, Matrix density	2.79 (gm/cc)
ρ_{fluid}, Fluid density	0.36 (gm/cc)
Δt_{matrix}, Interval transit time of matrix	41.956 ($\mu s/f$)
Δt_{fluid}, Interval transit time of fluid	264.178 ($\mu s/f$)

With the given condition, the correlation co-efficient R^2 for the three logs are 0.2813, 0.5294 and 0.1217 for sonic log, density log and neutron log respectively as Table 16 gives. The value selection of estimated porosity weights for Eq.(67) in this case are T_1 =0.6, T_2 =0.3, and T_3=0. Thus, the estimated porosity by the hybrid approach with three logs can be calculated in Eq.(64) and the prediction result is showed in Figure 36 with the correlation co-efficient R^2 = 0.5078

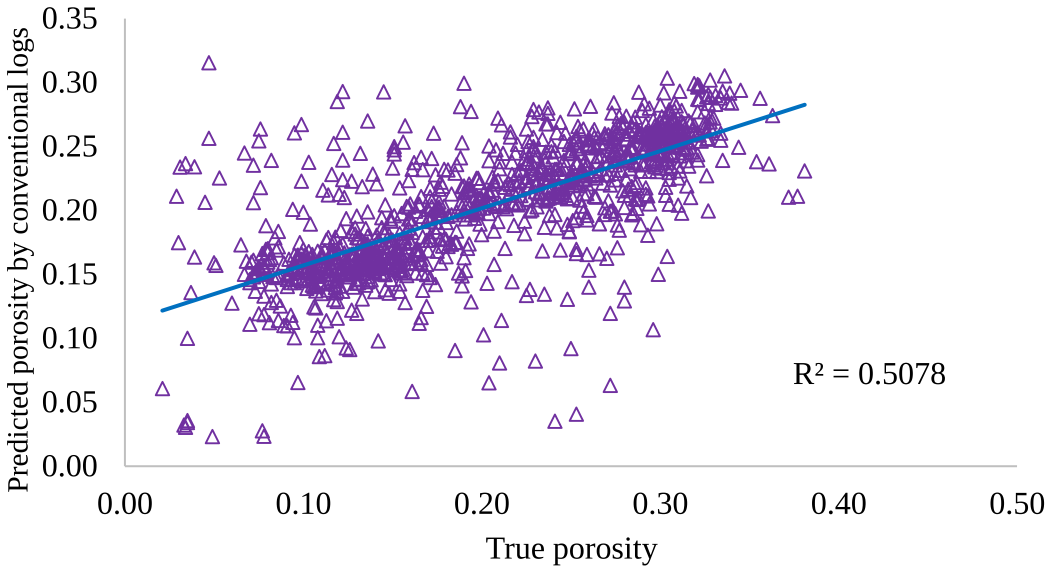

Figure 36 Regression plot of hybrid approach predicted porosity versus true porosity for blind well dataset

Among the proposed machine learning methods and conventional approach, Table 17 gives a summary of model prediction performance. It can be demonstrated that LSSVR-PSO model shows the best performance with highest correlation co-efficient $R^2 = 0.945$, lowest RMSE=0.01341 and MAE=0.01029 for porosity estimation in blind well among all the models.

Table 17 Summary of models for the blind well porosity prediction

Model Type	Model	R^2	RMSE	MAE
Hybrid approach	DT+ RHOB + CNC	0.508	0.04332	0.03424
Machine Learning methods	KNN	0.839	0.02076	0.01475
	SVR	0.898	0.01502	0.01164
	LSSVR-PSO	0.945	0.01341	0.01029

5.4 Sensitivity Analysis

Sensitivity analysis is defined as a process to show the relationship between a mathematical model output and the existing uncertainties in input features under some certain assumptions. Assumptions, input features and regression equations are key components of a regression model and the uncertainties can exist in every assumption, input parameter and regression equation in practical application, which may highly affect the regression performance of the model and cause errors. Hence, there are some advantages to employ sensitivity analysis on models as follows:

(1) Robustness testing.

(2) Model validation range for input features and output results.

(3) Accuracy priority on input features.

(4) Ease the calibration stage with large scale input features (Bahremand,2008).

(5) Clarify potential relationships between input features, observation and model output.

In this thesis, the sensitivity analysis is conducted in two parts: (a) Single feature variation for single data point; (b) A series of feature variations for prediction accuracy. Firstly, Table 18-20 represents the sensitivity outcome for a randomly selection of three data samples in the blind well dataset by varying a fixed input feature by increasing it with 20% and keep the others remain constant. The spread ratio is defined as the value difference between true porosity and predicted porosity. It can be observed that the variation of RHOB log values can cause a significantly high spread ratio between predicted porosity and true porosity.

Table 18 Sensitivity analysis on single dataset with 20% increase in each feature – Sample A

Item	DT	GR	DR	RHOB	CNC	True Porosity	Predicted Porosity (LSSVR-PSO)	Spread ratio
Reference	68.49	61.34	5.89	2.52	19.41	0.099	0.096	3.125%
Vary DT	82.18	61.34	5.89	2.52	19.41	0.099	0.101	-1.980%
Vary GR	68.49	73.61	5.89	2.52	19.41	0.099	0.102	-2.941%
Vary DR	68.49	61.34	7.06	2.52	19.41	0.099	0.099	0.000%
Vary RHOB	68.49	61.34	5.89	3.02	19.41	0.099	0.130	-23.846%
Vary CNC	68.49	61.34	5.89	2.52	23.29	0.099	0.096	3.125%

Table 19 Sensitivity analysis on single dataset with 20% increase in each feature – Sample B

Item	DT	GR	DR	RHOB	CNC	True Porosity	Predicted Porosity (LSSVR-PSO)	Spread ratio
Reference	66.15	43.99	7.48	2.57	12.88	0.119	0.124	-4.032%
Vary DT	79.38	43.99	7.48	2.57	12.88	0.119	0.127	-6.299%
Vary GR	66.15	52.79	7.48	2.57	12.88	0.119	0.123	-3.252%
Vary DR	66.15	43.99	8.98	2.57	12.88	0.119	0.127	-6.299%
Vary RHOB	66.15	43.99	7.48	3.08	12.88	0.119	0.153	-22.222%
Vary CNC	66.15	43.99	7.48	2.57	15.46	0.119	0.123	-3.252%

Table 20 Sensitivity analysis on single dataset with 20% increase in each feature – Sample C

Item	DT	GR	DR	RHOB	CNC	True Porosity	Predicted Porosity (LSSVR-PSO)	Spread ratio
Reference	80.08	16.36	12.13	2.35	14.25	0.069	0.078	-11.538%
Vary DT	96.09	16.36	12.13	2.35	14.25	0.069	0.082	-15.854%
Vary GR	80.08	19.63	12.13	2.35	14.25	0.069	0.076	-9.211%
Vary DR	80.08	16.36	14.56	2.35	14.25	0.069	0.08	-13.750%
Vary RHOB	80.08	16.36	12.13	2.82	14.25	0.069	0.113	-38.938%
Vary CNC	80.08	16.36	12.13	2.35	17.10	0.069	0.078	-11.538%

In the second part of the sensitivity analysis, this part of sensitivity analysis has been employed towards all the input features (DT, GR, DR, RHOB and CNC) with the LSSVR-PSO optimal model for blind well database. The sensitivity method is to fix four input features and make a prediction of porosity when the remaining input feature increases 10%, 20%, 30% and 50% for the blind well. Then, the first quartile and third quartile of true porosity in the blind well dataset can be computed by using Eq.(57)-(58) are: 0.091 and 0.192 and all the blind well data samples are divided into three groups in group intervals [0,0.091), [0.091, 0.192) and [0.192, 1). Hence, a series of 9 data samples are randomly selected from these three groups to show how the predicted porosity varies when the input features increases 10%, 20%, 30% and 50% for the blind well dataset.

In this way, a better illustration of relationship between input features and predicted porosity by scatter plots and the graphic sensitivity analysis results are showed in Figure 37-41 for DT, GR, DR, RHOB and CNC respectively.

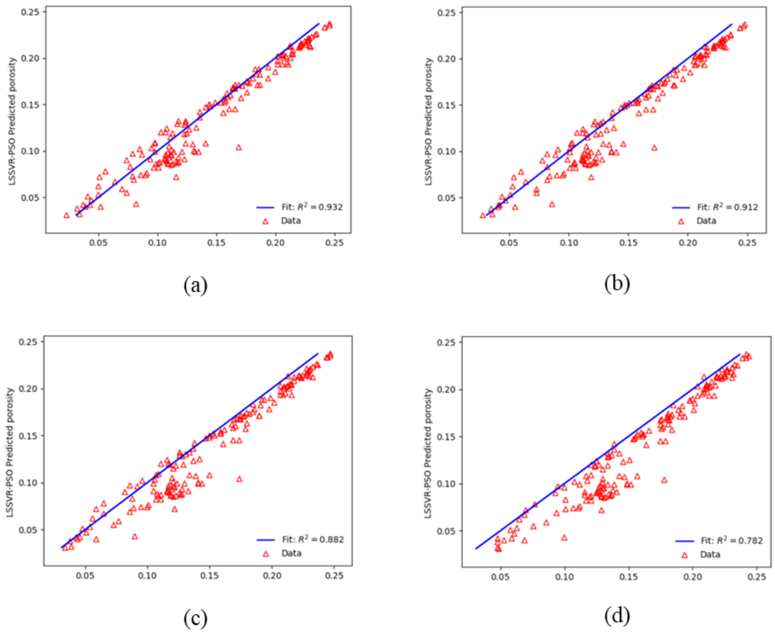

Figure 37 DT sensitivity analysis: (a) 10% (b) 20% (c)30% (d) 50%

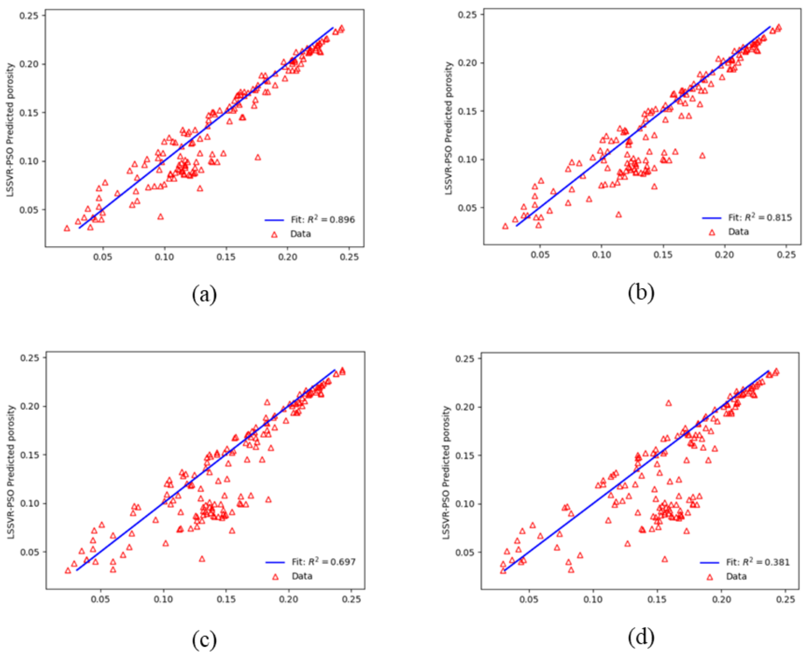

Figure 38 GR sensitivity analysis: (a) 10% (b) 20% (c)30% (d) 50%

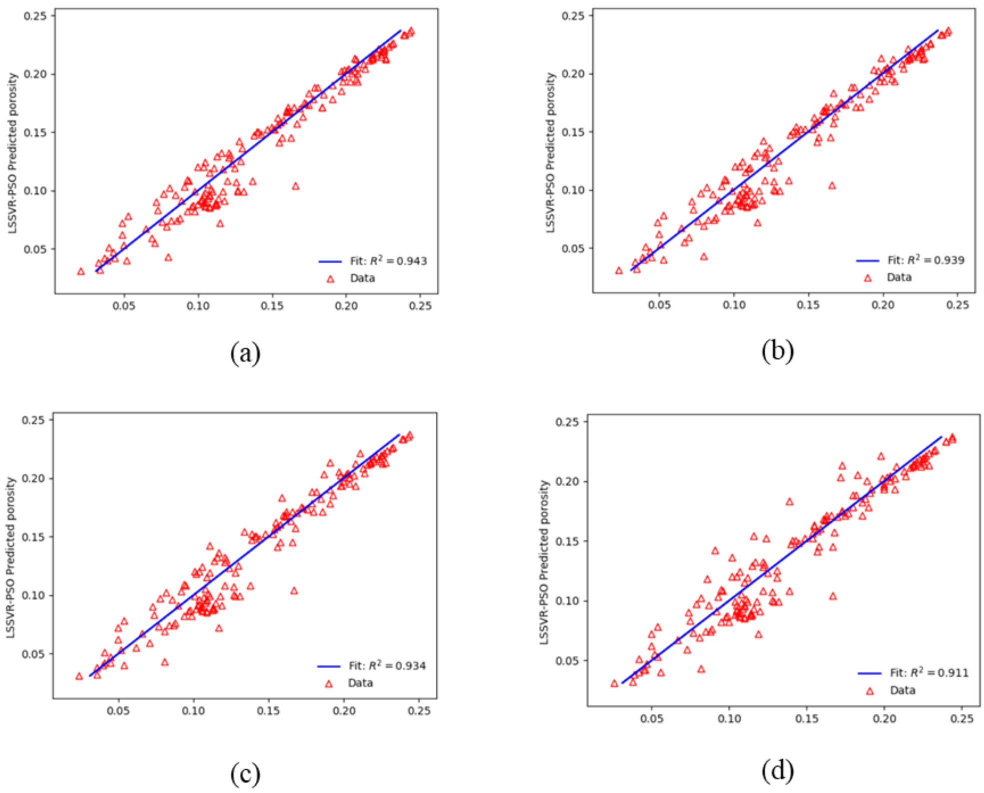

Figure 39 DR sensitivity analysis: (a) 10% (b) 20% (c)30% (d) 50%

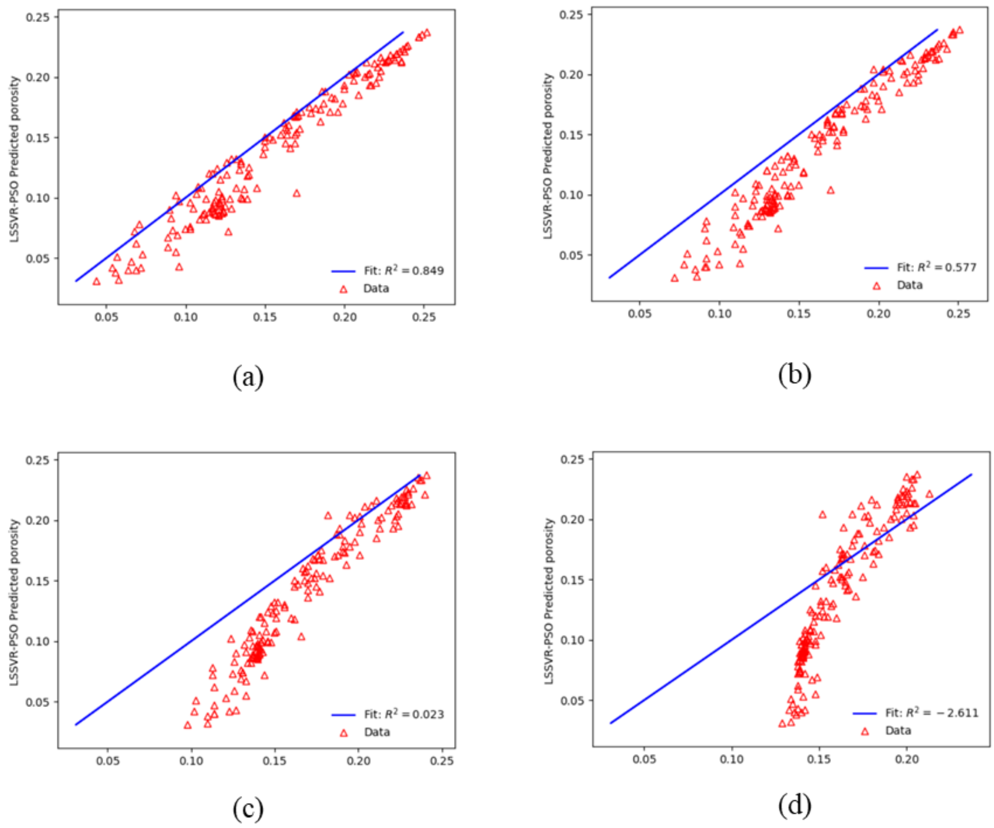

Figure 40 RHOB sensitivity analysis: (a) 10% (b) 20% (c)30% (d) 50%

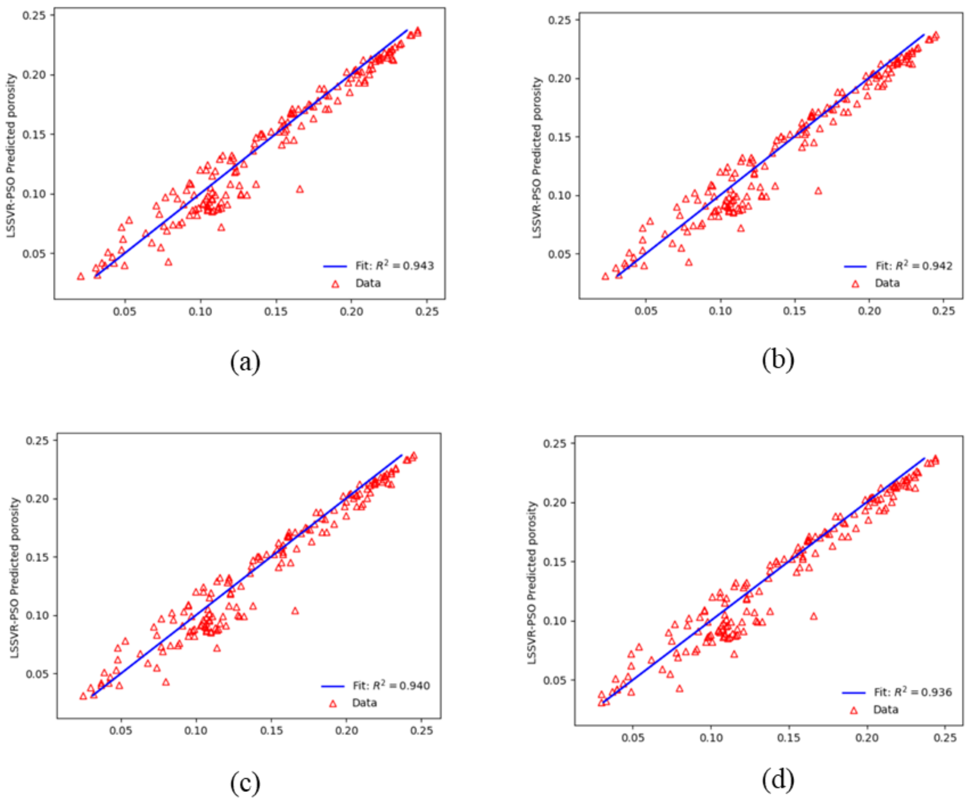

Figure 41 CNC sensitivity analysis: (a) 10% (b) 20% (c)30% (d) 50%

Meanwhile, a series of input feature variations versus LSSVR-PSO predicted porosity is illustrated in Figure 42. The data points marked with same color represents the original value of plotted log with the value increasing in 0%, 10%, 20%, 30% and 50%. Additionally, Table 21 provides a summary of sensitivity results by measurement of RMSE and R^2 for all the data samples in the blind well.

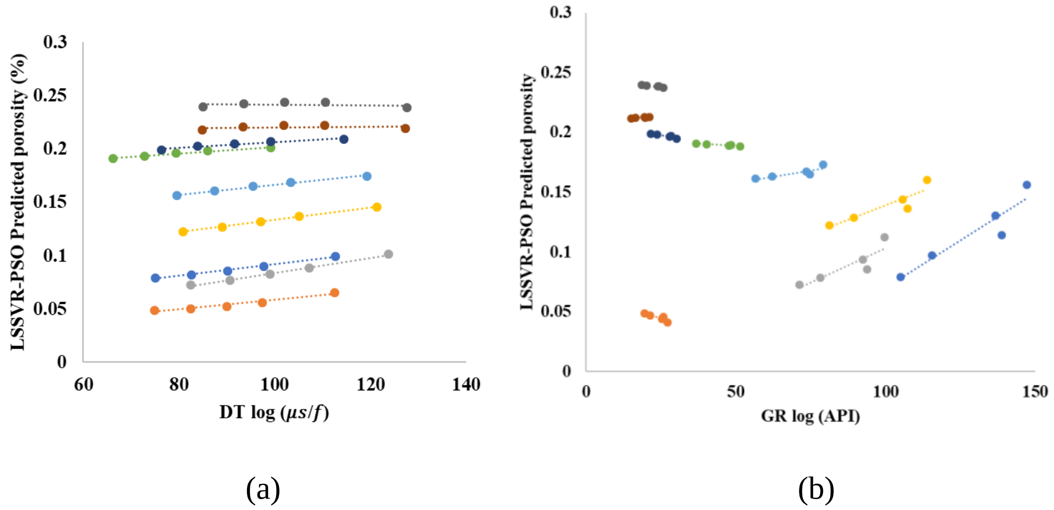

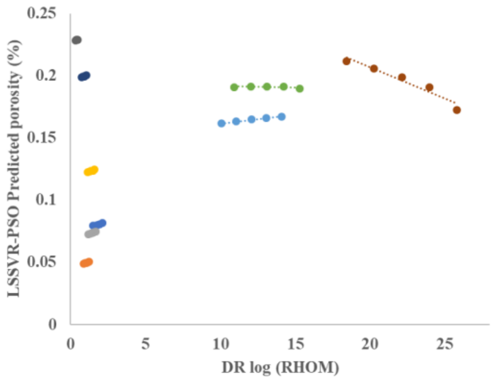

(c)

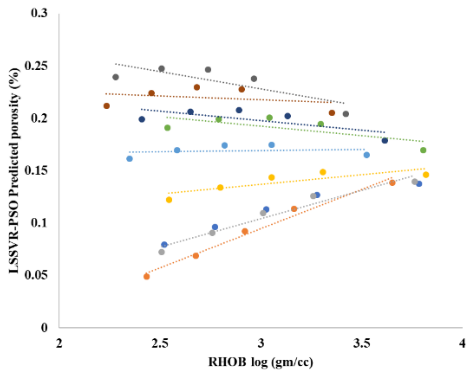

(d)

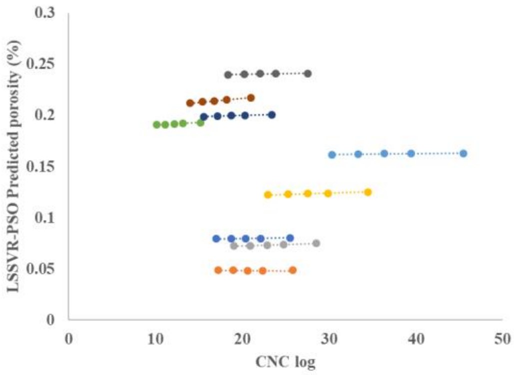

(e)

Figure 42 LSSVR-PSO predicted porosity with (a)DT, (b)GR, (c)DR, (d)RHOB and (e)CNC log variation

Table 21 Summary of LSSVR-PSO model accuracy of input feature for the blind well dataset

Input feature	Vary	RMSE	R^2
DT	10%	0.107	0.932
	20%	0.113	0.912
	30%	0.121	0.882
	50%	0.136	0.782
GR	10%	0.114	0.896
	20%	0.127	0.815
	30%	0.141	0.697
	50%	0.164	0.381
DR	10%	0.102	0.943
	20%	0.104	0.939
	30%	0.106	0.934
	50%	0.111	0.911
RHOB	10%	0.129	0.849
	20%	0.160	0.577
	30%	0.175	0.023
	50%	0.187	-2.611

CNC	10%	0.103	0.943
	20%	0.103	0.942
	30%	0.104	0.940
	50%	0.105	0.936

According to the sensitivity analysis results, some conclusions can be observed that how the uncertainties affect LSSVM-PSO model prediction performance and the relationships between different parameters and porosity:

(1) Porosity estimation is highly affected by the fluctuation in RHOB and the model may not be applicable with low R^2 value when the values changes in RHOB is varying over 30%.

(2) Porosity prediction is slightly influenced by the uncertainties in DT and GR and the model can maintain about 70%-80% prediction accuracy.

(3) Significant predicted porosity variation in high GR log values than those in low GR log values.

(4) CNC and DR are two input features that are stagnant and stable for the porosity prediction.

6 Discussion

In this chapter, more interpretation of the LSSVR-PSO model is discussed based on the porosity estimation results from the LSSVR-PSO model. Furthermore, the advantages and limitations of the LSSVR-PSO model are addressed as well.

For the interpretation of model results, the porosity estimation result of the LSSVR-PSO model has showed that accurate reservoir porosity estimation can be achieved only based on the well logging data from selected petrophysical logs with $R^2 = 0.945$. In this thesis, estimation results from KNN, SVR and the hybrid approach are utilized for comparison, the LSSVR-PSO model has the highest R^2 and lowest MSE and MAE among those comparison methods. However, the prediction performance of the LSSVR-PSO model is worse than the outcome of ADA-SVR model with $R^2 = 0.963$ (Li et al., 2019) or the prediction of HGAPSO-LSSVM model with $R^2 = 0.975$ (Ahmadi and Chen, 2019). The number of data points may not lead to the worse performance as 1260 data points are applied in the LSSVR-PSO model while 739 and 1000 data points are utilized in Li and Ahmadi ‘s work. Therefore, feature selection and data range may be the causes of lower estimation accuracy of the LSSVR-PSO in this thesis.

After the conduction of feature selection of the LSSVR-PSO model, the LSSVR-PSO model porosity estimation results are built on five petrophysical logs: DT, GR, DR, RHOB and CNC. However, only DT, CNC and RHOB are chosen as input features for ADA-SVR model (Li et al., 2019). Reduce the number of input features may increase the prediction accuracy, but the generalizability of model can be limited because the model performance would only rely on the data from few petrophysical logs.

On the other hand, the data range also have an impact on the model performance. Table 22 illustrates the data range comparison for petrophysical logs in HGAPSO-LSSVM model (Ahmadi and Chen, 2019) and LSSVR-PSO model. Both DT and porosity values in LSSVR-PSO is significantly larger than HGAPSO-LSSVM, which indicates that LSSVR-PSO model can be applied in a more general well with large applicable data range but slightly less accuracy.

Table 22 Data range comparison for HGAPSO-LSSVM model and LSSVR-PSO model for all dataset

Input feature	DT		RHOB		Porosity	
Model	HGAPSO-LSSVM	LSSVR-PSO	HGAPSO-LSSVM	LSSVR-PSO	HGAPSO-LSSVM	LSSVR-PSO
Min	48.39	44.08	2.28	1.98	0.03	0.02
Max	81.71	124.06	2.75	2.92	0.24	0.38
Average	57.88	83.75	2.57	2.36	0.08	0.17

The advantages of the LSSVR-PSO model are: (1) Provide a more efficient and economical method to obtain reservoir porosity than RCAL; (2) Reduce well logging service cost because some irrelevant well logs for porosity estimation can be notified during the process of feature selection, so these irrelevant well logging operations can be removed.

As for the limitations, the generalizability of the LSSVR-PSO model is limited by the training and validation dataset. The porosity prediction accuracy of the blind well is high, but it may not have the same performance for another well from Varg field with the same data in training and validation. The generalizability of applying LSSVR-PSO model in other fields in Varg field can be enhanced by increasing the number of wells used in training and validation dataset. The LSSVR-PSO model can be applied to predict reservoir porosity in North Sea by introducing more fields in North Sea. Additionally, variables used in the hybrid porosity estimation method are simplified by assigning the representative constant values from the perspective of theoretical calculation. However, constant variables may not be applicable for the real rock conditions. The performance of the hybrid porosity estimation method can be improved by calibrating by more true porosity data from RCAL. Besides, the hyper-parameter in KNN and SVR algorithms are not optimized and those parameters can be further optimized to achieve a higher prediction accuracy.

7 Conclusion

(1) Compared to the unoptimized KNN, SVR and the hybrid porosity estimation method, the LSSVR-PSO model have presented best porosity estimation result with R^2 = 0.945, RMSE= 0.01341 and MAE= 0.101029. The prediction application of LSSVR-PSO model on Varg field data has showed excellent performance, which may potentially provide a key method for reservoir rock property measurement and exploration.

(2) In the case of porosity estimation, distance correlation can provide a better illustration on the correlation relationship between different well logs and porosity where the data samples are in non-linear. Deep resistivity shows insignificant correlation between porosity in Pearson correlation and it may be ignored if only depending on Pearson correlation. On the contrary, relatively significant correlation can be observed between deep resistivity in distance correlation.

(3) Density log is found to be the most relevant log as input feature in porosity estimation by LSSVR-PSO model while Caliper log is discarded as the least relevance with porosity. Data quality of the density log can have a great impact on the model porosity estimation and the prediction result may not be reliable when the values changes in density log is varying over 30%.

(4) Well logging service cost can be reduced by removing some irrelevant well logs found during the process of feature selection for porosity estimation in LSSVR-PSO model.

Bibliography

Ahmadi, Mohammad Ali, and Zhangxing Chen. "Comparison of machine learning methods for estimating permeability and porosity of oil reservoirs via petro-physical logs." Petroleum 5.3 (2019): 271-284.

Amaefule, Jude O., Mehmet Altunbay, Djebbar Tiab, David G. Kersey, and Dare K. Keelan."Enhanced reservoir description: using core and log data to identify hydraulic (flow) units and predict permeability in uncored intervals/wells." SPE annual technical conference and exhibition. Society of Petroleum Engineers, 1993.

Asquith, George B., Daniel Krygowski, and Charles R. Gibson. Basic well log analysis. Vol. 16. Tulsa: American Association of Petroleum Geologists, 2004.

B. Schölkopf, A. Smola, Learning with Kernels, MIT Press, Cambridge, MA, 2002.

Bahremand, A., and F. De Smedt. "Distributed hydrological modeling and sensitivity analysis in Torysa Watershed, Slovakia." Water Resources Management 22.3 (2008): 393-408.

Bemani, A., Baghban, A., Mohammadi, A.H. and Andersen, P.Ø., 2020. Estimation of Adsorption Capacity of CO2, CH4, and their Binary Mixtures in Quidam Shale using LSSVR: Application in CO2 Enhanced Shale Gas Recovery and CO2 Storage. Journal of Natural Gas Science and Engineering, p.103204.

Bennett, Kristin P., and Olvi L. Mangasarian. "Robust linear programming discrimination of two linearly inseparable sets." Optimization methods and software 1.1 (1992): 23-34.

Bhattacharya, Shuvajit, and Srikanta Mishra. "Applications of machine learning for facies and fracture prediction using Bayesian Network Theory and Random Forest: Case studies from the Appalachian basin, USA." Journal of Petroleum Science and Engineering 170 (2018): 1005-1017.

British Petroleum Company plc. BP Energy Outlook, The British Petroleum Company plc, 2018

Bühlmann, Peter, and Sara Van De Geer. Statistics for high-dimensional data: methods, theory and applications. Springer Science & Business Media, 2011.

Burkov, Andriy. The hundred-page machine learning book. Quebec City, Can.: Andriy Burkov, 2019.

Chen, S., Li, H., Yang, D., & Tontiwachwuthikul, P."Optimal parametric design for water-alternating-gas (WAG) process in a CO2-miscible flooding reservoir." Journal of canadian petroleum technology 49.10 (2010): 75-82.

Conway, Drew, and John White. Machine learning for hackers. " O'Reilly Media, Inc.", 2012.

Crain, Eric Ross, and P. Eng. Crain's Petrophysical Pocket Pal. Ontario: ER Ross, 2006.

Dang, Ha Song, An Hai Le, and Duc Minh Do. "Correction and supplementingation of the well log curves for Cuu Long oil basin by using the Artificial Neural Networks." VNU Journal of Science: Earth and Environmental Sciences 33.1 (2017).

Dangeti, Pratap. Statistics for machine learning. Packt Publishing Ltd, 2017.

DELL'AVERSANA, Paolo. "Comparison of different Machine Learning algorithms for lithofacies classification from well logs." Bollettino di Geofisica Teorica ed Applicata 60.1 (2019).

Deng, C., Pan, H., Fang, S., Konaté, A. A., & Qin, R. "Support vector machine as an alternative method for lithology classification of crystalline rocks." Journal of Geophysics and Engineering 14.2 (2017): 341-349.

Donselaar, Marinus E., and Jasper M. Schmidt. "Integration of outcrop and borehole image logs for high-resolution facies interpretation: example from a fluvial fan in the Ebro Basin, Spain." Sedimentology 52.5 (2005): 1021-1042.

Fiacco, Anthony V., and Garth P. McCormick. Nonlinear programming: sequential unconstrained minimization techniques. Vol. 4. Siam, 1990.

Freedonia Group (2015), Logging & Measuring Services to Reach $6.2 Billion in 2019 from: https://www.upstreampumping.com/article/2015/logging-measuring-services-reach-62-billion-2019

Ghiasi-Freez, J., M. Ziaii, A. Kadkhodaie-Ilkhchi, and J. Honarmand. "A reservoir rock porosity estimation through image analysis and fuzzy logic techniques." Energy Sources, Part A: Recovery, Utilization, and Environmental Effects 36.12 (2014): 1276-1284.

Glover, Paul WJ. "Petrophysics." University of Aberdeen, UK (2000).

Glover, Paul. "Formation Evaluation MSC course notes." Aberdeen University (2001): 84-94.

Hastie, Trevor, Robert Tibshirani, and Jerome Friedman. The elements of statistical learning: data mining, inference, and prediction. Springer Science & Business Media, 2009.

Höök, Mikael. Coal and oil: The dark monarchs of global energy: understanding supply and extraction patterns and their importance for future production. Diss. Acta Acta Universitatis Upsaliensis, 2010.

Hsieh, Cho-Jui, Kai-Wei Chang, Chih-Jen Lin, S. Sathiya Keerthi, and Sellamanickam Sundararajan. "A dual coordinate descent method for large-scale linear SVM." Proceedings of the 25th international conference on Machine learning. 2008.

James, Gareth, Daniela Witten, Trevor Hastie, and Robert Tibshirani. An introduction to statistical learning. Vol. 112. New York: springer, 2013.

Kadkhodaie, Ali, and Reza Rezaee. "Intelligent sequence stratigraphy through a wavelet-based decomposition of well log data." Journal of Natural Gas Science and Engineering 40 (2017): 38-50.

Kalanaki, Moosa, Jaber Soltani, and Sajjad Tavassoli. "The use of hybrid SVR-PSO model to predict pipes failure rates." International journal of science and engineering research 4.11 (2013): 1022-1025.

Karmarkar, Narendra. "A new polynomial-time algorithm for linear programming." Proceedings of the sixteenth annual ACM symposium on Theory of computing. 1984.

Kennedy, James, and Russell Eberhart. "Particle swarm optimization." Proceedings of ICNN'95-International Conference on Neural Networks. Vol. 4. IEEE, 1995.

Krief, M., Garat, J., Stellingwerff, J., & Ventre, J. "A petrophysical interpretation using the velocities of P and S waves (full-waveform sonic)." The Log Analyst 31.06 (1990).

Li, Ning, Hongliang Wu, Qingfu Feng, Kewen Wang, Yujiang Shi, Qingfeng Li, and Xinping Luo. "Matrix porosity calculation in volcanic and dolomite reservoirs and its application." Applied Geophysics 6.3 (2009): 287.

Li, Zhongwei, Yuqi Xie, Xueqiang Li, and Wenyang Zhao. "Prediction and application of porosity based on support vector regression model optimized by adaptive dragonfly algorithm." Energy Sources, Part A: Recovery, Utilization, and Environmental Effects (2019): 1-14.

Liu, Hsiou-Hsiang, Lung-Cheng Chang, Chien-Wei Li, and Cheng-Hong Yang. "Particle swarm optimization-based support vector regression for tourist arrivals forecasting." Computational Intelligence and Neuroscience 2018 (2018).

Mazilu, Sinziana, and José Iria. "L1 vs. L2 regularization in text classification when learning from labeled features." 2011 10th International Conference on Machine Learning and Applications and Workshops. Vol. 1. IEEE, 2011.

Mitchell, Tom M. "Machine learning." (1997).

Mohagheghian, Erfan. An application of evolutionary algorithms for WAG optimisation in the Norne Field. Diss. Memorial University of Newfoundland, 2016.

Müller, Andreas C., and Sarah Guido. Introduction to machine learning with Python: a guide for data scientists. " O'Reilly Media, Inc.", 2016.

Müller, K. R., Smola, A. J., Rätsch, G., Schölkopf, B., Kohlmorgen, J., & Vapnik, V. "Predicting time series with support vector machines." International Conference on Artificial Neural Networks. Springer, Berlin, Heidelberg, 1997.

Norwegian Petroleum Directorate (2020), Factpages: Field Varg. Retrieved from: https://factpages.npd.no/en/field/pageview/shutdown/43451

Ohm, Georg Simon. The galvanic chain processed mathematically. TH Riemann, 1827.

Onalo, David, Sunday Adedigba, Faisal Khan, Lesley A. James, and Stephen Butt. "Data driven model for sonic well log prediction." Journal of Petroleum Science and Engineering 170 (2018): 1022-1037.

Osuna, Edgar, Robert Freund, and Federico Girosi. "An improved training algorithm for support vector machines." Neural networks for signal processing VII. Proceedings of the 1997 IEEE signal processing society workshop. IEEE, 1997.

Pirson, Sylvain J. "Handbook of well log analysis for oil and gas formation evaluation." (1963).

Platt, John. "Sequential minimal optimization: A fast algorithm for training support vector machines." (1998).

Pu, Xiugang, Zhilong Huang, Jiansheng Zhou, Dun-qing XIAO, and Sa LIU. "Quantitative characterization of the controlling effect of pore structure on the physical property of clastic reservoir." XIAN SHIYOU DAXUE XUEBAO ZIRAN KEXUE BAN 21.2 (2006): 15.

Raymer, L. L., E. R. Hunt, and John S. Gardner. "An improved sonic transit time-to-porosity transform." SPWLA 21st annual logging symposium. Society of Petrophysicists and Well-Log Analysts, 1980.

Salmachi A, Sayyafzadeh M, Haghighi M (2013) Infill well placement optimization in coal bed methane reservoirs using genetic algorithm. Fuel 111:248–258

Samuel, Arthur L. "Some studies in machine learning using the game of checkers." IBM Journal of research and development 3.3 (1959): 210-229.

Schlumberger. (1974). Log Interpretation Manual/Applications. Vol. 2. Houston Schlumberger Well Service Inc.

Shahabi, Himan, Bakhtyar Ali Ahmad, Baharin Bin Ahmad, Mohammad Javad Taheri Amiri, Soroush Keihanfard, and Saeed Ebrahimi. "Assessment of WLC and Fuzzy Logic Methods for Sit e Selection of Water Reservoirs in Malaysia." Polish Journal of Environmental Studies 25.3 (2016).

Shawe-Taylor, J. and Sun, S., 2011. A review of optimization methodologies in support vector machines. Neurocomputing, 74(17), pp.3609-3618.

Shi, Yuhui, and Russell Eberhart. "A modified particle swarm optimizer." 1998 IEEE international conference on evolutionary computation proceedings. IEEE world congress on computational intelligence (Cat. No. 98TH8360). IEEE, 1998.

Smola, Alex J., and Bernhard Schölkopf. "A tutorial on support vector regression." Statistics and computing 14.3 (2004): 199-222.

Statoil. Completion Report Well 15/12-5 PL 038. Statoil, 1986

Statoil. Completion Report Well 15/12-6S PL 038. Statoil, 1990

Statoil. Completion Report Well 15/12-9S PL 038. Statoil, 1993

Stitson, Mark, Alex Gammerman, Vladimir Vapnik, Volodya Vovk, Chris Watkins, and Jason Weston. "Support vector regression with ANOVA decomposition kernels." Advances in kernel methods—Support vector learning (1999): 285-292.

Suykens, Johan AK, and Joos Vandewalle. "Least squares support vector machine classifiers." Neural processing letters 9.3 (1999): 293-300.

Székely, Gábor J., Maria L. Rizzo, and Nail K. Bakirov. "Measuring and testing dependence by correlation of distances." The annals of statistics 35.6 (2007): 2769-2794.

Tittman, Jay, and J. S. Wahl. "The physical foundations of formation density logging (gamma-gamma)." Geophysics 30.2 (1965): 284-294.

Tukey, John W. "Comparing individual means in the analysis of variance." Biometrics (1949): 99-114.

Vapnik V. 1995. The Nature of Statistical Learning Theory. Springer, New York.

Vapnik, Vladimir, Steven E. Golowich, and Alex J. Smola. "Support vector method for function approximation, regression estimation and signal processing." Advances in neural information processing systems. 1997.

Vapnik, Vladimir. Estimation of dependences based on empirical data. Springer Science & Business Media, 2006.

Wang, Dahai, Jun Peng, Qian Yu, Yuanyuan Chen, and Hanghang Yu. "Support vector machine algorithm for automatically identifying depositional microfacies using well logs." Sustainability 11.7 (2019): 1919.

Wendt, W.A., Sakurai, S., Nelson, P.H., 1985. Permeability prediction from well logs using multiple regression. In: Lake, L.W., Caroll, H.B.J. (Eds.), Reservoir Characterization. Academic Press, New York.

Wyllie, M. R. J., A. R. Gregory, and G. H. F. Gardner. "An experimental investigation of factors affecting elastic wave velocities in porous media." Geophysics 23.3 (1958): 459-493.

Yaeger, Larry S., Richard F. Lyon, and Brandyn J. Webb. "Effective training of a neural network character classifier for word recognition." Advances in neural information processing systems. 1997.

Yann LeCun, Yoshua Bengio, and Geoffrey E. Hinton. Deep learning. Nature, 521(7553):436–444, 2015.

Zhang, Jie, Xin Nie, Suyun Xiao, Chong Zhang, Chaomo Zhang, and Zhansong Zhang. "Generating porosity spectrum of carbonate reservoirs using ultrasonic imaging log." Acta Geophysica 66.2 (2018): 191-201.

Zhou, Qi, Wei Wu, Dongpeng Liu, Kaikai Li, and Qiao Qiao. "Estimation of corrosion failure likelihood of oil and gas pipeline based on fuzzy logic approach." Engineering Failure Analysis 70 (2016): 48-55.

Appendix

Well logs dataset (Well 15/12-5)

DT	CA	GR	DR	RHOB	CNC	POR
81.2153	9.3052	88.8625	1.7826	2.4832	20.297	0.082
81.6998	9.2371	90.1049	1.7768	2.4732	20.6701	0.07
82.5162	9.1621	90.986	1.7742	2.4825	21.6049	0.075
82.2469	9.1285	89.7354	1.7827	2.4848	21.013	0.07
81.3693	9.0664	88.6989	1.8328	2.4347	21.4587	0.078
81.6266	9.0454	87.7778	1.8398	2.4216	21.4248	0.072
81.5932	9.033	88.8979	1.8381	2.4269	21.3466	0.08
81.4977	9.0292	89.4596	1.8388	2.4531	20.9949	0.073
81.3992	9.0375	87.018	1.8413	2.4585	20.6543	0.072
81.4856	9.0434	84.17	1.8439	2.4564	21.0363	0.077
81.924	9.0405	86.8776	1.8431	2.4459	21.6084	0.078
82.5582	9.0355	90.3839	1.8419	2.4314	21.7267	0.071
82.2426	8.862	90.1166	1.9158	2.4633	21.748	0.074
81.1013	8.8594	90.9492	1.8959	2.4581	21.4412	0.077
81.2744	8.8571	91.0568	1.8863	2.4611	21.6233	0.073
81.4863	8.8457	91.0797	1.8706	2.4616	21.0303	0.086
81.4655	8.8479	90.2372	1.8495	2.4428	20.4283	0.075
81.4448	8.8592	87.7521	1.8049	2.4169	20.1886	0.078
81.5385	8.8556	86.6512	1.7713	2.4187	20.533	0.081
81.6706	8.8489	86.0969	1.738	2.3895	20.52	0.08
81.4465	8.8496	85.095	1.7258	2.383	19.9895	0.086
81.1163	8.8447	85.4208	1.7212	2.4424	20.1898	0.097
81.3283	8.8423	88.2352	1.7267	2.4757	20.966	0.099
81.6166	8.8368	89.9677	1.7451	2.4667	21.4572	0.072
81.022	8.8669	87.1616	1.7387	2.3973	20.3133	0.08
81.0191	8.8713	88.4046	1.7197	2.411	20.2809	0.082
81.1255	8.8652	88.51	1.7154	2.4377	20.028	0.078
81.0932	8.8578	84.8589	1.7109	2.4595	19.0967	0.105
80.8822	8.8555	85.5083	1.7222	2.4535	18.2637	0.091
81.0614	8.853	87.2752	1.7388	2.4161	18.6288	0.102
82.0434	8.8338	87.7814	1.7575	2.3945	20.5869	0.085
82.6952	8.8299	87.8393	1.7636	2.4248	22.2563	0.092
82.4709	8.8433	88.6685	1.7651	2.4605	22.6234	0.092
81.9391	8.8221	89.86	1.7613	2.4589	21.2079	0.093
81.5825	8.7802	91.3703	1.7488	2.467	19.5299	0.085
81.6968	8.776	91.1501	1.735	2.4811	19.6407	0.095
82.2392	8.7729	90.2003	1.7121	2.4748	20.2518	0.091
82.452	8.7587	88.3284	1.6933	2.4297	19.8046	0.095
82.0751	8.7581	84.0868	1.6738	2.3734	18.9427	0.098
81.7539	8.7635	82.6781	1.6678	2.3905	19.4734	0.1
81.6354	8.75	82.5153	1.6674	2.4373	20.195	0.105

81.4879	8.7351	81.7564	1.6717	2.4314	19.4358	0.105
81.3925	8.7282	79.7869	1.6934	2.4204	20.1153	0.097
81.4379	8.7088	78.8932	1.7184	2.4381	19.6708	0.102
81.4046	8.6976	78.6662	1.7388	2.4552	19.6048	0.105
81.2822	8.6828	78.9616	1.754	2.4661	20.0694	0.096
81.1234	8.6709	80.2364	1.7337	2.4394	20.2844	0.095
80.8677	8.6504	81.4071	1.6394	2.4045	20.5391	0.095
80.577	8.6175	79.8648	1.5176	2.398	20.0329	0.077
80.2065	8.5487	73.1844	1.3286	2.3891	18.1566	0.103
80.4977	8.4939	66.9379	1.2037	2.3875	17.0316	0.132
82.4211	8.4548	59.7404	1.0744	2.3844	17.1535	0.158
84.9536	8.4573	54.8894	1.0173	2.3834	18.5224	0.185
87.6901	8.4557	52.2188	0.9639	2.3564	20.8129	0.144
87.563	8.4325	55.6613	0.9359	2.3267	20.9943	0.171
85.6203	8.4023	58.6538	0.9081	2.3035	20.4308	0.195
85.0906	8.4027	54.9105	0.8959	2.3075	20.5253	0.204
86.8995	8.4221	49.1352	0.8915	2.2819	21.1969	0.172
88.5705	8.4235	48.0837	0.8984	2.2491	21.6364	0.178
86.9131	8.358	48.9096	1.0298	2.309	21.5034	0.19
88.5053	8.3316	45.9838	1.1123	2.2776	22.9691	0.166
88.1855	8.3035	44.3991	1.1842	2.2535	22.6247	0.171
84.8228	8.2899	41.0182	1.2797	2.2335	20.8149	0.243
82.4152	8.2863	38.974	1.3342	2.2477	20.1287	0.215
82.4678	8.2746	39.3202	1.3692	2.2908	20.567	0.227
84.0398	8.2846	40.8985	1.3551	2.2951	21.3121	0.19
85.3402	8.3131	43.5492	1.3097	2.2835	21.2578	0.16
85.3966	8.3092	45.7288	1.2787	2.2722	20.8857	0.231
85.2712	8.2856	46.9411	1.2607	2.2665	20.9262	0.238
85.674	8.2768	46.1244	1.274	2.2763	21.2281	0.271
87.1687	8.2835	44.1411	1.3154	2.2688	22.3684	0.247
88.6282	8.2998	43.1315	1.3474	2.2467	22.868	0.272
85.9776	8.2965	40.3213	1.4597	2.2463	21.7799	0.243
83.7541	8.3264	38.6701	1.4215	2.3212	20.4433	0.251
85.2752	8.3592	41.2052	1.3533	2.357	21.4642	0.207
87.8702	8.3455	43.9509	1.3091	2.3075	22.8186	0.287
89.6494	8.3189	44.2498	1.3006	2.2841	22.8596	0.264
89.7487	8.3091	42.9095	1.3531	2.2972	22.8488	0.176
89.7096	8.3241	41.017	1.4628	2.2777	23.9664	0.12
87.467	8.355	40.1137	1.5195	2.2516	23.9476	0.292
80.94	8.3803	38.5666	1.5301	2.2487	22.0003	0.244
79.3221	8.3797	37.418	1.4851	2.2822	21.7877	0.257
84.1986	8.3672	37.6819	1.376	2.2909	23.4613	0.28
88.0658	8.3581	39.1537	1.2899	2.2507	24.1987	0.284
90.403	8.3644	39.4657	1.211	2.1997	25.7574	0.29
91.7111	8.3778	38.4556	1.1949	2.184	26.3936	0.311
93.5121	8.3815	38.0609	1.201	2.1858	26.2148	0.296

94.2867	8.3852	37.84	1.2003	2.1904	26.4781	0.321
95.0268	8.4255	37.201	1.177	2.1621	27.0015	0.305
96.0013	8.5058	35.7702	1.0428	2.129	27.8144	0.225
94.9074	8.5517	36.887	0.8471	2.1697	26.5165	0.307
93.5638	8.5483	37.7182	0.8232	2.2135	25.1124	0.296
92.9794	8.5569	37.1798	0.8261	2.2118	25.183	0.286
93.5063	8.5793	35.9196	0.8778	2.1569	25.8665	0.117
91.409	8.5908	38.934	0.8972	2.1741	24.4048	0.249
86.81	8.575	40.6705	0.8784	2.2205	22.2545	0.264
81.387	8.5179	43.8274	0.8225	2.3238	20.8842	0.289
81.8831	8.4865	44.4202	0.776	2.3276	21.7792	0.276
86.7765	8.467	40.5898	0.7263	2.2344	24.1152	0.287
90.6019	8.479	38.568	0.7147	2.1825	25.4639	0.166
93.7318	8.5263	38.1696	0.7374	2.1299	25.9464	0.173
93.619	8.5344	38.2079	0.7855	2.1232	25.7523	0.274
90.1791	8.4972	38.5699	0.8911	2.1537	24.076	0.291
86.7893	8.4823	39.1619	1.001	2.1761	22.8064	0.271
85.8051	8.472	39.2539	1.177	2.1982	22.4902	0.262
88.677	8.462	36.5885	1.3329	2.1858	22.0329	0.225
93.0887	8.4419	30.2455	1.7207	2.1085	21.3412	0.279
90.8501	8.428	31.876	1.856	2.1179	19.9634	0.307
89.2854	8.4228	32.8702	1.8209	2.1544	19.6744	0.299
94.5016	8.379	33.3102	1.4975	2.2042	23.2257	0.204
99.3743	8.4056	32.8298	1.2884	2.1823	23.8192	0.26
91.0277	8.4651	37.2691	0.9578	2.2054	22.889	0.306
91.7656	8.473	37.4442	0.9268	2.1782	23.4244	0.307
97.2183	8.4882	36.2823	0.8814	2.1124	24.9403	0.3
100.9357	8.5056	35.2956	0.8466	2.0999	25.3179	0.306
102.287	8.5359	35.6845	0.7846	2.1174	24.4933	0.301
102.0598	8.5307	35.8561	0.7266	2.1268	24.0543	0.316
102.3975	8.4974	34.4574	0.6439	2.1167	23.7428	0.328
102.62	8.4923	35.3538	0.5876	2.1072	23.8061	0.273
101.7951	8.5225	36.8547	0.5298	2.1139	24.4101	0.281
100.0515	8.5414	35.8536	0.5102	2.127	24.0659	0.236
96.5401	8.5487	35.4521	0.5119	2.166	22.9372	0.26
93.108	8.5509	36.2453	0.5255	2.1975	21.6539	0.269

Well logs dataset (Well 15/12-6S)

80.641	10.000	53.261	1.824	2.449	14.662	0.107
80.469	12.000	59.179	1.845	2.432	16.002	0.109
79.969	8.000	54.741	1.801	2.539	18.498	0.106
80.063	8.000	50.302	1.791	2.436	15.763	0.102
79.836	9.500	56.590	1.777	2.480	15.704	0.106
80.109	10.000	51.042	1.766	2.450	18.453	0.114
80.281	11.000	56.220	1.749	2.493	14.775	0.107

80.094	10.000	56.960	1.714	2.431	20.127	0.103
80.266	15.000	60.658	1.680	2.415	16.005	0.102
80.313	15.000	52.521	1.658	2.471	14.941	0.110
80.141	11.000	51.782	1.615	2.449	15.170	0.112
79.766	11.000	54.741	1.601	2.465	14.271	0.114
80.578	10.000	50.302	1.678	2.438	18.641	0.119
80.156	11.500	54.371	1.693	2.464	19.587	0.101
79.063	14.000	60.658	1.727	2.543	17.245	0.127
79.156	10.000	59.179	1.757	2.480	18.280	0.107
79.469	9.500	58.069	1.712	2.440	17.336	0.103
79.500	10.000	56.220	1.670	2.399	20.282	0.101
78.813	6.000	53.261	1.620	2.397	25.078	0.128
79.703	6.500	45.864	1.619	2.498	20.186	0.122
79.313	8.000	51.042	1.626	2.480	16.539	0.128
77.094	9.000	50.302	1.658	2.507	18.044	0.117
78.406	12.000	54.001	1.683	2.422	15.629	0.144
78.250	11.000	56.220	1.713	2.440	17.649	0.134
78.586	10.000	52.891	1.751	2.494	17.759	0.118
78.547	11.000	49.562	1.796	2.428	14.636	0.095
77.086	11.500	53.631	1.828	2.421	19.630	0.129
83.898	8.500	53.261	2.089	2.378	17.062	0.117
84.609	7.000	48.823	2.246	2.376	19.086	0.113
78.195	9.500	44.384	2.384	2.430	21.222	0.136
79.531	11.000	37.727	2.640	2.327	15.835	0.121
79.711	11.000	39.576	2.845	2.387	17.802	0.108
79.250	12.000	39.946	2.908	2.412	16.692	0.119
79.391	11.000	43.275	2.824	2.340	16.847	0.148
79.422	12.000	44.384	2.677	2.324	13.945	0.121
77.852	7.500	45.494	2.462	2.341	19.163	0.171
76.781	11.000	53.261	2.250	2.438	15.286	0.158
76.727	9.500	54.371	2.112	2.462	16.760	0.154
77.438	13.000	58.439	2.053	2.313	15.907	0.159
77.141	12.000	54.001	2.043	2.516	18.673	0.157
75.563	11.000	53.261	2.116	2.427	15.980	0.163
71.250	12.500	54.371	2.264	2.464	14.517	0.110
70.266	12.000	48.823	2.511	2.537	17.449	0.113
71.578	14.500	55.850	2.809	2.551	14.484	0.108
71.750	13.000	70.275	3.174	2.481	14.922	0.133
70.180	12.500	60.289	3.941	2.513	14.109	0.130
68.938	15.000	58.439	5.145	2.608	14.943	0.126
66.680	15.000	51.412	7.344	2.505	14.727	0.093
60.391	15.000	42.165	10.442	2.587	12.093	0.112
57.383	13.500	32.548	13.785	2.579	12.440	0.109
57.281	11.000	28.110	18.673	2.395	7.854	0.119
57.016	12.000	26.261	21.572	2.643	8.398	0.097
61.281	11.000	28.110	22.854	2.536	6.415	0.095

62.258	10.500	25.521	23.197	2.497	5.684	0.094
66.281	8.000	24.411	22.585	2.524	7.127	0.091
72.297	13.000	24.041	23.298	2.439	8.423	0.135
77.000	13.000	23.672	25.273	2.292	8.938	0.104
71.844	12.500	22.562	26.554	2.392	13.334	0.075
57.531	15.000	27.370	27.210	2.433	11.350	0.060
59.898	14.000	21.452	30.019	2.532	7.864	0.108
66.125	11.000	21.452	33.868	2.552	6.363	0.120
56.117	11.000	23.302	36.112	2.527	9.182	0.142
44.078	12.000	21.452	36.821	2.418	7.575	0.119
50.203	10.500	23.302	36.075	2.434	11.982	0.075
54.156	11.000	23.672	33.851	2.478	8.939	0.089
74.797	12.000	24.041	28.049	2.391	11.836	0.160
84.219	16.500	23.672	20.760	2.228	14.794	0.076
89.359	12.000	25.891	17.601	2.299	18.939	0.146
99.547	14.500	26.261	16.402	2.232	26.058	0.103
106.141	13.000	25.891	15.749	2.136	17.690	0.136
100.750	12.000	25.151	15.039	2.041	21.566	0.145
98.031	11.000	25.151	14.348	2.175	16.286	0.262
94.773	11.000	25.521	13.552	2.261	16.767	0.141
98.625	9.000	25.891	11.474	2.121	21.395	0.211
107.313	13.000	33.288	8.681	2.222	22.634	0.289
95.633	14.500	28.850	7.596	2.147	24.606	0.229
84.969	12.000	29.589	7.308	2.187	21.659	0.283
86.102	13.000	29.959	7.670	2.196	19.494	0.294
87.359	16.000	31.069	8.499	2.059	21.292	0.303
95.055	17.500	29.589	9.591	2.319	15.545	0.310
106.234	16.000	28.850	10.511	2.267	23.773	0.297
111.375	13.500	25.151	11.498	2.143	16.683	0.228
110.547	13.000	25.891	12.016	2.108	20.993	0.274
112.109	14.500	27.370	11.480	2.127	23.745	0.188
105.125	15.000	28.850	11.065	2.133	25.488	0.209
102.867	10.500	27.740	10.925	2.050	20.028	0.302
102.797	11.000	30.329	10.932	2.100	21.893	0.308
102.328	16.500	25.521	10.831	2.209	22.281	0.291
103.031	13.000	26.631	10.414	2.185	18.673	0.301
98.219	12.000	27.000	9.717	2.191	22.210	0.295
93.891	15.000	28.110	8.873	2.162	19.349	0.315
93.586	15.500	26.631	7.857	2.196	19.016	0.297
96.078	14.000	31.069	6.922	2.144	17.635	0.296
95.695	14.000	30.699	6.496	2.196	19.043	0.282
93.750	14.000	33.288	6.625	2.208	18.744	0.291
92.289	11.500	31.439	7.068	2.195	20.230	0.210
92.109	12.000	31.069	7.647	2.299	20.251	0.255
92.195	13.500	26.631	8.140	2.217	19.451	0.278
89.641	11.000	27.370	8.433	2.165	22.543	0.212

87.773	13.000	26.631	8.365	2.191	16.704	0.228
86.594	14.000	30.329	8.390	2.186	20.693	0.233
83.594	12.500	31.439	8.248	2.262	18.572	0.287
81.141	12.000	27.370	7.999	2.227	23.549	0.246
74.852	10.500	27.000	7.660	2.157	19.346	0.229
70.078	12.000	28.110	7.281	2.126	19.137	0.267
72.102	9.500	29.220	6.765	2.155	20.898	0.326
90.891	11.000	29.589	6.307	2.147	18.901	0.304
89.992	13.000	25.521	6.263	2.239	22.174	0.225
90.563	11.000	40.686	6.493	2.262	25.290	0.238
85.055	10.000	34.398	6.932	2.208	22.227	0.241
86.328	10.000	30.329	7.836	2.266	20.555	0.377
91.938	10.500	28.480	9.452	2.176	19.357	0.301
98.563	10.000	26.631	10.536	2.223	22.763	0.295
94.070	13.000	26.261	11.167	2.107	20.642	0.254
82.047	15.000	22.192	11.546	2.204	20.159	0.281
87.906	12.000	23.672	11.556	2.186	19.421	0.275
91.188	13.000	33.288	10.837	2.165	14.038	0.307
84.063	14.500	27.740	10.076	2.221	14.993	0.286
77.875	9.000	28.110	9.973	2.335	17.203	0.293
93.313	10.000	25.891	10.229	2.180	17.152	0.229
102.578	10.000	27.370	9.970	2.096	22.325	0.229
89.508	12.000	22.932	9.487	2.017	21.458	0.322
90.500	14.000	22.932	9.024	2.286	20.909	0.317
95.367	12.500	25.521	8.550	2.107	17.674	0.157
97.594	12.000	26.631	7.938	2.069	23.396	0.261
95.172	10.500	22.562	7.553	1.999	22.028	0.321
94.375	10.000	23.672	7.446	1.981	28.975	0.336
95.242	12.000	21.822	7.113	2.020	23.432	0.122
89.672	10.000	21.452	6.542	2.107	32.989	0.325
96.539	11.500	22.562	5.967	2.185	31.268	0.344
101.203	10.000	26.631	5.525	2.093	19.491	0.194
104.844	12.000	29.220	5.188	2.076	26.981	0.326
102.750	10.000	34.028	5.161	2.096	25.327	0.237
103.680	10.000	29.959	5.381	2.143	24.328	0.099
104.828	9.000	25.151	5.689	2.032	21.324	0.190
103.289	9.000	29.589	6.018	2.114	30.108	0.232
101.930	9.500	29.959	6.138	2.029	27.349	0.319
98.375	7.000	29.589	6.264	2.005	31.866	0.304
93.234	11.000	28.480	6.511	2.018	27.754	0.288
90.266	9.000	28.110	6.536	2.131	21.654	0.334
81.164	8.000	26.631	6.228	2.154	22.260	0.354
84.578	8.000	24.411	5.700	2.260	19.603	0.372
92.711	8.500	26.631	5.485	2.223	21.726	0.381
97.438	8.000	26.631	5.345	2.090	19.427	0.363
85.352	8.000	32.918	5.411	2.077	22.051	0.309

77.500	12.000	31.809	5.467	2.244	26.226	0.288
75.375	20.000	27.740	5.467	2.372	15.288	0.253
77.563	12.000	34.768	5.320	2.302	15.008	0.248
77.148	10.500	32.918	4.748	2.265	15.779	0.327
82.641	11.000	37.727	4.088	2.405	11.497	0.304
85.406	10.500	42.535	3.339	2.306	18.441	0.312
84.500	11.000	42.165	2.784	2.257	22.159	0.114
76.211	10.000	39.206	2.493	2.425	18.292	0.191
73.547	7.000	42.905	2.327	2.511	12.872	0.107
76.320	9.000	45.864	2.181	2.410	18.281	0.132
79.813	10.000	49.562	2.012	2.466	10.916	0.203
83.281	9.500	46.603	1.898	2.416	16.016	0.190
82.563	9.000	45.864	1.927	2.367	18.301	0.150
81.078	10.000	50.302	1.919	2.403	21.433	0.127
81.641	8.500	45.124	2.010	2.342	19.501	0.086
81.016	9.000	40.686	2.146	2.425	15.902	0.142
81.813	9.500	45.494	2.241	2.410	18.367	0.180
84.406	13.000	44.384	2.328	2.404	21.392	0.164
87.422	10.000	37.727	2.664	2.239	27.517	0.177
83.297	9.000	33.658	2.934	2.345	25.056	0.242
81.953	11.000	41.425	3.044	2.292	30.114	0.201
81.008	12.500	34.398	3.028	2.272	18.520	0.176
78.672	13.000	31.809	2.840	2.308	29.352	0.160
92.750	10.000	44.384	2.828	2.351	19.611	0.149
96.203	10.500	42.165	2.687	2.500	29.823	0.207
91.922	9.000	32.548	2.705	2.295	20.806	0.248
90.758	11.000	35.138	2.870	2.196	34.174	0.172
89.547	11.000	36.247	2.916	2.183	32.452	0.231
89.711	9.500	37.727	2.773	2.243	24.748	0.099
90.063	10.000	30.329	2.665	2.231	25.620	0.261
90.938	10.500	34.398	2.586	2.169	19.095	0.281
91.219	11.000	31.809	2.528	2.211	27.195	0.259
90.828	10.000	36.617	2.509	2.176	39.806	0.253
88.188	8.000	41.425	2.529	2.168	31.330	0.255
88.016	7.500	38.096	2.589	2.280	21.123	0.286
86.969	8.000	33.288	2.608	2.192	19.218	0.210
85.422	8.500	38.466	2.520	2.281	20.324	0.210
83.109	9.000	41.425	2.464	2.222	24.641	0.231
82.555	7.000	39.946	2.434	2.360	27.371	0.224
84.063	9.000	36.987	2.377	2.381	18.861	0.186
88.250	9.000	38.466	2.332	2.263	16.938	0.257
90.563	9.000	38.466	2.318	2.289	21.015	0.203
91.711	7.500	38.096	2.310	2.264	26.456	0.227
89.313	8.000	39.206	2.317	2.129	25.863	0.234
77.414	9.500	36.987	2.598	2.357	15.312	0.065
73.891	10.000	27.370	2.478	2.446	18.110	0.217

70.789	6.500	35.877	2.304	2.481	17.688	0.248
72.297	13.000	42.905	2.184	2.459	15.861	0.227
76.695	10.500	35.507	2.004	2.466	13.353	0.280
84.828	10.000	40.686	1.784	2.407	19.470	0.234
83.789	9.500	39.576	1.740	2.305	19.721	0.194
78.813	9.000	49.562	1.748	2.363	21.764	0.160
77.055	10.500	45.124	1.792	2.492	20.429	0.148
84.594	9.000	39.206	1.854	2.518	20.430	0.140
90.461	10.500	35.138	1.977	2.301	21.630	0.072
92.328	13.000	31.069	2.062	2.314	27.573	0.217
92.695	12.000	27.000	2.099	2.276	18.349	0.230
89.453	10.000	26.631	2.174	2.338	18.753	0.159
87.063	7.000	30.329	2.156	2.476	18.858	0.123
90.453	11.000	32.548	2.087	2.322	17.557	0.100
97.484	7.500	34.398	2.110	2.223	26.047	0.217
95.219	8.000	42.905	2.176	2.269	22.125	0.207
92.156	11.000	45.124	2.203	2.222	26.109	0.241
90.703	12.000	42.905	2.254	2.271	17.506	0.245
92.672	11.000	30.329	2.333	2.319	22.956	0.165
98.031	12.000	30.329	2.381	2.311	21.803	0.197
100.414	11.500	32.918	2.337	2.154	24.457	0.247
90.766	16.000	36.987	2.191	2.265	21.306	0.282
89.211	13.500	32.179	1.975	2.306	13.193	0.228
91.219	14.000	38.466	1.842	2.263	15.125	0.206
89.070	14.000	42.905	1.777	2.254	23.897	0.189
84.578	17.000	39.946	1.816	2.452	17.509	0.141
90.109	18.500	38.836	1.927	2.418	18.674	0.276
94.219	14.000	34.768	2.128	2.383	15.353	0.277
100.086	15.000	31.439	2.347	2.243	16.700	0.179
96.266	13.000	30.329	2.468	2.246	24.760	0.185
99.211	9.000	28.850	2.578	2.273	20.316	0.209
92.234	12.000	34.768	2.911	2.239	28.757	0.116
89.313	13.000	32.918	3.317	2.335	18.160	0.196
88.875	13.000	33.288	3.819	2.312	18.963	0.176
55.398	12.000	28.110	9.304	2.497	11.832	0.296
52.438	9.000	26.631	12.095	2.634	8.663	0.272
50.023	10.500	27.000	14.418	2.698	4.936	0.253
51.938	12.000	22.932	16.410	2.643	3.970	0.161
51.297	9.000	24.041	17.192	2.721	3.808	0.241
53.594	9.000	28.850	14.997	2.735	5.126	0.035
55.508	13.000	26.631	9.764	2.767	6.965	0.077
56.484	16.000	25.891	6.327	2.756	8.358	0.033
64.125	16.500	25.891	4.753	2.773	7.544	0.035
85.641	16.000	27.370	3.520	2.379	11.793	0.030
101.344	17.000	28.850	2.942	2.321	18.063	0.029
102.906	15.000	30.329	2.604	2.246	24.175	0.034

104.602	16.000	31.439	2.463	2.216	17.616	0.067
101.656	17.000	31.069	2.374	2.250	23.739	0.039
101.305	14.500	33.288	2.289	2.162	16.050	0.047
98.781	11.000	34.028	2.166	2.185	25.131	0.151
87.172	18.000	42.165	2.116	2.310	20.361	0.272
77.391	17.500	37.357	2.077	2.440	17.486	0.299
77.266	15.000	37.727	2.044	2.514	20.730	0.280
86.984	16.000	33.288	2.068	2.321	15.378	0.253
95.203	16.500	36.247	2.125	2.298	17.419	0.171
96.188	14.000	31.809	2.088	2.172	22.329	0.229
93.398	14.000	33.288	1.991	2.286	18.993	0.243
91.531	13.000	32.548	1.955	2.128	19.746	0.260
88.648	14.000	36.617	1.892	2.275	19.514	0.234
87.375	15.000	36.987	1.815	2.322	22.701	0.269
88.430	15.000	36.617	1.849	2.350	22.029	0.266
83.469	15.000	41.425	2.002	2.284	22.026	0.256
76.297	13.000	38.836	2.184	2.380	17.958	0.266
71.547	15.000	36.987	2.270	2.519	14.295	0.272
77.328	15.500	30.699	2.256	2.468	12.640	0.260
85.672	21.000	29.589	2.148	2.299	15.345	0.197
91.469	17.500	33.288	1.946	2.269	17.062	0.204
92.031	14.000	31.809	1.713	2.293	19.193	0.200
88.344	16.500	34.028	1.542	2.254	17.287	0.111
85.844	10.000	41.425	1.494	2.309	29.168	0.170
85.664	14.000	36.987	1.563	2.246	22.701	0.217
86.172	8.000	35.507	1.868	2.200	23.783	0.222
80.836	14.500	38.466	2.279	2.690	19.400	0.230
67.906	16.000	34.028	2.803	2.454	15.554	0.235
57.234	13.500	25.151	3.450	2.557	13.209	0.250
59.266	11.000	25.151	3.918	2.525	10.618	0.201
62.555	10.000	27.370	3.671	2.666	8.825	0.204
64.250	17.000	25.891	2.818	2.585	9.010	0.185
63.820	13.500	27.370	2.315	2.501	14.853	0.166
69.969	14.000	29.589	1.982	2.443	12.177	0.102
83.234	13.000	30.329	1.601	2.411	13.874	0.039
93.516	10.000	34.028	1.398	2.312	22.079	0.045
97.883	10.500	30.329	1.290	2.162	21.560	0.075
98.406	12.000	31.809	1.190	2.140	19.471	0.095
96.898	13.500	36.247	1.108	2.219	17.195	0.072
94.891	13.000	33.288	1.036	2.211	28.642	0.082
91.047	14.500	37.727	0.933	2.330	25.942	0.273
89.016	11.000	38.466	0.829	2.307	27.365	0.220
88.453	15.000	44.754	0.795	2.377	26.409	0.249
88.922	16.000	41.425	0.772	2.362	30.766	0.266
90.453	11.000	34.028	0.790	2.342	29.863	0.241
92.289	11.000	36.247	0.846	2.269	24.226	0.213

91.703	12.000	35.507	0.932	2.267	19.911	0.192
88.313	12.500	38.466	1.036	2.340	18.295	0.209
88.438	10.000	45.124	1.124	2.331	30.183	0.178
89.086	11.500	38.096	1.254	2.255	19.974	0.193
82.984	10.000	36.247	1.362	2.354	18.295	0.200
70.500	11.500	32.179	1.325	2.471	18.504	0.225
66.438	11.000	34.028	1.182	2.634	14.672	0.210
77.461	8.500	35.507	1.011	2.349	11.969	0.182
88.625	12.000	34.028	0.849	2.292	17.369	0.205
90.430	14.500	38.836	0.770	2.265	22.626	0.194
90.188	9.000	39.946	0.759	2.355	19.668	0.199
88.906	9.500	37.727	0.801	2.343	17.033	0.161
81.922	11.000	39.946	0.833	2.528	28.332	0.078
79.914	14.000	38.466	0.866	2.503	24.220	0.073
83.953	16.000	42.165	0.907	2.398	24.813	0.181
83.391	15.000	42.905	0.871	2.464	21.431	0.187
82.688	13.000	40.316	0.857	2.470	22.454	0.189
82.609	16.000	38.466	0.822	2.445	31.317	0.177
86.625	14.500	37.727	0.757	2.364	24.191	0.158
83.344	15.000	36.987	0.733	2.431	20.573	0.068
81.805	15.000	35.877	0.733	2.588	16.230	0.165
82.172	15.000	39.946	0.731	2.308	17.747	0.124
87.234	15.500	45.864	0.694	2.421	23.066	0.143
88.813	12.000	41.425	0.723	2.336	25.532	0.181
91.734	12.500	42.165	0.744	2.308	22.323	0.192
93.078	11.000	41.425	0.770	2.215	16.194	0.167
92.359	11.500	38.836	0.768	2.181	25.919	0.151
85.414	13.500	35.877	0.793	2.336	22.865	0.180
83.891	13.000	34.768	0.848	2.371	16.877	0.171
85.531	12.000	34.768	0.978	2.280	19.339	0.190
82.703	13.000	39.206	1.118	2.398	19.623	0.170
74.016	13.000	35.877	1.163	2.550	16.723	0.211
70.406	10.000	34.768	1.194	2.485	16.042	0.194
78.695	14.000	40.686	1.161	2.376	24.882	0.178
84.227	11.000	39.576	0.960	2.378	21.129	0.154
81.797	11.000	40.686	0.980	2.503	18.734	0.154
81.016	12.000	41.055	1.064	2.534	12.306	0.169
82.781	14.000	45.124	1.205	2.367	22.145	0.084
83.633	13.000	52.151	1.317	2.447	24.405	0.051
81.344	14.000	42.905	1.394	2.437	25.930	0.130
78.727	14.500	44.014	1.446	2.463	21.799	0.149
78.984	11.000	41.425	1.455	2.447	18.169	0.146
83.391	12.000	42.165	1.328	2.480	19.729	0.130
83.648	12.000	44.014	1.279	2.547	26.255	0.119
82.656	14.000	42.905	1.279	2.443	21.707	0.125
82.320	14.500	49.562	1.298	2.450	46.889	0.099

82.813	13.000	47.343	1.321	2.490	33.233	0.094
82.102	13.500	42.165	1.346	2.501	18.184	0.167
82.453	12.000	51.042	1.380	2.448	27.380	0.116
100.828	12.000	45.864	1.866	2.496	25.759	0.111
101.492	11.500	45.864	2.254	2.453	34.578	0.114
98.016	16.000	43.644	2.877	2.522	24.171	0.121
99.445	18.000	40.316	3.797	2.066	25.258	0.119
85.563	16.000	27.370	6.921	2.230	31.907	0.122
80.922	14.500	29.220	6.770	2.406	22.765	0.126
70.227	14.000	29.220	3.309	2.579	12.191	0.035
77.359	16.000	26.631	3.588	2.563	11.287	0.081
75.109	18.000	33.288	3.862	2.634	21.165	0.124
83.531	16.000	31.809	3.658	2.433	17.846	0.050
87.109	13.000	43.644	3.372	2.256	54.266	0.053
77.828	15.000	65.837	2.393	2.298	47.526	0.094
86.375	12.000	51.412	2.117	2.918	21.138	0.078
124.063	15.000	44.384	1.838	2.061	29.312	0.047
59.703	14.000	38.096	3.409	2.809	16.230	0.049
57.781	11.500	38.096	3.272	2.774	14.338	0.034
56.234	13.000	37.727	2.936	2.666	17.299	0.021
56.344	13.000	44.014	2.524	2.405	15.515	0.037
75.688	10.000	54.371	2.329	2.543	19.073	0.078
76.906	10.000	49.562	2.140	2.577	20.591	0.070
75.813	12.000	51.412	1.978	2.512	24.884	0.085
77.344	15.000	43.644	1.821	2.528	20.171	0.087
77.000	12.000	45.864	1.717	2.557	12.303	0.086
76.266	12.000	48.083	1.700	2.413	22.155	0.110

Well logs dataset (Well 15/12-9S)

DT	CA	GR	DR	RHOB	CNC	POR
87.698	8.771	61.666	2.649	2.340	19.387	0.174
87.803	8.755	60.079	2.668	2.332	19.673	0.191
88.219	8.754	59.949	2.680	2.310	20.450	0.176
88.253	8.754	60.308	2.704	2.287	20.531	0.202
87.615	8.754	60.851	2.744	2.298	20.222	0.179
87.137	8.753	61.166	2.779	2.321	20.360	0.177
87.572	8.738	60.731	2.813	2.321	20.686	0.183
88.365	8.698	61.124	2.875	2.302	20.932	0.172
88.595	8.665	61.764	2.990	2.286	20.908	0.236
87.961	8.656	60.283	3.125	2.290	20.419	0.221
86.719	8.656	57.822	3.217	2.297	20.084	0.159
86.222	8.656	56.818	3.307	2.288	20.507	0.213
86.678	8.654	56.356	3.434	2.296	20.768	0.231
87.171	8.640	54.801	3.523	2.311	20.452	0.186
87.593	8.608	54.572	3.553	2.299	20.439	0.158

88.412	8.575	55.698	3.584	2.281	21.240	0.237
88.772	8.560	55.862	3.624	2.270	22.059	0.232
88.346	8.557	55.884	3.594	2.267	22.119	0.233
87.889	8.559	57.411	3.528	2.265	22.402	0.190
87.757	8.581	59.571	3.519	2.258	23.221	0.192
87.741	8.622	59.329	3.553	2.275	23.201	0.241
87.363	8.646	58.093	3.603	2.303	22.398	0.198
86.473	8.625	58.391	3.675	2.299	22.303	0.193
85.950	8.583	57.872	3.806	2.261	23.023	0.204
86.552	8.561	55.134	4.029	2.221	23.545	0.198
87.943	8.557	52.160	4.275	2.205	23.944	0.181
89.627	8.556	51.184	4.482	2.217	24.629	0.257
90.538	8.534	52.854	4.625	2.239	24.849	0.197
91.731	8.493	54.005	4.705	2.245	24.032	0.235
95.103	8.464	53.765	4.740	2.244	23.177	0.217
97.785	8.459	54.372	4.807	2.254	22.685	0.238
99.613	8.459	54.689	4.892	2.259	21.929	0.231
104.341	8.466	53.623	4.953	2.245	21.724	0.226
109.552	8.501	53.847	5.037	2.237	21.953	0.239
111.535	8.552	55.163	5.102	2.242	21.630	0.241
111.427	8.572	55.081	5.004	2.239	21.387	0.208
110.093	8.564	54.180	4.775	2.234	21.571	0.229
104.035	8.568	53.578	4.576	2.264	21.232	0.251
91.525	8.605	55.198	4.542	2.317	20.086	0.269
81.431	8.642	58.836	4.659	2.314	19.748	0.149
78.463	8.653	59.529	5.006	2.258	20.948	0.165
81.871	8.632	56.534	5.924	2.213	22.185	0.252
87.715	8.585	55.026	7.706	2.180	23.039	0.236
93.092	8.524	54.054	10.275	2.168	23.497	0.314
99.915	8.481	51.490	12.360	2.180	22.914	0.269
103.395	8.472	49.223	13.318	2.215	20.962	0.250
95.001	8.476	46.955	13.508	2.290	18.068	0.259
84.831	8.467	45.183	13.585	2.336	17.587	0.079
84.482	8.459	45.135	13.720	2.270	18.394	0.236
91.656	8.459	45.743	13.688	2.192	22.099	0.315
97.361	8.459	46.971	13.406	2.157	23.971	0.301
99.001	8.459	48.680	13.190	2.143	24.458	0.283
95.557	8.459	50.833	13.403	2.139	24.474	0.296
87.925	8.459	51.373	13.830	2.134	24.173	0.292
80.440	8.459	50.027	14.091	2.129	23.819	0.297
76.321	8.459	50.216	13.847	2.126	23.601	0.276
77.903	8.459	49.649	13.028	2.119	23.891	0.275
88.565	8.459	47.629	11.633	2.109	24.401	0.269
97.757	8.459	47.762	10.181	2.105	24.629	0.307
100.300	8.459	50.214	9.104	2.110	24.892	0.286
99.990	8.459	52.801	8.313	2.137	24.639	0.299

98.316	8.459	52.439	7.603	2.192	23.192	0.250
94.770	8.459	50.362	7.038	2.240	21.873	0.236
90.586	8.459	50.180	6.717	2.250	21.320	0.259
88.276	8.459	52.854	6.546	2.238	21.131	0.215
88.438	8.460	56.796	6.446	2.227	21.142	0.251
89.736	8.474	58.238	6.488	2.221	21.067	0.258
90.730	8.493	57.126	6.747	2.195	21.166	0.225
91.545	8.500	55.646	7.314	2.156	22.044	0.284
92.407	8.520	53.562	8.457	2.128	23.211	0.288
93.868	8.557	46.078	12.110	2.127	22.338	0.334
94.540	8.557	44.730	13.279	2.124	20.960	0.288
94.414	8.557	44.908	13.562	2.125	20.198	0.262
93.724	8.557	44.680	13.364	2.136	20.159	0.265
93.952	8.557	44.348	13.576	2.150	20.290	0.297
95.320	8.557	43.732	14.830	2.165	20.045	0.273
98.158	8.557	30.881	33.965	2.157	18.276	0.253
97.581	8.557	31.398	35.438	2.162	18.819	0.251
96.949	8.557	33.179	33.979	2.174	18.584	0.264
95.135	8.554	33.986	32.418	2.219	16.729	0.234
90.905	8.544	33.637	31.339	2.296	13.679	0.218
83.561	8.541	33.526	29.111	2.385	10.799	0.213
74.807	8.551	33.665	24.985	2.462	8.769	0.114
67.190	8.557	35.578	20.243	2.466	8.827	0.082
66.099	8.557	40.600	16.023	2.416	10.955	0.174
71.516	8.557	43.878	12.755	2.381	12.787	0.144
76.871	8.557	43.352	10.647	2.342	14.436	0.133
79.041	8.557	44.225	9.681	2.278	16.570	0.198
81.494	8.557	47.706	9.369	2.219	18.346	0.226
85.049	8.557	50.620	9.488	2.174	19.704	0.257
89.125	8.557	50.309	9.769	2.141	20.940	0.254
93.158	8.557	47.872	9.849	2.131	21.467	0.289
97.734	8.557	48.318	9.579	2.155	20.648	0.296
103.493	8.557	51.557	9.155	2.207	18.849	0.274
106.803	8.557	52.922	8.836	2.256	17.540	0.186
106.445	8.557	52.149	8.790	2.244	18.139	0.122
107.030	8.557	51.004	9.063	2.173	20.507	0.122
104.448	8.517	44.510	11.277	2.106	23.721	0.305
103.854	8.548	44.370	11.412	2.109	23.490	0.325
99.864	8.557	46.711	11.495	2.122	23.342	0.280
91.603	8.557	45.478	10.894	2.181	22.203	0.282
90.255	8.557	45.489	10.409	2.190	21.848	0.228
89.542	8.557	48.040	9.865	2.189	22.198	0.285
89.854	8.557	50.980	9.158	2.182	22.336	0.235
91.080	8.557	52.997	8.351	2.179	22.637	0.283
92.170	8.557	53.866	7.693	2.193	21.883	0.258
91.884	8.557	57.142	7.309	2.215	20.516	0.242

90.593	8.557	60.477	7.179	2.230	20.378	0.206
89.914	8.557	60.132	7.477	2.234	20.847	0.237
89.438	8.557	57.314	8.522	2.242	19.212	0.231
86.303	8.557	51.512	10.615	2.287	14.001	0.212
77.564	8.557	43.587	13.823	2.362	9.303	0.153
67.686	8.557	36.939	17.406	2.407	6.463	0.118
63.750	8.557	34.963	19.338	2.374	6.243	0.067
67.728	8.557	38.002	17.555	2.289	9.362	0.136
76.915	8.557	44.180	13.698	2.229	15.693	0.251
86.339	8.557	51.505	10.370	2.224	20.209	0.248
89.918	8.557	56.617	8.437	2.241	19.536	0.221
88.623	8.558	56.562	7.617	2.231	19.148	0.218
87.110	8.569	53.790	7.632	2.192	20.426	0.258
87.853	8.604	52.993	8.028	2.163	21.631	0.278
89.894	8.644	52.093	8.718	2.159	21.944	0.299
90.813	8.655	49.606	10.212	2.184	21.411	0.304
90.044	8.667	47.823	12.971	2.277	18.738	0.293
85.774	8.703	45.618	17.298	2.457	14.270	0.260
83.132	8.532	54.094	8.687	2.209	20.617	0.257
88.216	8.528	52.968	7.509	2.199	20.954	0.244
89.788	8.525	52.885	7.076	2.189	20.819	0.253
90.141	8.530	54.559	6.847	2.184	20.884	0.246
90.466	8.544	54.999	6.513	2.191	20.973	0.254
88.943	8.557	55.147	5.192	2.243	20.100	0.243
88.472	8.557	56.045	4.960	2.271	19.607	0.222
87.621	8.557	59.724	4.686	2.297	19.264	0.208
86.743	8.546	62.010	4.487	2.300	18.865	0.214
86.413	8.510	62.349	4.525	2.291	18.696	0.208
86.620	8.473	60.302	5.096	2.271	19.023	0.199
86.885	8.460	54.992	6.281	2.248	17.880	0.221
85.817	8.470	46.564	7.957	2.266	13.858	0.226
80.463	8.506	38.631	9.403	2.329	9.880	0.145
72.551	8.544	34.981	9.723	2.390	8.187	0.100
72.949	8.557	49.444	6.689	2.337	14.501	0.193
80.439	8.557	57.527	5.133	2.307	17.547	0.224
84.948	8.557	58.166	4.250	2.294	18.535	0.195
86.369	8.557	58.279	3.834	2.273	19.793	0.226
87.403	8.557	59.288	3.664	2.249	20.513	0.243
88.678	8.557	59.095	3.624	2.243	20.231	0.251
88.822	8.557	58.636	3.656	2.247	20.119	0.190
88.481	8.557	59.005	3.733	2.239	20.477	0.268
88.950	8.557	60.768	3.824	2.229	21.012	0.258
89.908	8.557	61.519	3.904	2.227	21.429	0.251
90.926	8.557	59.494	3.945	2.228	21.378	0.255
91.555	8.557	57.249	3.979	2.233	20.674	0.241
91.334	8.557	56.724	4.046	2.243	19.889	0.221

90.320	8.557	56.486	4.086	2.249	19.410	0.216
89.375	8.557	55.961	4.021	2.232	19.468	0.250
88.940	8.557	57.238	3.865	2.213	20.067	0.220
88.853	8.557	61.773	3.623	2.225	20.435	0.250
88.456	8.557	66.436	3.327	2.266	19.976	0.201
87.441	8.557	67.656	3.058	2.300	19.545	0.175
86.196	8.557	63.582	2.907	2.317	19.567	0.238
85.568	8.557	61.082	2.855	2.316	19.301	0.167
85.811	8.557	62.629	2.910	2.294	19.018	0.199
86.703	8.557	63.700	3.156	2.261	19.686	0.183
88.180	8.560	61.907	3.685	2.210	21.629	0.255
91.206	8.580	57.302	4.643	2.128	23.962	0.216
96.379	8.622	51.956	6.278	2.057	24.810	0.340
105.832	8.656	45.864	11.807	2.044	22.114	0.322
105.195	8.656	42.065	14.451	2.076	20.064	0.321
101.759	8.656	38.124	15.382	2.108	18.374	0.277
98.020	8.660	36.591	13.001	2.141	17.553	0.271
95.567	8.693	37.152	8.713	2.203	17.442	0.274
94.106	8.767	41.349	5.005	2.288	17.738	0.292
91.750	8.830	53.339	3.270	2.353	18.439	0.171
88.497	8.850	65.960	2.485	2.373	19.080	0.146
85.985	8.838	73.623	2.157	2.364	19.757	0.154
85.069	8.815	76.773	2.133	2.357	20.295	0.174
84.860	8.795	75.860	2.371	2.358	20.661	0.161
84.865	8.745	71.085	2.892	2.315	21.548	0.130
86.942	8.677	62.562	3.758	2.182	22.546	0.361
105.673	8.640	40.879	13.155	2.027	21.181	0.328
104.975	8.652	34.896	19.241	2.043	20.763	0.321
104.294	8.656	32.284	19.042	2.052	20.590	0.335
103.599	8.656	30.221	18.448	2.057	19.969	0.327
104.057	8.656	29.349	18.050	2.049	19.244	0.311
104.998	8.656	28.685	18.629	2.050	19.522	0.345
105.227	8.660	28.184	18.609	2.059	19.526	0.339
104.504	8.686	29.230	16.349	2.083	19.080	0.327
103.506	8.739	35.851	11.769	2.153	18.738	0.329
98.007	8.878	90.454	4.474	2.368	19.311	0.144
92.045	8.924	97.977	3.044	2.399	19.314	0.130
87.467	8.911	85.906	2.292	2.399	19.221	0.122
85.442	8.864	76.033	1.957	2.391	19.487	0.135
84.926	8.805	72.271	1.885	2.373	19.484	0.131
84.803	8.738	70.879	1.911	2.353	19.034	0.186
84.740	8.710	70.898	1.983	2.344	18.780	0.129
84.419	8.729	71.604	2.167	2.341	19.170	0.176
84.172	8.728	71.480	2.490	2.310	20.551	0.151
86.061	8.690	67.606	2.895	2.224	22.400	0.159
91.640	8.678	60.957	3.224	2.164	22.640	0.277

97.906	8.728	57.665	3.361	2.214	20.912	0.335
99.049	8.797	62.626	3.258	2.336	19.200	0.305
94.002	8.834	72.210	2.987	2.405	18.316	0.118
86.830	8.849	80.758	2.608	2.413	18.500	0.112
83.726	8.852	85.688	2.257	2.404	19.354	0.117
85.050	8.853	91.646	2.056	2.404	19.347	0.079
86.988	8.853	95.200	2.001	2.414	18.402	0.116
85.694	8.853	92.560	1.993	2.416	17.885	0.099
83.028	8.853	90.798	1.970	2.415	17.883	0.097
82.201	8.853	91.639	1.925	2.415	17.784	0.104
82.675	8.853	90.075	1.862	2.408	17.559	0.097
82.905	8.853	86.559	1.791	2.407	17.474	0.105
83.087	8.853	84.410	1.724	2.413	17.589	0.111
82.996	8.853	84.047	1.654	2.417	17.708	0.122
82.538	8.853	84.473	1.577	2.412	17.790	0.118
82.350	8.852	85.882	1.509	2.404	17.908	0.129
82.801	8.848	87.470	1.460	2.406	18.117	0.116
83.548	8.836	89.392	1.429	2.405	18.281	0.136
84.030	8.838	89.663	1.413	2.393	18.143	0.140
84.171	8.845	87.011	1.409	2.384	18.023	0.136
84.141	8.838	85.259	1.418	2.391	18.204	0.145
84.144	8.836	87.377	1.444	2.405	18.059	0.117
83.947	8.847	87.791	1.485	2.392	17.618	0.120
83.501	8.852	82.867	1.517	2.371	17.374	0.142
83.397	8.853	80.062	1.519	2.378	17.066	0.157
83.303	8.853	83.113	1.507	2.392	16.991	0.192
82.790	8.853	87.091	1.498	2.393	17.004	0.133
82.467	8.853	87.827	1.472	2.395	16.848	0.165
82.608	8.853	86.113	1.426	2.383	17.071	0.145
83.421	8.853	83.849	1.388	2.368	17.621	0.149
84.441	8.853	82.307	1.379	2.371	18.193	0.179
84.869	8.853	80.253	1.395	2.375	18.576	0.180
84.793	8.853	79.038	1.411	2.370	18.630	0.156
85.036	8.853	79.234	1.417	2.376	18.764	0.177
85.571	8.853	79.501	1.423	2.392	19.244	0.183
85.868	8.853	81.771	1.440	2.390	19.594	0.143
85.937	8.853	87.159	1.460	2.377	19.737	0.157
85.967	8.853	93.532	1.463	2.374	19.746	0.167
85.678	8.853	97.209	1.460	2.381	19.168	0.169
85.594	8.852	94.529	1.480	2.393	18.257	0.142
85.809	8.834	88.108	1.556	2.395	17.811	0.140
85.629	8.774	84.953	1.713	2.366	18.106	0.141
85.397	8.698	81.987	1.936	2.307	18.265	0.155
85.174	8.675	72.251	2.131	2.278	18.042	0.188
84.767	8.719	66.062	2.245	2.321	17.903	0.259
84.123	8.798	75.104	2.273	2.398	17.777	0.253

82.881	8.837	89.890	2.174	2.444	17.798	0.122
81.102	8.826	97.709	2.028	2.477	17.623	0.093
78.974	8.790	93.966	2.015	2.481	17.610	0.118
77.871	8.752	83.541	2.279	2.412	17.434	0.124
79.635	8.708	74.870	2.760	2.323	16.473	0.135
83.588	8.685	67.934	3.193	2.291	15.787	0.163
86.113	8.741	64.260	3.296	2.339	16.026	0.218
86.064	8.853	76.415	3.064	2.419	17.210	0.259
84.525	8.927	96.920	2.652	2.453	18.260	0.116
83.660	8.949	104.368	2.255	2.461	18.396	0.098
83.434	8.951	104.727	1.952	2.470	18.313	0.083
82.976	8.951	106.087	1.767	2.460	18.446	0.126
82.736	8.951	107.232	1.661	2.449	18.493	0.119
82.701	8.951	108.287	1.600	2.453	18.222	0.096
82.164	8.951	106.324	1.559	2.445	17.955	0.121
81.656	8.951	102.052	1.536	2.439	17.967	0.124
81.919	8.951	102.467	1.535	2.457	18.240	0.127
82.605	8.951	105.817	1.547	2.467	18.498	0.126
83.094	8.951	104.065	1.570	2.458	18.335	0.107
83.100	8.951	100.231	1.565	2.453	17.890	0.114
82.920	8.951	100.848	1.472	2.455	17.443	0.129
82.840	8.951	103.527	1.346	2.455	17.131	0.124
82.776	8.951	105.528	1.297	2.456	17.208	0.109
82.600	8.952	105.859	1.288	2.453	17.407	0.106
82.321	8.965	104.222	1.284	2.449	17.359	0.127
81.929	8.995	99.896	1.282	2.462	17.165	0.109
81.596	9.023	95.324	1.280	2.463	17.124	0.125
81.576	9.041	93.872	1.281	2.441	17.240	0.130
81.840	9.049	93.295	1.301	2.429	17.129	0.144
82.019	9.049	92.197	1.350	2.439	16.823	0.133
81.713	9.049	91.539	1.418	2.454	16.710	0.145
81.192	9.049	91.411	1.486	2.464	16.774	0.103
80.792	9.049	91.382	1.539	2.463	16.639	0.115
80.424	9.049	90.691	1.561	2.455	16.269	0.107
80.204	9.049	91.167	1.570	2.461	16.109	0.132
80.372	9.049	92.880	1.577	2.472	16.226	0.131
80.554	9.049	93.082	1.584	2.478	16.234	0.118
80.104	9.049	91.843	1.583	2.480	15.917	0.120
79.304	9.049	90.197	1.574	2.474	15.557	0.105
79.130	9.049	90.838	1.565	2.470	15.444	0.110
79.694	9.049	91.934	1.557	2.471	15.433	0.130
80.485	9.049	91.964	1.546	2.464	15.355	0.138
80.812	9.049	92.268	1.540	2.449	15.419	0.126
80.798	9.049	91.843	1.533	2.434	15.744	0.114
80.844	9.049	91.426	1.509	2.422	16.110	0.132
81.084	9.049	91.206	1.462	2.421	16.272	0.115

81.559	9.049	91.084	1.397	2.426	16.437	0.113
81.942	9.049	90.930	1.324	2.429	16.812	0.128
82.043	9.049	88.906	1.256	2.425	17.145	0.119
82.118	9.049	84.527	1.197	2.407	17.215	0.140
82.373	9.049	78.874	1.154	2.399	17.139	0.137
82.565	9.049	77.146	1.133	2.412	17.214	0.151
82.458	9.049	80.183	1.138	2.430	17.393	0.161
81.964	9.049	80.931	1.159	2.431	17.263	0.154
81.432	9.049	79.613	1.191	2.416	16.932	0.133
81.258	9.049	80.343	1.245	2.413	16.782	0.143
81.299	9.049	82.511	1.331	2.439	16.880	0.138
81.380	9.049	84.551	1.445	2.456	17.116	0.169
80.845	9.049	82.542	1.561	2.452	16.729	0.124
78.963	9.049	77.829	1.629	2.466	15.801	0.109
76.808	9.049	75.160	1.626	2.476	15.473	0.146
77.043	9.049	77.192	1.575	2.470	15.982	0.091
79.223	9.049	80.437	1.507	2.465	16.691	0.136
80.762	9.049	80.693	1.427	2.459	17.122	0.136
80.796	9.049	80.209	1.363	2.448	17.573	0.143
80.898	9.049	81.445	1.325	2.433	18.171	0.132
81.441	9.049	81.507	1.307	2.418	18.377	0.124
81.827	9.049	81.220	1.292	2.415	18.387	0.156
81.722	9.049	83.205	1.268	2.427	18.355	0.166
81.472	9.049	84.868	1.243	2.429	18.196	0.147
81.660	9.049	85.776	1.232	2.410	17.997	0.116
82.109	9.049	85.885	1.237	2.401	17.660	0.153
82.207	9.049	84.201	1.267	2.405	17.514	0.164
81.845	9.049	83.761	1.317	2.410	17.562	0.150
81.264	9.049	84.541	1.358	2.420	17.487	0.154
80.846	9.049	85.116	1.371	2.434	17.214	0.121
80.844	9.049	86.172	1.367	2.445	17.234	0.121
81.149	9.049	88.019	1.346	2.450	17.395	0.155
81.349	9.049	88.953	1.307	2.445	17.136	0.139
81.445	9.049	87.970	1.259	2.424	16.749	0.089
81.559	9.049	86.887	1.218	2.401	16.602	0.164
81.890	9.049	81.766	1.233	2.408	16.192	0.145
82.232	9.049	81.601	1.289	2.435	16.556	0.152
82.404	9.049	87.221	1.348	2.455	16.985	0.167
82.285	9.049	91.409	1.393	2.449	17.206	0.154
82.019	9.049	87.272	1.403	2.435	17.192	0.130
81.590	9.049	80.948	1.390	2.438	16.914	0.119
81.104	9.049	78.081	1.368	2.444	16.551	0.140
80.858	9.048	80.486	1.346	2.439	16.181	0.155
80.880	9.033	82.997	1.316	2.435	16.321	0.136
81.108	8.993	81.661	1.270	2.421	16.826	0.150
81.424	8.960	81.809	1.215	2.408	17.190	0.148

81.825	8.951	83.418	1.163	2.405	17.409	0.110
82.756	8.951	86.367	1.124	2.393	17.163	0.150
82.468	8.951	87.685	1.132	2.402	17.442	0.165
81.879	8.951	84.936	1.145	2.417	17.293	0.166
81.551	8.951	81.636	1.151	2.426	17.487	0.141
81.437	8.951	80.521	1.138	2.432	17.435	0.143
81.619	8.951	80.758	1.107	2.430	17.433	0.136
82.159	8.951	79.444	1.071	2.420	17.896	0.139
82.769	8.951	78.037	1.044	2.419	18.103	0.143
82.809	8.951	78.659	1.028	2.431	18.039	0.152
82.379	8.951	80.299	1.014	2.429	17.694	0.159
83.044	8.951	80.668	1.000	2.414	17.538	0.137
84.872	8.951	78.545	0.997	2.414	17.461	0.137
84.435	8.951	76.112	1.002	2.416	17.563	0.157
82.283	8.951	75.214	1.009	2.400	18.221	0.154
81.906	8.952	74.693	1.033	2.400	18.639	0.123
82.125	8.988	73.457	1.091	2.388	19.299	0.148
81.063	9.330	71.783	1.177	2.286	18.884	0.136
80.178	9.837	71.628	1.244	2.216	17.459	0.154
83.717	9.796	72.372	1.277	2.213	18.495	0.127
90.097	9.419	78.508	1.299	2.209	21.980	0.161
94.840	9.170	91.480	1.295	2.243	23.801	0.139
95.446	8.943	95.946	1.242	2.308	23.014	0.123
88.992	8.860	86.178	1.181	2.377	19.750	0.129
81.649	8.868	79.119	1.157	2.416	18.224	0.134
79.565	8.892	80.789	1.162	2.431	17.687	0.150
79.808	8.923	82.074	1.156	2.436	17.348	0.151
80.729	8.946	81.512	1.139	2.435	17.411	0.112
81.416	8.951	79.468	1.126	2.435	17.670	0.127
81.598	8.951	78.317	1.121	2.442	17.740	0.136
81.825	8.951	79.992	1.123	2.444	17.888	0.134
82.367	8.951	81.733	1.129	2.435	18.307	0.130
82.990	8.951	81.195	1.136	2.428	18.347	0.115
83.527	8.951	79.004	1.141	2.420	17.948	0.133
83.665	8.951	77.104	1.147	2.414	17.760	0.139
83.423	8.951	76.429	1.158	2.424	17.589	0.140
83.115	8.951	76.396	1.171	2.432	17.067	0.139
82.814	8.951	76.884	1.181	2.426	16.796	0.140
82.745	8.951	76.685	1.189	2.416	17.066	0.146
83.431	8.951	76.130	1.193	2.407	17.180	0.120
84.372	8.951	77.074	1.193	2.408	17.050	0.134
84.976	8.950	76.773	1.188	2.409	17.359	0.140
85.282	8.941	74.539	1.185	2.403	18.210	0.163
85.578	8.922	73.496	1.175	2.402	18.922	0.152
85.703	8.893	74.393	1.171	2.408	19.168	0.153
85.294	8.864	76.600	1.187	2.418	19.187	0.155

84.484	8.835	76.978	1.223	2.437	19.219	0.163
84.270	8.770	74.651	1.293	2.442	19.761	0.169
85.196	8.669	74.212	1.433	2.413	20.485	0.135
85.827	8.588	75.138	1.644	2.386	20.563	0.160
83.993	8.561	72.938	1.846	2.405	19.446	0.175
79.946	8.557	66.613	1.937	2.459	17.770	0.171
77.409	8.557	61.897	1.913	2.470	17.548	0.189
80.134	8.557	65.872	1.832	2.412	18.759	0.123
84.658	8.557	73.484	1.762	2.354	19.474	0.127
87.488	8.557	78.521	1.743	2.320	19.344	0.190
88.972	8.557	78.723	1.848	2.303	19.158	0.189
90.881	8.557	75.951	2.115	2.288	19.236	0.198
93.421	8.557	71.397	2.574	2.255	19.442	0.199
96.169	8.557	65.084	3.238	2.200	19.864	0.188
98.803	8.557	58.580	4.024	2.140	20.867	0.216
100.644	8.557	54.078	4.709	2.098	21.632	0.237
101.093	8.557	51.340	4.970	2.080	21.685	0.309
100.712	8.557	49.635	4.791	2.084	21.849	0.294
100.502	8.557	50.442	4.379	2.087	22.617	0.252
101.179	8.557	53.646	3.998	2.073	23.376	0.308
102.077	8.557	56.017	3.757	2.065	23.427	0.356
101.583	8.557	56.050	3.746	2.079	22.565	0.331
100.264	8.557	53.948	3.934	2.109	21.096	0.330
99.757	8.557	46.615	4.704	2.114	19.776	0.307
100.732	8.559	49.001	5.484	2.074	20.266	0.300
101.244	8.586	47.632	5.507	2.091	20.052	0.290
101.417	8.615	48.671	5.524	2.091	19.950	0.312
101.583	8.644	48.534	5.397	2.074	20.176	0.291
102.018	8.655	46.775	5.005	2.059	20.779	0.328
102.420	8.656	45.758	4.441	2.056	21.314	0.331
102.549	8.656	46.798	3.772	2.064	21.358	0.334
102.533	8.657	46.868	3.140	2.075	20.778	0.338
101.944	8.712	45.899	1.920	2.098	20.763	0.321
101.165	8.745	48.193	1.287	2.126	20.952	0.325
99.473	8.754	49.961	0.826	2.145	21.276	0.305
97.043	8.754	50.301	0.625	2.173	21.444	0.298
94.291	8.754	48.722	0.553	2.222	21.134	0.304
90.602	8.741	46.097	0.509	2.267	20.285	0.279
85.319	8.677	45.007	0.468	2.306	19.091	0.285
80.578	8.597	45.516	0.424	2.325	18.266	0.235
78.697	8.559	45.719	0.366	2.295	18.424	0.170
81.770	8.557	46.044	0.299	2.221	19.819	0.133
87.505	8.557	48.113	0.245	2.155	21.509	0.132
89.737	8.557	49.700	0.215	2.132	22.155	0.304
85.583	8.557	48.560	0.216	2.148	21.893	0.304
82.052	8.557	46.171	0.234	2.181	21.067	0.311

83.345	8.557	45.395	0.260	2.205	19.978	0.310
86.465	8.558	46.259	0.283	2.197	19.369	0.289
89.253	8.564	46.504	0.292	2.169	19.919	0.265
92.064	8.581	47.193	0.283	2.148	21.341	0.220
94.564	8.609	47.933	0.264	2.145	22.695	0.281
95.973	8.639	47.480	0.249	2.150	23.277	0.294
96.244	8.654	46.412	0.242	2.149	23.802	0.301
95.982	8.656	45.656	0.240	2.141	24.312	0.313
95.784	8.656	45.867	0.239	2.135	24.430	0.321
96.512	8.672	46.289	0.238	2.133	24.478	0.312
97.482	8.712	45.896	0.238	2.135	24.530	0.297
97.800	8.746	44.702	0.242	2.136	24.775	0.307
97.834	8.754	43.854	0.254	2.128	25.350	0.310
97.907	8.749	44.784	0.274	2.119	25.960	0.317
93.206	8.709	46.324	0.306	2.203	22.169	0.302
87.222	8.678	44.838	0.307	2.224	21.559	0.305
84.681	8.652	45.845	0.303	2.170	21.988	0.162
88.529	8.617	47.937	0.285	2.131	23.898	0.156
94.215	8.576	48.412	0.255	2.128	23.922	0.242
96.578	8.559	47.379	0.232	2.128	23.917	0.308
96.821	8.557	46.055	0.221	2.125	25.408	0.311
96.780	8.557	46.108	0.220	2.127	26.819	0.328
96.683	8.557	47.118	0.221	2.135	27.194	0.318
96.356	8.554	46.472	0.223	2.138	27.150	0.308
95.975	8.543	45.163	0.223	2.137	26.868	0.321
95.613	8.541	44.937	0.222	2.140	26.480	0.319
95.327	8.552	45.312	0.219	2.149	26.236	0.312
95.131	8.557	46.213	0.212	2.156	25.893	0.311
94.998	8.557	46.985	0.206	2.155	25.799	0.307
95.239	8.557	46.064	0.210	2.153	26.319	0.306
94.849	8.550	42.948	0.239	2.173	25.945	0.311
91.452	8.520	40.337	0.302	2.222	23.225	0.298
84.881	8.493	40.037	0.405	2.280	19.644	0.294
78.466	8.517	41.243	0.537	2.306	17.419	0.298
76.027	8.549	42.682	0.632	2.277	17.613	0.175
77.973	8.557	43.862	0.612	2.223	19.140	0.238
82.447	8.557	44.487	0.494	2.180	21.157	0.232
87.308	8.557	44.262	0.382	2.153	22.597	0.294
90.264	8.557	43.411	0.318	2.140	23.089	0.301
90.931	8.557	43.275	0.297	2.144	23.190	0.273
90.649	8.557	43.522	0.295	2.156	22.810	0.285
89.918	8.557	44.559	0.288	2.162	22.271	0.318
89.637	8.557	44.401	0.270	2.156	22.488	0.272
90.993	8.557	42.039	0.245	2.139	23.326	0.275
93.844	8.557	41.379	0.223	2.126	24.276	0.314
96.035	8.557	42.875	0.212	2.125	24.680	0.302

96.853	8.557	42.645	0.214	2.139	23.799	0.298
96.082	8.557	40.968	0.234	2.157	22.844	0.308
96.014	8.557	42.113	0.242	2.154	23.220	0.306
96.257	8.560	43.127	0.244	2.154	23.152	0.297
96.351	8.580	43.359	0.243	2.151	23.165	0.298
96.086	8.622	43.831	0.240	2.150	23.392	0.303
95.502	8.650	44.167	0.239	2.146	23.862	0.314
95.083	8.656	44.497	0.239	2.137	24.374	0.317
95.412	8.656	45.252	0.236	2.133	24.668	0.292
96.011	8.656	44.026	0.232	2.134	24.931	0.307
96.314	8.656	42.449	0.233	2.138	25.102	0.312
95.843	8.656	42.978	0.245	2.145	25.120	0.301
94.641	8.655	43.947	0.267	2.151	25.259	0.311
93.049	8.640	45.067	0.294	2.158	25.431	0.310
91.290	8.600	45.428	0.316	2.171	24.913	0.306
89.503	8.566	44.573	0.318	2.173	24.160	0.267
88.959	8.558	43.809	0.299	2.157	24.173	0.295
90.624	8.550	45.210	0.268	2.135	24.872	0.281
93.109	8.519	47.252	0.238	2.116	25.815	0.257
95.369	8.478	47.674	0.217	2.106	26.677	0.312
97.191	8.462	47.661	0.206	2.109	27.285	0.296
98.027	8.473	48.103	0.204	2.118	27.428	0.328
97.408	8.492	48.940	0.213	2.124	26.945	0.319
96.323	8.489	49.651	0.230	2.134	26.206	0.326
95.282	8.480	48.427	0.244	2.149	25.406	0.327
94.102	8.474	45.627	0.245	2.155	24.846	0.266
92.914	8.463	44.618	0.238	2.148	24.902	0.312
92.331	8.459	46.154	0.231	2.134	25.597	0.291
92.827	8.459	47.669	0.227	2.123	26.128	0.297
93.977	8.459	47.299	0.229	2.131	25.151	0.290
95.102	8.459	46.086	0.244	2.154	23.478	0.323
93.449	8.471	46.628	0.346	2.214	22.079	0.316
90.460	8.476	47.641	0.398	2.255	21.432	0.255
87.428	8.467	45.288	0.424	2.267	20.084	0.303
85.421	8.459	42.306	0.425	2.250	20.316	0.241
85.697	8.459	44.051	0.408	2.214	20.522	0.235
87.470	8.459	46.185	0.392	2.176	19.807	0.264
89.364	8.459	45.918	0.387	2.177	19.667	0.279
89.076	8.459	45.976	0.380	2.217	18.580	0.269
87.374	8.459	45.589	0.364	2.192	18.796	0.300
87.997	8.459	44.741	0.347	2.158	19.844	0.299
90.734	8.459	43.242	0.334	2.138	20.662	0.189
92.533	8.459	44.334	0.341	2.154	20.188	0.204
91.368	8.459	46.509	0.375	2.202	18.508	0.310
87.683	8.459	45.504	0.417	2.239	16.893	0.315
84.021	8.459	41.330	0.453	2.249	16.019	0.283

82.741	8.459	39.760	0.486	2.244	15.686	0.280
82.961	8.459	41.590	0.492	2.228	16.068	0.176
83.110	8.459	43.861	0.444	2.203	17.574	0.238
83.818	8.459	45.224	0.382	2.172	19.352	0.229
85.819	8.459	45.717	0.340	2.157	19.949	0.240
87.683	8.459	45.542	0.308	2.151	20.153	0.236
89.529	8.459	45.666	0.281	2.139	21.504	0.249
92.296	8.459	46.622	0.270	2.138	23.146	0.326
94.387	8.459	47.324	0.274	2.143	23.866	0.297
94.777	8.459	47.116	0.293	2.142	23.948	0.274
94.030	8.459	46.758	0.330	2.137	23.786	0.253
92.748	8.459	45.707	0.384	2.135	23.485	0.263
91.384	8.459	44.661	0.451	2.154	23.032	0.264
90.440	8.459	45.999	0.528	2.186	22.291	0.321
89.225	8.470	48.277	0.591	2.202	21.156	0.246
87.471	8.506	50.900	0.615	2.206	20.426	0.255
86.607	8.539	53.981	0.586	2.207	20.617	0.265
87.296	8.527	55.693	0.536	2.208	20.609	0.244
88.720	8.485	53.594	0.496	2.216	20.158	0.271
89.259	8.470	49.784	0.468	2.243	19.112	0.193
87.844	8.497	46.543	0.426	2.257	18.118	0.245
86.335	8.538	44.100	0.374	2.231	18.631	0.230
88.442	8.556	44.177	0.341	2.195	20.290	0.031
92.451	8.557	46.534	0.325	2.174	21.497	0.219
94.348	8.557	48.626	0.316	2.172	21.278	0.151
94.254	8.557	49.870	0.320	2.174	20.696	0.275
93.686	8.557	50.621	0.334	2.171	20.466	0.225
93.411	8.557	50.570	0.333	2.162	20.269	0.292
94.032	8.557	50.413	0.327	2.147	20.151	0.226
95.402	8.557	49.388	0.331	2.142	20.449	0.269
96.221	8.557	48.026	0.340	2.152	21.075	0.260
96.439	8.557	49.189	0.346	2.157	21.405	0.246
96.767	8.557	51.600	0.351	2.149	21.486	0.300
97.012	8.557	51.558	0.339	2.142	21.701	0.300
97.106	8.557	48.853	0.304	2.141	22.187	0.294
97.591	8.557	46.626	0.262	2.132	23.210	0.263
98.335	8.557	46.725	0.232	2.122	24.157	0.301
98.809	8.557	47.377	0.217	2.122	24.272	0.278
99.216	8.557	47.953	0.216	2.119	23.855	0.285
99.809	8.557	48.547	0.222	2.118	23.359	0.308
100.023	8.557	50.092	0.232	2.125	23.101	0.306
99.631	8.557	52.067	0.247	2.129	23.053	0.304
99.297	8.557	52.498	0.268	2.132	23.068	0.311
98.972	8.557	52.465	0.291	2.131	22.628	0.310
98.699	8.557	52.846	0.310	2.122	22.317	0.292
98.964	8.557	53.144	0.326	2.117	22.436	0.306

99.539	8.557	54.463	0.336	2.121	22.158	0.313
99.936	8.557	55.686	0.339	2.127	21.853	0.301
100.109	8.557	55.267	0.343	2.130	22.184	0.284
100.066	8.557	55.574	0.354	2.130	23.077	0.313
99.938	8.553	59.639	0.371	2.133	23.854	0.297
99.666	8.528	64.395	0.391	2.144	23.537	0.255
98.892	8.485	64.583	0.404	2.157	22.612	0.299
97.926	8.462	61.820	0.404	2.156	21.833	0.273
97.950	8.459	58.321	0.397	2.140	21.257	0.312
99.022	8.459	55.470	0.388	2.134	20.706	0.286
99.552	8.459	53.596	0.381	2.145	20.151	0.276
98.678	8.459	54.292	0.380	2.158	20.075	0.294
96.956	8.459	57.059	0.395	2.169	20.316	0.239
95.463	8.459	59.396	0.427	2.183	20.348	0.314
94.710	8.459	59.902	0.474	2.208	19.684	0.253
93.125	8.459	57.574	0.519	2.265	17.724	0.303
88.378	8.459	54.599	0.543	2.319	16.032	0.284
82.662	8.459	53.411	0.539	2.299	16.634	0.259
81.713	8.459	53.613	0.495	2.245	18.123	0.263
85.694	8.459	53.413	0.401	2.197	18.992	0.257
90.712	8.459	51.771	0.299	2.150	20.196	0.283
94.481	8.459	50.901	0.233	2.117	21.607	0.076
96.700	8.459	50.648	0.202	2.107	22.260	0.244
97.189	8.459	50.123	0.191	2.114	22.598	0.237
96.856	8.459	50.948	0.199	2.119	22.911	0.276
96.346	8.459	53.671	0.219	2.119	22.734	0.301
95.797	8.459	54.891	0.230	2.123	22.225	0.310
95.268	8.459	52.757	0.232	2.131	21.854	0.295
94.908	8.459	50.110	0.230	2.134	22.326	0.304
95.209	8.459	49.931	0.215	2.135	23.230	0.281
95.506	8.459	52.232	0.217	2.138	22.962	0.322
95.495	8.459	53.234	0.220	2.140	22.662	0.297
95.229	8.459	51.112	0.221	2.139	22.325	0.298
95.068	8.459	48.357	0.218	2.138	22.367	0.298
94.942	8.459	48.316	0.213	2.139	22.845	0.313
94.872	8.459	49.339	0.212	2.138	23.209	0.292
95.125	8.459	49.722	0.218	2.137	23.304	0.289
95.529	8.459	50.779	0.225	2.142	22.792	0.288
95.730	8.459	51.569	0.235	2.158	22.322	0.316
93.677	8.459	48.674	0.263	2.232	20.399	0.275
93.947	8.459	45.841	0.265	2.231	20.224	0.305
94.713	8.459	46.309	0.267	2.204	21.477	0.282
93.797	8.459	51.228	0.267	2.195	22.098	0.296
93.229	8.459	55.286	0.264	2.193	21.766	0.224
93.321	8.459	54.347	0.289	2.203	21.258	0.304
91.730	8.459	53.713	0.347	2.242	20.172	0.275

87.983	8.461	53.978	0.428	2.318	18.474	0.275
82.742	8.481	54.114	0.509	2.393	16.904	0.244
78.044	8.514	54.301	0.546	2.397	16.790	0.270
76.803	8.532	57.036	0.522	2.321	18.331	0.249
90.611	8.552	65.499	0.361	2.206	20.877	0.150
90.569	8.557	67.094	0.348	2.224	20.587	0.174
89.357	8.552	68.691	0.358	2.227	20.604	0.225
88.663	8.531	68.758	0.380	2.236	20.420	0.207

Well logs dataset (Well 15/12-20S)

DT	CA	GR	DR	RHOB	CNC	POR
68.485	8.601	61.344	5.886	2.519	19.410	0.099
66.146	8.567	43.991	7.483	2.566	12.880	0.119
65.456	8.476	38.238	8.649	2.581	11.130	0.171
66.183	8.454	36.687	10.940	2.537	10.130	0.178
69.931	8.397	8.935	20.865	2.312	9.300	0.136
75.959	8.397	8.959	12.298	2.331	12.100	0.185
79.063	8.420	16.579	12.909	2.343	13.960	0.171
80.076	8.420	16.356	12.130	2.349	14.250	0.069
76.615	8.420	12.629	19.497	2.342	12.610	0.152
70.578	8.420	7.256	23.660	2.359	9.570	0.142
67.801	8.420	9.861	24.205	2.425	8.510	0.055
66.969	8.408	9.439	23.320	2.446	7.850	0.118
66.779	8.420	8.428	21.195	2.496	8.070	0.183
68.514	8.420	9.294	22.060	2.473	10.310	0.154
74.665	8.420	28.444	9.973	2.380	15.470	0.193
81.625	8.420	20.433	11.459	2.386	13.440	0.040
77.293	8.595	46.527	7.838	2.406	21.350	0.042
74.117	8.567	36.350	5.099	2.492	14.820	0.038
73.768	8.510	26.244	3.417	2.515	14.200	0.053
80.263	8.567	45.523	3.705	2.507	25.190	0.031
87.422	8.567	56.575	10.063	2.350	30.340	0.145
85.499	8.601	37.032	16.676	2.310	16.330	0.163
78.826	8.454	26.970	9.321	2.464	14.260	0.141
77.691	8.420	21.345	9.643	2.341	12.530	0.212
80.564	8.420	14.452	17.242	2.219	13.950	0.203
82.731	8.397	14.210	15.960	2.218	15.590	0.221

82.455	8.397	15.815	16.658	2.278	14.730	0.205
82.060	8.397	18.003	15.344	2.298	14.250	0.200
82.738	8.420	15.056	18.442	2.235	14.010	0.213
84.333	8.420	14.140	12.886	2.224	15.670	0.193
85.370	8.420	13.791	11.678	2.221	17.440	0.195
85.741	8.420	12.156	4.162	2.251	19.300	0.213
82.509	8.420	14.812	2.700	2.264	18.420	0.214
82.866	8.437	12.113	1.515	2.273	18.390	0.173
83.304	8.420	11.534	0.941	2.284	18.420	0.182
83.878	8.397	10.805	0.623	2.307	19.040	0.216
82.650	8.420	12.869	0.556	2.283	19.300	0.219
84.523	8.420	18.484	0.823	2.265	19.430	0.219
85.057	8.420	18.506	0.540	2.281	18.380	0.233
83.953	8.397	10.580	0.360	2.265	18.800	0.221
83.721	8.420	10.065	0.289	2.276	18.800	0.237
83.281	8.420	9.708	0.259	2.297	19.100	0.219
82.851	8.420	7.757	0.341	2.269	19.660	0.226
82.687	8.420	8.625	0.388	2.277	18.730	0.200
83.323	8.420	13.625	0.602	2.284	18.420	0.214
84.916	8.454	8.444	0.461	2.239	20.610	0.213
85.791	8.454	8.505	0.389	2.218	21.340	0.214
86.174	8.420	9.653	0.350	2.208	21.460	0.174
84.819	8.397	13.331	0.365	2.279	19.070	0.208
83.303	8.420	11.905	0.482	2.305	17.840	0.212
80.211	8.420	7.844	0.547	2.328	16.770	0.235
79.125	8.420	8.629	0.505	2.315	17.170	0.225
80.674	8.420	6.483	0.342	2.284	17.890	0.223
81.046	8.408	5.149	0.360	2.271	18.890	0.202
77.240	8.397	14.646	1.203	2.357	15.180	0.051
77.780	8.420	23.542	1.571	2.378	14.970	0.178
75.479	8.420	24.775	1.644	2.422	10.870	0.148
68.957	8.420	32.365	1.973	2.516	6.690	0.152
65.470	8.420	33.396	2.111	2.557	5.730	0.067
66.517	8.476	28.382	2.031	2.561	7.460	0.042
71.450	8.454	17.237	1.196	2.475	14.420	0.152

74.162	8.454	22.247	0.995	2.463	15.410	0.096
74.990	8.476	22.208	0.979	2.452	15.940	0.128
73.906	8.454	23.408	0.970	2.476	16.090	0.119
74.978	8.454	19.510	0.881	2.434	17.220	0.062
76.324	8.420	21.560	0.759	2.409	15.610	0.197
77.700	8.420	19.152	0.658	2.397	16.950	0.130
77.893	8.454	15.620	0.588	2.382	17.770	0.156
76.797	8.454	13.474	0.506	2.324	17.790	0.190
80.105	8.437	12.123	0.417	2.305	19.610	0.170
79.220	8.476	10.848	0.511	2.289	19.170	0.233
76.205	8.454	21.073	1.239	2.320	16.480	0.218
70.724	8.454	42.788	2.679	2.443	15.670	0.216
69.327	8.476	69.423	2.782	2.566	16.180	0.040
69.287	8.544	72.745	3.024	2.547	16.870	0.032
68.975	8.476	90.149	3.324	2.544	18.370	0.088
67.853	8.510	110.097	3.481	2.582	20.150	0.072
70.249	8.510	84.331	2.774	2.571	18.460	0.059
71.414	8.510	72.195	2.521	2.539	18.480	0.047
75.551	8.567	52.149	1.722	2.492	19.150	0.090
78.653	8.510	40.578	1.098	2.410	18.150	0.078
80.363	8.493	34.213	0.963	2.400	16.120	0.167
78.688	8.544	39.559	0.979	2.465	15.390	0.168
75.428	8.476	46.442	0.998	2.451	16.710	0.124
76.383	8.527	34.758	0.982	2.428	16.890	0.072
77.612	8.544	31.126	1.073	2.423	14.830	0.150
75.829	8.544	41.059	1.319	2.498	15.280	0.147
73.457	8.544	44.779	1.336	2.482	16.510	0.097
74.093	8.544	47.685	1.215	2.465	17.070	0.132
75.336	8.544	51.982	1.081	2.450	17.310	0.120
76.191	8.567	75.606	0.990	2.455	19.870	0.132
78.117	8.544	71.480	0.763	2.356	21.450	0.102
79.388	8.544	66.883	0.732	2.353	22.630	0.188
80.865	8.567	74.978	1.064	2.372	19.740	0.202
77.993	8.510	105.125	1.412	2.475	18.050	0.193
75.135	8.565	105.067	1.512	2.522	17.030	0.043

76.228	8.558	142.719	1.252	2.486	19.470	0.104
77.248	8.587	105.720	0.954	2.493	20.190	0.107
79.414	8.493	89.839	0.842	2.408	20.830	0.158
80.846	8.476	81.578	0.849	2.445	21.650	0.175
80.157	8.454	68.637	1.048	2.379	19.800	0.171
78.884	8.510	88.728	1.144	2.445	20.110	0.204
76.151	8.454	79.567	1.197	2.499	17.990	0.115
74.836	8.476	71.711	1.163	2.488	19.130	0.108
74.970	8.420	68.107	1.058	2.455	19.070	0.129
76.331	8.420	70.451	0.975	2.426	20.400	0.120
79.862	8.454	75.235	0.893	2.397	21.580	0.168
81.360	8.420	77.144	0.820	2.392	21.050	0.162
82.839	8.420	81.387	0.688	2.368	22.160	0.167
84.616	8.420	74.555	0.601	2.337	20.890	0.188
85.421	8.420	75.448	0.612	2.319	20.230	0.212
84.874	8.420	93.801	0.651	2.333	21.100	0.203
85.334	8.454	118.546	0.833	2.375	20.950	0.211
85.454	8.510	163.591	1.151	2.550	27.760	0.204
75.940	8.454	91.994	1.205	2.660	19.860	0.090
77.939	8.454	88.637	1.140	2.468	18.830	0.073
78.876	8.476	93.109	1.134	2.513	22.050	0.076
79.155	8.595	98.569	1.153	2.564	21.360	0.157
79.564	8.510	97.022	1.170	2.605	21.630	0.145
79.998	8.584	99.661	1.188	2.580	24.360	0.085
81.084	8.567	90.822	1.223	2.609	25.830	0.108
82.635	8.601	91.497	1.318	2.646	29.090	0.099
81.584	8.748	89.209	1.422	2.614	29.440	0.089
79.040	8.805	88.087	1.515	2.623	26.120	0.096
77.958	8.658	86.555	1.554	2.587	23.500	0.098
79.294	8.641	89.347	1.543	2.567	22.970	0.082
80.015	8.658	88.807	1.551	2.571	22.980	0.074
80.977	8.601	89.148	1.558	2.580	21.240	0.091
83.329	8.624	93.909	1.518	2.587	23.620	0.086
84.328	8.601	95.630	1.457	2.591	26.330	0.086
85.358	8.748	99.310	1.383	2.546	27.560	0.087

85.392	8.777	99.197	1.333	2.547	29.220	0.088
85.669	8.703	103.091	1.308	2.553	29.940	0.099
85.543	8.714	106.285	1.257	2.542	28.410	0.108
85.532	8.675	102.835	1.233	2.540	28.960	0.100
86.122	8.641	106.926	1.250	2.534	27.840	0.099
86.108	8.805	101.360	1.287	2.558	26.230	0.091
84.980	8.771	95.710	1.365	2.578	26.560	0.093
83.394	8.714	97.241	1.466	2.594	23.730	0.089
80.889	8.641	91.538	1.548	2.588	18.680	0.093
78.677	8.612	86.600	1.611	2.593	19.770	0.101
79.838	8.601	84.353	1.683	2.590	20.100	0.074
82.417	8.601	84.345	1.704	2.608	21.790	0.087
83.274	8.601	86.561	1.696	2.583	21.780	0.092
82.152	8.646	89.032	1.671	2.598	21.960	0.095
81.680	8.612	86.655	1.560	2.584	20.340	0.086
82.833	8.658	78.234	1.449	2.531	20.690	0.091
82.496	8.658	71.141	1.201	2.508	19.050	0.083
81.908	8.624	69.195	1.018	2.502	19.140	0.103
83.941	8.624	61.187	0.889	2.469	19.800	0.109
85.880	8.601	56.273	0.862	2.433	19.830	0.150
84.798	8.624	61.490	0.924	2.430	20.190	0.171
81.760	8.612	75.295	0.981	2.525	23.000	0.160
80.929	8.692	81.256	1.150	2.545	22.980	0.123
80.217	8.567	80.533	1.234	2.587	23.520	0.105
79.615	8.567	83.867	1.291	2.603	24.250	0.125
79.960	8.601	85.299	1.327	2.599	25.500	0.096
81.140	8.584	89.167	1.374	2.636	25.260	0.082
81.697	8.624	93.419	1.406	2.586	26.100	0.087
81.654	8.567	89.653	1.410	2.579	23.260	0.099